

กลไกของลิโปโซมในการนำส่งแคลซินเอเอ็มซึ่งเป็นแบบจำลองยับยั้งของ
พี-ไกลโคโปรตีนเข้าสู่เซลล์คาโค-2

นางสาวอิงอร ประสารชัยมนตรี

วิทยานิพนธ์นี้เป็นส่วนหนึ่งของการศึกษาตามหลักสูตรปริญญาเภสัชศาสตรมหาบัณฑิต
สาขาวิชาเภสัชกรรม ภาควิชาวิทยาการเภสัชกรรมและเภสัชอุตสาหกรรม
คณะเภสัชศาสตร์ จุฬาลงกรณ์มหาวิทยาลัย
ปีการศึกษา 2552
ลิขสิทธิ์ของจุฬาลงกรณ์มหาวิทยาลัย

MECHANISMS OF LIPOSOMES IN THE DELIVERY OF
THE P-GLYCOPROTEIN SUBSTRATE MODEL CALCEIN AM
INTO CACO-2 CELLS

Miss Ing-orn Prasanchaimontri

A Thesis Submitted in Partial Fulfillment of the Requirements
for the Degree of Master of Science in Pharmacy Program in Pharmaceutics

Department of Pharmaceutics and Industrial Pharmacy

Faculty of Pharmaceutical Sciences

Chulalongkorn University

Academic Year 2009

Copyright of Chulalongkorn University

Thesis Title MECHANISMS OF LIPOSOMES IN THE DELIVERY
OF THE P-GLYCOPROTEIN SUBSTRATE MODEL
CALCEIN AM INTO CACO-2 CELLS
By Miss Ing-orn Prasanchaimontri
Field of Study Pharmaceutics
Thesis Advisor Assistant Professor Nontima Vardhanabhuti, Ph.D.
Thesis Co-Advisor Associate Professor Thitima Pengsuparp, Ph.D.

Accepted by the Faculty of Pharmaceutical Sciences, Chulalongkorn
University in Partial Fulfillment of the Requirements for the Master's Degree

..... Dean of the Faculty
of Pharmaceutical Sciences
(Associate Professor Pornpen Pramyothin, Ph.D.)

THESIS COMMITTEE

..... Chairman
(Associate Professor Uthai Suvanakoot, Ph.D.)

..... Thesis Advisor
(Assistant Professor Nontima Vardhanabhuti, Ph.D.)

..... Thesis Co-Advisor
(Associate Professor Thitima Pengsuparp, Ph.D.)

..... Examiner
(Associate Professor Parkpoom Tengamnuay, Ph.D.)

..... External Examiner
(Associate Professor Nusara Piyapolrunroj, Ph.D.)

อิงอร ประสารชัยมนตรี : กลไกของลิโปโซมในการนำส่งแคลซินเอเอ็มซึ่งเป็นแบบจำลอง
 ซับซ้อนของพี-ไกลโคโปรตีนเข้าสู่เซลล์คาโค-2. (MECHANISMS OF LIPOSOMES
 IN THE DELIVERY OF THE P-GLYCOPROTEIN SUBSTRATE MODEL CALCEIN
 AM INTO CACO-2 CELLS) อ.ที่ปรึกษาวิทยานิพนธ์หลัก : ผศ. ดร.นนทิมา วรธนะภูติ,
 อ.ที่ปรึกษาวิทยานิพนธ์ร่วม : รศ. ดร.ธิดิมา เฟื่องสุภาพ, 116 หน้า.

การศึกษานี้มีวัตถุประสงค์เพื่อหากลไกที่เป็นไปได้ของลิโปโซมในการเพิ่มการนำส่งสารที่เป็นซับซ้อนของ
 พี-ไกลโคโปรตีนเข้าสู่เซลล์คาโค-2 รวมถึงศึกษาผลของปัจจัยต่าง ๆ ด้านสูตรตำรับของลิโปโซม (ได้แก่
 การเติมลิพิดที่มีประจุ ปริมาณคอเลสเตอรอล และชนิดของฟอสฟาติดีลโคลีน) ในการศึกษาใช้แคลซินเอเอ็มเป็นตัวแทน
 ของสารที่เป็นซับซ้อนของพี-ไกลโคโปรตีน เตรียมลิโปโซมซึ่งบรรจุแคลซินเอเอ็มด้วยวิธีฟิล์มไฮเดรชันและนำมาลด
 ขนาดด้วยการกอดผ่านเมมเบรนที่ทำจากโพลีคาร์บอนเนตซึ่งมีช่องเปิดขนาด 100 นาโนเมตร การสืบหากลไกที่เป็นไปได้
 ในการนำส่งแคลซินเอเอ็มเข้าสู่เซลล์ของลิโปโซมทำโดยใช้หลายเทคนิคร่วมกัน ในการศึกษาผลของปัจจัยต่าง ๆ ด้าน
 สูตรตำรับของลิโปโซม ทำโดยเปรียบเทียบปริมาณแคลซินเอเอ็มที่นำส่งเข้าสู่เซลล์คาโค-2 โดยใช้ลิโปโซมที่มี
 ส่วนประกอบแตกต่างกัน ผลการศึกษาแสดงให้เห็นว่าลิโปโซมชนิดไม่มีประจุ (ซึ่งประกอบด้วยฟอสฟาติดีลโคลีน:
 คอเลสเตอรอล ในสัดส่วน 7:3 โดยโมล) สามารถเพิ่มการนำส่งแคลซินเอเอ็มเข้าสู่เซลล์คาโค-2 ได้ ในลักษณะที่ขึ้นกับ
 เวลาในการบ่มและความเข้มข้นของลิโปโซมที่ใช้ ผลจากการศึกษาด้วยกล้องจุลทรรศน์เลเซอร์ชนิดส่องกราดแบบ
 คอนโฟคัล และการใช้เทคนิคฟลูออเรสเซนส์ดีควินซิงบ่งชี้ถึงการเกิดกระบวนการเอนโดไซโตซิสของลิโปโซมที่บรรจุ
 แคลซินเอเอ็มเข้าสู่เซลล์คาโค-2 ผลการยับยั้งด้วยตัวยับยั้งกระบวนการเอนโดไซโตซิส/เมแทบอลิซึม และผลของอุณหภูมิ
 สนับสนุนการเกิดกระบวนการเอนโดไซโตซิสเช่นกัน ในขณะที่ไม่มีหลักฐานที่สนับสนุนว่าการนำส่งแคลซินเอเอ็มเข้า
 เซลล์ที่เพิ่มขึ้นเกิดจากการเปลี่ยนแปลงสภาพให้ซึมของเยื่อหุ้มเซลล์ หรือการปรับเปลี่ยนการทำงานของพี-ไกลโคโปรตีน
 โดยลิโปโซม ลิพิดที่มีประจุและชนิดของฟอสฟาติดีลโคลีนมีอิทธิพลต่อการนำส่งแคลซินเอเอ็มของลิโปโซมอย่างมาก
 ประสิทธิภาพในการนำส่งแคลซินเอเอ็มเข้าสู่เซลล์ของลิโปโซมที่ไม่มีประจุ และชนิดประจุลบ (ซึ่งประกอบด้วย
 ฟอสฟาติดีลโคลีน:โดซิทิลฟอสเฟต:คอเลสเตอรอล ในสัดส่วน 6:3:1 โดยโมล) เท่าเทียมกันและมากกว่าการนำส่งในรูป
 สารละลายแคลซินเอเอ็ม แต่ลิโปโซมชนิดประจุบวก (ซึ่งประกอบด้วย ฟอสฟาติดีลโคลีน:สเตอรอลเอมีน:คอเลสเตอรอล
 ในสัดส่วน 6:3:1 โดยโมล) ไม่สามารถเพิ่มการนำส่งแคลซินเอเอ็มเข้าสู่เซลล์ได้ ลิโปโซมที่เตรียมโดยใช้ฟอสฟาติดีลโคลีน
 จากถั่วเหลืองทั้งที่มีและไม่มีคอเลสเตอรอลสามารถเพิ่มการนำส่งแคลซินเอเอ็มเข้าสู่เซลล์ได้ดีกว่าผลจากการนำส่งโดยใช้
 ลิโปโซมที่เตรียมจากไดพามีโทอิลฟอสฟาติดีลโคลีน ในขณะที่ปริมาณคอเลสเตอรอลในลิโปโซมมีผลเพียงเล็กน้อย
 ต่อการนำส่งสารแคลซินเอเอ็ม ลิโปโซมที่ประกอบด้วยคอเลสเตอรอล 20-40 เปอร์เซ็นต์โดยโมล ลดการนำส่งแคลซิน-
 เอเอ็มเข้าสู่เซลล์อย่างมีนัยสำคัญ แต่ผลที่เกิดขึ้นน้อยกว่าผลของการเติมลิพิดที่มีประจุและชนิดของฟอสฟาติดีลโคลีน
 ผลการศึกษาโดยรวมชี้ให้เห็นว่ากระบวนการเอนโดไซโตซิสเป็นกระบวนการหลักของลิโปโซมที่ช่วยเพิ่มการนำส่งสาร
 แคลซินเอเอ็มเข้าสู่เซลล์คาโค-2 และส่วนประกอบของลิโปโซมมีบทบาทสำคัญในการนำส่งแคลซินเอเอ็มซึ่งเป็น
 ซับซ้อนของพี-ไกลโคโปรตีนเข้าสู่เซลล์คาโค-2 เช่นกัน

ภาควิชาวิทยาการเภสัชกรรมและเภสัชอุตสาหกรรม ลายมือชื่อนิติศ.....
 สาขาวิชา...เภสัชกรรม..... ลายมือชื่ออ.ที่ปรึกษาวิทยานิพนธ์หลัก.....
 ปีการศึกษา...2552..... ลายมือชื่ออ.ที่ปรึกษาวิทยานิพนธ์ร่วม.....

4976614933: MAJOR PHARMACEUTICS

KEYWORDS: P-glycoprotein / Liposomes / Endocytosis / Caco-2 / Calcein AM

ING-ORN PRASANCHAIMONTRI: MECHANISMS OF LIPOSOMES IN THE DELIVERY OF THE P-GLYCOPROTEIN SUBSTRATE MODEL CALCEIN AM INTO CACO-2 CELLS. THESIS ADVISOR: ASST. PROF. NONTIMA VARDHANABHUTI, Ph.D., THESIS CO-ADVISOR: ASSOC. PROF. THITIMA PENGSUPARP, Ph.D., 116 pp.

The aim of this present study was to investigate the probable mechanisms by which liposomes enhance delivery of P-glycoprotein (P-gp) substrates into Caco-2 cells. The effect of liposomal formulation factors (inclusion of charged lipids, cholesterol content, and type of phosphatidylcholine) was also determined. Calcein AM was used as a model molecule for P-gp substrates. Calcein AM-loaded liposomes were prepared by the film-hydration method followed by extrusion through 100 nm polycarbonate membranes. The possible mechanisms of calcein AM uptake from liposomes were investigated by several techniques. To identify the effect of liposomal formulation factors, the extents of calcein AM uptake into Caco-2 cells were compared among liposomes with different compositions. The result demonstrated that neutral liposomes (phosphatidylcholine:cholesterol at 7:3 molar ratio) could enhance the delivery of calcein AM into Caco-2 cells in a time- and concentration-dependent manner. The results from confocal laser scanning microscopy and fluorescence dequenching technique studies substantiated endocytosis of calcein AM-loaded liposomes into Caco-2 cells. This mechanism was also supported by the inhibitory effect of endocytosis/metabolic inhibitors and the effect of temperature. On the contrary, the enhancement in calcein AM uptake via either the changing in cell membrane permeability or the modulation of P-gp function by liposomes was not evident. Charged lipids and type of phosphatidylcholine showed a strong influence on calcein AM uptake from liposomes. Calcein AM from both neutral and negatively charged (phosphatidylcholine: cholesterol:dicetyl phosphate at 6:3:1 molar ratio) liposomes was taken up by Caco-2 cells similarly and more efficiently than that from calcein AM solution. Positively charged (phosphatidylcholine: cholesterol:stearylamine at 6:3:1 molar ratio) liposomes failed to enhance calcein AM uptake into Caco-2 cells. Soybean phosphatidylcholine liposomes, either with or without cholesterol, could increase cellular uptake of calcein AM better than dipalmitoyl phosphatidylcholine liposomes did. On the other hand, cholesterol content inserted only a minimal effect on calcein AM uptake. The presence of 20-40 mole% of cholesterol in liposomes significantly reduced calcein AM uptake into Caco-2 cells, but with much less magnitude than the effects seen with the inclusion of charged lipids and the type of phosphatidylcholine. Overall results indicate that endocytosis was the main mechanism by which liposomes enhanced the uptake of calcein AM into Caco-2 cells. The liposomal composition also played a significant role in the delivery of the P-gp substrate calcein AM into Caco-2 cells.

Department: Pharmaceutics and Industrial Pharmacy Student's Signature

Field of Study: Pharmaceutics Advisor's Signature

Academic Year: 2009 Co-Advisor's Signature

ACKNOWLEDGEMENTS

I would like to express my sincere appreciation to my advisor, Assistant Professor Nontima Vardhanabhuti, Ph.D., for her scientific guidance, kindness, encouragement, and understanding throughout this study.

I would also like to thank Associate Professor Thitima Pengsuparp, Ph.D., my co-advisor, for her guidance, support, and kindness.

I would also like to thank the thesis committee for their valuable suggestions and helpful discussion.

I sincerely thank Assistant Professor Surachai Unchern, Ph.D., and Associate Professor Parkpoom Tengamnuay, Ph.D., for providing cell culture facilities which are the most important facility for the completion of this study. I also wish to express my gratitude to Assistant Professor Suree Jianmongkol, Ph.D., for her kindness when I was working in the cell culture laboratory under her care.

I am deeply thankful to Mrs. Wassana Wijagkanalan for her advice and kindness, to Ms. Araya Lukanawonakul and Ms. Somrudee Chuenkitiyanon for their helpful suggestions on cell culture techniques, and to Mr. Noppadol Sa-Ard-Iam for his assistance in flow cytometric study.

Sincere thanks are also given to all my friends in the Department of Pharmaceutics and Industrial Pharmacy and the Department of Pharmacology and Physiology and to other persons whose names have not been mentioned for their friendship and valuable help. In addition, I would like to thank all the faculty members in both departments for their support and encouragement.

Special thanks are extended to the members of the Bioequivalence Study Center, Department of Medical Sciences, Ministry of Public Health for encouraging me to pursue my graduate study and their moral support during my study. Thanks are also due to the grant from Center of Innovative Nanotechnology, Chulalongkorn University.

Above all, I would like to express my deepest gratitude to my family for the unconditional encouragement, care, love, and support given to me throughout the years.

CONTENTS

	PAGE
ABSTRACT [THAI].....	iv
ABSTRACT [ENGLISH].....	v
ACKNOWLEDGEMENTS.....	vi
CONTENTS.....	vii
LIST OF TABLES.....	ix
LIST OF FIGURES.....	x
LIST OF ABBREVIATIONS.....	xiv
CHAPTER	
I INTRODUCTION.....	1
II LITERATURE REVIEW.....	6
Transport of drugs across cell membranes.....	6
P-glycoprotein (P-gp).....	10
Strategies to enhance P-gp substrate delivery.....	16
Liposomes as drug carriers.....	19
Interactions of liposomes with cells.....	19
Techniques used in investigation of liposome-cell interactions.....	24
Caco-2 as a cell culture model.....	27
Liposomes and the delivery of P-gp substrates.....	29
III MATERIALS AND METHODS.....	30
Materials.....	30
Equipment.....	31
Methods.....	33
Preparation of liposomes.....	33
Characterization of the physical properties of liposomes.....	35
Maintenance of Caco-2 cells.....	35
Characterization of Caco-2 monolayers.....	36
Uptake of calcein AM into Caco-2 cells as a function of time.....	39

CHAPTER	PAGE
Uptake of calcein AM into Caco-2 cells as a function of concentration.....	40
Investigation of the possible mechanisms of liposomes in the delivery of calcein AM into Caco-2 cells.....	40
Effect of liposomal composition on calcein AM uptake into Caco-2 cells.....	45
Cell viability study	46
Statistical analysis.....	46
IV RESULTS AND DISCUSSION.....	47
Characterization of the physical properties of liposomes.....	47
Characterization of Caco-2 monolayers.....	48
Uptake of calcein AM into Caco-2 cells as a function of time.....	54
Uptake of calcein AM into Caco-2 cells as a function of concentration.....	55
Investigation of the possible mechanisms of liposomes in the delivery of calcein AM into Caco-2 cells.....	56
Effect of liposomal composition on calcein AM uptake into Caco-2 cells.....	75
Cell viability study	79
V CONCLUSIONS.....	81
REFERENCES.....	83
APPENDICES.....	98
VITA.....	116

LIST OF TABLES

TABLE		PAGE
1	Examples of P-gp substrates.....	12
2	Acceptable in vitro P-gp substrates.....	15
3	In vitro P-gp inhibitors.....	16
4	Examples of studies on drug delivery systems using Caco-2 cells as a model.....	28
5	Mean diameters and zeta potential values of blank neutral liposomes and calcein AM-loaded liposomes.....	47
6	Apparent permeability coefficients of rhodamine 123 and the efflux activity of P-gp in the absorptive and the secretory directions across Caco-2 monolayers in the absence and in the presence of verapamil.....	50
7	Uptake of rhodamine 123 and calcein AM from solutions in the absence and in the presence of 100 μ M verapamil.....	52
8	Fluorescence intensity from Caco-2 cells incubated with Alexa Fluor [®] 488-conjugated dextran and serum-free DMEM (Control)...	54
9	Fluorescence intensity of calcein from the uptake of calcein solution and calcein-loaded liposomes into Caco-2 cells by flow cytometry.....	65
10	Uptake of calcein AM-loaded liposomes and Alexa Fluor [®] 488-conjugated dextran into Caco-2 cells in the presence of various metabolic inhibitors.....	73

LIST OF FIGURES

FIGURE		PAGE
1	Transport pathways of drug across cell membrane: (A) passive transcellular, (B) passive paracellular, (C) carrier-mediated apical transport, (D) apical efflux transport, (E) basolateral efflux transport, and (F) carrier-mediated basolateral transport.....	6
2	Intracellular transport of vesicles in enterocytes	9
3	Topological map and domain organization of P-gp (NBD1 and NBD2 = nucleotide-binding domains)	10
4	A schematic showing the drug-substrate binding pocket of P-gp. Two drugs are depicted as simultaneously bound in the drug-binding pocket. The drug shown in orange appears to have a greater affinity for P-gp than the one depicted in red.....	11
5	Models proposed to explain the possible mechanisms of drug efflux by P-gp: (a) pore model, (b) flippase model, and (c) hydrophobic vacuum cleaner model.....	14
6	Possible ways by which liposomes can interact with cells and deliver their contents: 1. Adsorption of a liposome followed by release of the liposomal contents, 2. Adsorption of a liposome followed by transfer of lipophilic compounds from the liposomal bilayer to the plasma membrane, 3. Endocytosis/phagocytosis of a liposome followed by intracellular degradation of the liposome via endolysosomal pathway, and 4. Fusion of liposomal membrane with plasma membrane followed by release of liposomal contents into the cytoplasm	20
7	Physical appearances of liposomal preparations: blank = blank PC liposomes, neutral = calcein AM-loaded neutral liposomes, positive = calcein AM-loaded positively charged liposomes, and negative = calcein AM-loaded negatively charged liposomes.....	48

FIGURE		PAGE
8	TEER values of Caco-2 monolayers as a function of time	49
9	Absorptive (A-to-B) and secretory (B-to-A) permeability coefficients of rhodamine 123 across Caco-2 monolayers in the absence and in the presence of verapamil.....	50
10	Overlay of fluorescence histograms from Caco-2 cells incubated with Alexa Fluor [®] 488-conjugated dextran and serum-free DMEM (Control).....	53
11	Calcein AM uptake profiles from calcein AM solution and calcein AM-loaded liposomes	54
12	Calcein AM uptake from calcein AM solution and calcein AM-loaded liposomes at various concentrations.....	56
13	Calcein uptake into Caco-2 cells from calcein solution with blank liposomes in the pre-treatment and the co-treatment conditions.....	57
14	Calcein AM uptake from calcein AM solution with either verapamil or blank liposomes in the pre-treatment and the co-treatment conditions.....	58
15	CLSM images (with bright field images on the left panel and fluorescence field images on the right panel) of Caco-2 cells treated with various conditions: (A) control, (B) liposomes labeled with NBD-PE (0.35 mg/ml of total lipid concentration), (C and D) calcein AM solution and calcein AM-loaded liposomes (250 nM of final calcein AM concentration), (E and F) calcein solution and calcein-loaded liposomes (16 μ M of final calcein concentration).....	61-62
16	CLSM images of Caco-2 cells treated with liposomes double-labeled with NBD-PE and rhodamine 123 (0.35 mg/ml total lipid concentration, 5.28 μ M of final NBD-PE concentration, and 2 μ M of final rhodamine 123 concentration). The pictures were taken using FITC and TRITC filters for NBD and rhodamine 123, respectively.....	64

FIGURE	PAGE
17	Intracellular accumulation of calcein from calcein solution and calcein-loaded liposomes (80 μ M of calcein) determined by spectrofluorometric method..... 66
18	Uptake of calcein AM from calcein AM-loaded liposomes into Caco-2 cells after pre-treatment with cytochalasin B at 1.25 μ g/ml (CB 1.25) and 2.5 μ g/ml (CB 2.5) for 60 min..... 67
19	Uptake of liposomes labeled with NBD-PE into Caco-2 cells after pre-treatment with cytochalasin B at 1.25 μ g/ml (CB 1.25) and 2.5 μ g/ml (CB 2.5) for 60 min..... 68
20	Uptake of calcein from calcein-loaded liposomes into Caco-2 cells after pre-treatment with cytochalasin B at 1.25 μ g/ml (CB 1.25) and 2.5 μ g/ml (CB 2.5) for 60 min 68
21	Fluorescence histograms from Caco-2 cells incubated with Alexa Fluor [®] 488-conjugated dextran after pre-treatment with cytochalasin B at 2.5 μ g/ml (Cytochalasin B) and with DMEM (Control)..... 70
22	Fluorescence histograms from Caco-2 cells incubated with Alexa Fluor [®] 488-conjugated dextran in the presence of various metabolic inhibitors: (A) sodium azide 15 mM, (B) sodium azide 15 mM + sodium fluoride 10 mM, and (C) sodium azide 15 mM + deoxyglucose 50 mM. Cells incubated with the fluorescent dextran in the absence of metabolic inhibitor were used as the control group. 71
23	Intracellular accumulation of calcein AM in Caco-2 cells incubated with calcein AM solution and calcein AM-loaded liposomes at 37 °C and 4 °C..... 74
24	Intracellular accumulation of calcein AM from calcein AM solution, calcein AM-loaded neutral (PC:CH), positively charged (PC:CH:SA), and negatively charged (PC:CH:DCP) liposomes 76

FIGURE		PAGE
25	Intracellular accumulation of calcein AM from calcein AM solution, calcein AM-loaded neutral liposomes with the different PC:CH ratios	77
26	Intracellular accumulation of calcein AM from calcein AM solution, calcein AM-loaded neutral liposomes with either soybean PC or DPPC and CH at 7:3 and 10:0 molar ratios.....	78
27	Cytotoxicity of calcein AM solution, calcein AM-loaded neutral (PC:CH), positively charged (PC:CH:SA), and negatively charged (PC:CH:DCP) liposomes to Caco-2 cells.....	80
28	A representation of calibration curve of calcein in 1% Triton [®] X-100 in PBS.....	114
29	A representation of calibration curve of rhodamine 123 in 1% Triton [®] X-100 in PBS.....	114
30	A representation of calibration curve of rhodamine 123 in the apical buffer.....	115
31	A representation of calibration curve of rhodamine 123 in the basolateral buffer.....	115

LIST OF ABBREVIATIONS

ABC	=	ATP-binding cassette
ANOVA	=	analysis of variance
BALB/c	=	dermal fibroblast
BHK21	=	hamster fibroblast
Caco-2	=	human colon adenocarcinoma
CH	=	cholesterol
CV1	=	African green monkey kidney cell line
CYP	=	cytochrome P450
DCP	=	dicetylphosphate
DMEM	=	Dulbecco's Modified Eagle's Medium
DMSO	=	dimethyl sulphoxide
DODAP	=	1,2-dioleoyl-3-dimethylammoniumpropanediol
DOPC	=	1,2-dioleoyl- <i>sn</i> -glycero- β -phosphatidylcholine
DPPE	=	dipalmitoyl phosphatidylcholine
DPPE	=	dipalmitoyl phosphatidylethanolamine
EDTA	=	ethylenediaminetetraacetic acid
FBS	=	fetal bovine serum
FITC	=	fluorescein isothiocyanate
HeLa	=	human ovarian carcinoma cell line
HEPES	=	N-[2-hydroxyethyl]piperazine-N'-(2-ethanesulfonic acid)]
J774A.1 and J774	=	murine macrophage cell line
kDa	=	kilodalton
MDR1	=	multidrug resistance protein
MES	=	2-[N-morpholino]ethanesulfonic acid
mg	=	milligram
ml	=	milliliter
mm	=	millimeter
mM	=	millimolar

MRP	=	multidrug resistance-associated protein
MW	=	molecular weight
NBD	=	Nitro-2-1,3-BenzoxaDiazol-4-yl
nm	=	nanometer
OAT-A	=	organic anion transporting polypeptides
PA	=	phosphatidic acid
P_{app}	=	apparent permeability coefficient
$P_{app, AB}$	=	apparent permeability coefficient, apical to basolateral
$P_{app, BA}$	=	apparent permeability coefficient, basolateral to apical
P-gp	=	P-glycoprotein
PBS	=	phosphate buffered saline
PC	=	phosphatidylcholine
PE	=	phosphatidylethanolamine
PG	=	phosphatidylglycerol
PS	=	phosphatidylserine
RAW264.7	=	murine macrophage cell line
SA	=	stearylamine
SD	=	standard deviation
SEM	=	standard error of means
TEER	=	transepithelial electrical resistance
TRITC	=	tetramethylrhodamine isothiocyanate
μg	=	microgram
μl	=	microliter
μm	=	micrometer
μM	=	micromolar

CHAPTER I

INTRODUCTION

To exert their therapeutic effects systemically, drugs administered by extravascular routes must first be absorbed into the systemic circulation. Subsequently, the drugs need to diffuse or to be transported across various barriers to their sites of action at the target cells. The efflux transporters have been reported to be important barriers in the drug absorption process (Chan, Lowes, and Hirst, 2004; Krishna and Mayer, 2000; Takano, Yumoto, and Murakami, 2006). These transporters include P-glycoprotein (P-gp) or multidrug resistance protein (MDR1) and multidrug resistance-associated proteins (MRP1-7).

P-gp, an ATP-binding cassette (ABC) transporter, is known to decrease the absorption efficacy of many drugs. P-gp is the apical membrane protein of 170-180 kDa, which is encoded in the multidrug resistance gene (Hidalgo and Li, 1996). This transporter binds with the drug substrates and effluxes them out of the cells. The result from P-gp function is the decrease in intracellular accumulation of the substrates. The expression of P-gp transporters can be found in normal tissues. High levels of P-gp expression have been observed in the epithelia of brain capillaries, adrenal glands, kidneys, lungs, liver, and small intestine (Chan et al., 2004). The overexpression of P-gp has been found in tumors (Fardel, Lecureur, and Guillouzo, 1996).

The substrates of P-gp comprise many structurally and pharmacologically unrelated hydrophobic compounds. Therapeutic agents that have been demonstrated to be the substrates of P-gp include analgesics, anticancers, HIV protease inhibitors, H₂-receptor antagonists, antigout agents, antidiarrhea agents, antiemetics, calcium channel blockers, cardiac glycosides, immunosuppressive agents, and antibiotics (Schinkel and Jonker, 2003). Special interest has been directed to anticancer agents due to overexpression of this efflux protein in cancer cells. The result of this efflux phenomenon is the multidrug resistance of cancer cells to anticancer drugs and, consequently, the failure in clinical therapy (Krishna and Mayer, 2000; Mamot et al., 2003; Mayer and Shabbits, 2001; Ozben, 2006).

The approaches to overcome multidrug resistance can be classified into two major categories. The first one is modulation of P-gp function by P-gp modulators. Another approach is avoidance of P-gp function via the use of appropriate drug carriers. P-gp modulators reverse the function of P-gp by several pathways. Most P-gp modulators inhibit P-gp function by blocking the binding site of substrate (Varma et al., 2003). The use of P-gp modulators (such as LY 335979, cyclosporin A, verapamil, PSC 833, and XR9576) has been successful in enhancing the delivery of P-gp substrates to various cells (Dantzig et al., 1996; Eneroth et al., 2001; Hunter, Hirst, and Simmons, 1993; Lo, Liu, and Cherng, 2001; Mistry et al., 2001). However, most of these modulators, such as the immunosuppressive agent cyclosporin A, still have intrinsic pharmacological effects that lead to side effects and toxicity (Ozben, 2006). Though researchers have succeeded in developing non-toxic P-gp modulators, the problems due to possible drug interactions remain. The P-gp inhibitor PSC 833 (valsopodar) with 20-fold potency of that of cyclosporin A has been developed (Varma et al., 2003). However, co-administration of PSC 833 with anticancer drugs (daunorubicin, doxorubicin, and paclitaxel) results in the pharmacokinetic alteration of the anticancer drugs and increase in drug toxicity (Mamot et al., 2003). The use of drug delivery systems is an alternative approach to enhance the delivery of P-gp substrates. Most studies used nanoparticles to overcome the efflux mechanism. For example, daunorubicin encapsulated in liposomes effectively reduces the drug resistance in both in vitro and in vivo studies (Michieli et al., 1999). Doxorubicin-loaded nanospheres (Cuvier et al., 1992) and paclitaxel-loaded micellar systems (Dabholkar et al., 2006) can better deliver the drugs to cells by bypassing the P-gp function. Furthermore, uptake of rhodamine 123 into cancer cells increases when the dye is loaded in a micellar system (Zastre et al., 2002).

Liposomes are nanoparticles successfully used as drug delivery systems for many drugs. They can entrap both hydrophilic and lipophilic substances in the aqueous compartment and in the lipid bilayer, respectively. The liposomal components are biodegradable and rather similar to structural components of most biological membranes. Properties of liposomes can be modified by changing their compositions (Hatzi et al., 2007; Imura et al., 2002). When liposomes are taken up into biological systems, they can interact with cells in many ways including

adsorption/binding, fusion, contact release, intermembrane lipid transfer, and endocytosis/phagocytosis (Torchilin and Weissig, 2003). The composition, bilayer fluidity, and size of liposomes can affect the interaction between liposomes and cells that leads to different uptake mechanisms (Lee, Hong, and Papahadjopoulos, 1992; Manconi et al., 2007; Miller et al., 1998; Poste and Papahadjopoulos, 1976). The liposome uptake into cells is also influenced by cell type (Lee et al., 1992; Miller et al., 1998). Liposomes composed of negatively charged phospholipids are taken up into BHK21, 3T3, and L929 via a non-endocytotic pathway or fusion (Papahadjopoulos, Poste, and Schaefer, 1973). PC-based liposomes spiked with phosphatidylserine, phosphatidylglycerol, or phosphatidic acid are efficiently endocytosed into CV1 (Lee et al., 1992). Positively charged liposomes may adsorb around the cell membrane without being internalized into the cells (Manconi et al., 2007). Several techniques have been used to study liposome-cell interactions. Fluorescent markers with or without specific inhibitors are commonly used to investigate the interactions by fluorescence microscopy (Chu et al., 1990; Connor and Huang, 1985; Fretz et al., 2004; Hwang et al., 2007; Khalil et al., 2006; Lee et al., 1992; Manconi et al., 2007).

The interaction of liposomes with cells may be a useful means to enhance the delivery of P-gp substrates into the cells. The release of encapsulated compounds from liposomes after the liposomes have passed through the cell membrane into the cytoplasm compartment may bypass the P-gp function. Many studies have given scientific evidence that encapsulation of P-gp substrates in liposomes can enhance the uptake of P-gp substrates into cells. Most research groups focused on anticancer drugs such as cisplatin (Hwang et al., 2007), daunorubicin (Michieli et al., 1999), doxorubicin (Kobayashi et al., 2007), epirubicin (Lo, 2000), and 9-nitrocamptothecin (Chen et al., 2006). In the liposome delivery systems, drug uptake into cells can be affected by the liposomal composition. Liposomes composed of negatively charged phospholipids can increase the intracellular accumulation of many drugs that are P-gp substrates (Mamot et al., 2003). The liposomal composition may also affect uptake efficiency. In a previous study, neutral liposomes were shown to be better than charged liposomes in the delivery of rhodamine 123 to Caco-2 cells and the presence of charge on liposomal surface reduced the uptake of rhodamine 123 when compared

with the uptake from solution (Lukanawonakul, 2005). In addition, liposomes as well as their components may act as P-gp modulators. Blank liposomes composed of either dipalmitoyl phosphatidylcholine or dipalmitoyl phosphatidylethanolamine enhance the uptake of epirubicin solution into Caco-2 cells (Lo, 2000). Neutral phospholipids such as phosphatidylcholine and phosphatidylethanolamine are also known to be P-gp substrates (Bosh et al., 1997), which can compete with drugs to bind with P-gp (Romsicki and Sherom, 1999). Cholesterol, which is often present as a liposomal component, can bind with P-gp and result in changing in intracellular accumulation of drugs given concomitantly (Wang et al., 2000; Troost et al., 2004). Therefore, liposomes may play a variety of roles in the enhancing of P-gp substrate delivery.

In order to develop liposomal systems for P-gp substrates delivery, various liposomal formulations have been studied. In most studies, the uptake efficiency was evaluated (Massing and Fuxius, 2000; Warren et al., 1992). However, the mechanism of liposomes in the delivery of P-gp substrates is still unclear. The insight into the mechanism by which liposomes interact with cells that can increase the uptake of P-gp substrates may be useful in development of more successful delivery systems. To promote the specific liposome-cell interaction that leads to a more efficient P-gp substrate uptake, the liposomal composition can be tailored. For example, if fusion was the predominant mechanism, effective fusogens might be incorporated into liposomes to increase the efficiency of the process. On the other hand, if endocytosis was the major pathway, liposomes might be designed to promote endocytosis as well as release of the P-gp substrate from the endosomes into the cytoplasm and, consequently, to its site of action in the cell. In addition, the liposomal composition can affect the interaction between liposomes and cells. Thus, the knowledge on the effects of liposomal formulation factors on P-gp substrate delivery is also useful. The formulation factors that may be easily modified include charge-imposing lipids, cholesterol content, and type of the phospholipid.

In this study, the probable mechanisms of liposomes in the delivery of a model P-gp substrate into Caco-2 cells were investigated. The effect of liposomal formulation factors including charged lipids, cholesterol content, and type of phosphatidylcholine, on the delivery of the P-gp substrate was also determined. Caco-2 cells were selected for the target cells. This model culture system has been

widely used to study both P-gp efflux and drug transport (Artursson and Borchardt, 1997; Balimane and Chong, 2005; Gan and Thakker, 1997). The characteristics of this adenocarcinoma cell line are well established. The cells are known to express P-gp when cultured in a suitable condition (Anderle et al., 1998; Sambuy et al., 2005). For P-gp substrates, calcein AM was chosen as a model. Calcein AM has been used in several studies involving P-gp function (Eneroth et al., 2001; Essodaigui, Broxterman, and Garnier-Suillerot, 1998; Utoguchi et al., 2000). This compound is an insoluble, neutral, lipophilic molecule that does not display any fluorescence. When it is taken up into the cells, the non-fluorescent calcein AM is hydrolyzed by cytosolic enzymes and is converted into the fluorescent calcein, which is water-soluble and not a P-gp substrate. This property of calcein AM is useful for spectrofluorometric analysis since there will be no interference from intact molecules outside the cells.

Objectives

The overall objectives of this study were to investigate:

1. The probable mechanisms by which liposomes enhance delivery of P-gp substrates into Caco-2 cells
2. The effect of liposomal composition on delivery of P-gp substrates into Caco-2 cells

CHAPTER II

LITERATURE REVIEW

Transport of drugs across cell membranes

Transport of drug substances across the cell membrane is a complex and dynamic process that includes the passage of compounds across several functional barriers in parallel. Drugs transport occurs mainly in several pathways as depicted in Figure 1:

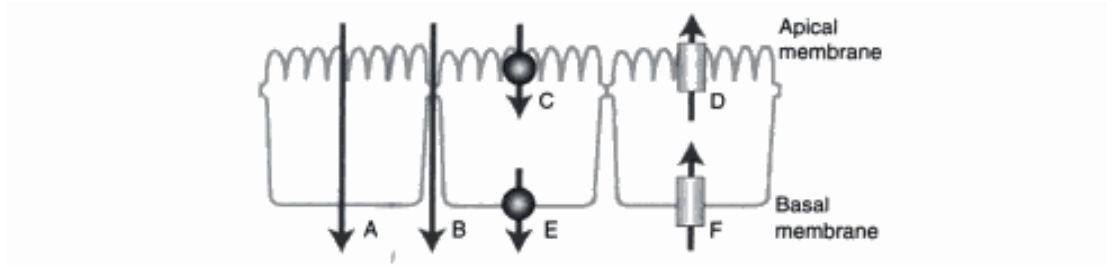


Figure 1: Transport pathways of drug across cell membrane: (A) passive transcellular, (B) passive paracellular, (C) carrier-mediated apical transport, (D) apical efflux transport, (E) basolateral efflux transport, and (F) carrier-mediated basolateral transport (Source: Smith and O'Donnell, 2006)

1. Passive diffusion (Daugherty and Mrsny, 1999; Shargel, Wu-Pong, and Yu, 2005; Ward, Tippin, and Thakker, 2000; Smith and O'Donnell, 2006)

Passive diffusion is the process by which molecules spontaneously diffuse from a region of higher concentration to a region of lower concentration or by an electrochemical gradient. Drug molecules move forward and backward across a membrane. If the two sides have the same drug concentration, forward-moving drug molecules are balanced by molecules moving back, resulting in no net transfer of drug. When one side is higher in drug concentration, at any given time, the number of forward-moving drug molecules will be higher than the number of backward-moving molecules; the net result will be transfer of molecules to the other side. This process requires no external energy.

1.1 Passive paracellular transport

Passive paracellular pathway is an aqueous, extracellular route across the epithelium (Figure 1). The small hydrophilic molecules (MW < 200) that are not recognized by carriers are transported across the epithelial barrier via paracellular pathway. The available surface area for paracellular transport has been estimated to be 0.01% of the total surface area of the epithelial layer. The driving force for this pathway is the electrochemical potential gradient resulting from the differences in concentration, electrical potential, and hydrostatic pressure between the two sides of the epithelial membrane. The paracellular transport pathway is restricted by the tightness of the intercellular junction. The physiology of the tight junctions can be modulated by paracellular permeability enhancers. The paracellular permeability enhancers include Ca^{2+} chelators, bile salts, surfactants, medium-chain fatty acids, fatty acid esters, phosphate esters, and cationic polymers. The change in the function of the tight junction can be monitored by measuring the transepithelial electrical resistance (TEER).

1.2 Passive transcellular transport

Passive transcellular pathway is the process that involves the movement of solute molecules across the apical membrane, through the cell cytoplasm, and across the basolateral membrane (Figure 1). The importance of this route is that it can take place along the majority (99.9%) of the epithelial surface area.

2. Carrier-mediated transport (Shargel et al., 2005)

Carrier-mediated transport systems are presented for the absorption of ions and nutrients for the body. Carrier-mediated transport is a specialized process, requiring a carrier that binds the drug to form a carrier-drug complex that shuttles the drug across the membrane and then dissociates the drug on the other side of the membrane. The carrier may become saturated if the drug concentration is very high. If a drug is absorbed by the carrier-mediated process, the absorption rate increases with the drug concentration until the carrier molecules are completely saturated.

2.1 Active transport

Active transport is a carrier-mediated process that plays an important role in gastrointestinal absorption and in renal and biliary secretion of many drugs and metabolites. Active transport is characterized by the ability to transport the drug against a concentration gradient. This process is an energy-consuming system.

2.2 Facilitated diffusion

Facilitated diffusion is also a carrier-mediated transport system, differing from active transport in that the drug moves along a concentration gradient rather than against the gradient. Therefore, this system does not require energy other than the thermal energy. In terms of drug absorption, facilitated diffusion seems to play a minor role.

3. Vesicular transport (Cooper, 2000; Shargel et al., 2005)

Vesicular transport is the process of engulfing particles or dissolved materials by the cell. It is a major cellular activity, responsible for molecular traffic among a variety of specific membrane-enclosed compartments. Vesicular transport can be classified by size of particles and type of materials. Pinocytosis is a non-specific uptake process by which solute molecules dissolved in the luminal fluid are incorporated by bulk transport into the fluid-phase of endocytotic vesicles. On the other hand, phagocytosis refers to the engulfment of larger particles or macromolecules into cell. A few cell types (e.g., macrophages) can take up whole bacteria and other large particles by this process. Endocytosis and exocytosis are the processes of moving specific macromolecules into and out of a cell, respectively. After macromolecules are taken up into endosomes, maturation of endosomes from early to late endosomes occurs. Subsequently, the late endosomes are sequestered by the lysosomes, where the macromolecules are enzymatically digested. The digested materials and/or the undigested particles exit the basolateral membrane into the microvasculature (Figure 2).

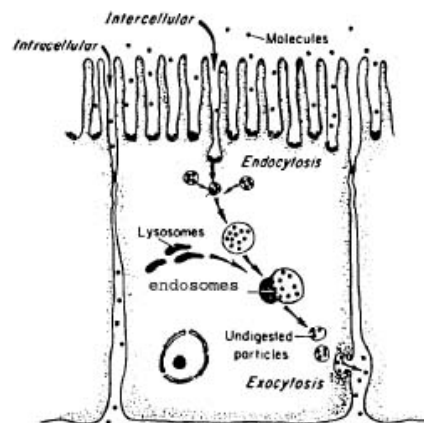


Figure 2: Intracellular transport of vesicles in enterocytes (Source: Ho et al., 1990)

The transport of receptor-associated macromolecules into cytoplasm refers to a receptor-mediated endocytosis. Transferrin and low-density lipoprotein receptors are the one group of receptors that are endocytosed independent of ligand binding and then recycled back to the plasma membrane. The other group of receptors is signaling receptors that are internalized immediately following ligand binding. These latter receptors include the tyrosine kinase receptors for epidermal growth factors, insulin receptors, and the heterotrimeric G-protein-coupled receptors (Jones, Gumbleton, and Duncan, 2003).

Transcytosis is vesicular transport of macromolecules from one side of the cell to the other within a membrane-bounded carrier. It is a strategy used by multicellular organisms to move materials selectively between two different environments without altering the unique compositions of those environments. A variety of cell types use transcytosis as a transport process. The most familiar cell type that expresses transcytosis is the epithelial cells. In these polarized epithelial cells, the net movement of material can be in either direction, apical to basolateral or the reverse, depending on the cargo and particular cellular contents. However, transcytosis is not restricted to only epithelial cells. Osteoclasts and neurons also carry vesicular cargos between two environments by transcytosis. In normal enterocytes, the transcytotic capacity is low, most of the endocytosed material is localized to and degraded in the lysosomes (Tuma and Hubbard, 2003).

4. Efflux transport (Takano et al., 2006)

The efflux transport has the opposite function when compared with the absorption processes described earlier. The efflux transporters play the role in limiting the intracellular accumulation of their substrates. They mediate the extrusion of compounds from the cell cytoplasm to the outside. Two families of efflux transporters are the multidrug resistance (MDR) and multidrug-resistance-associated protein (MRP) families. P-glycoprotein (P-gp or MDR1) is the most extensively studied efflux protein.

P-glycoprotein (P-gp)

Structure of P-gp

P-gp, a member of the ATP-binding cassette family of transport proteins, is a typical transmembrane efflux pump. P-gp consists of 1280 amino acids and has a molecular weight of approximately 170 kDa. It is encoded by the human MDR1 gene. The structure of P-gp is composed of two homologous parts of approximately equal length. Each homologous part contains one hydrophobic integral membrane domain and one hydrophilic nucleotide-binding domain (Figure 3). Two integral membrane domains form the binding sites for drug efflux, while the two nucleotide-binding domains bind and hydrolyze ATP (Fardel et al., 1996; Higgins et al., 1997).

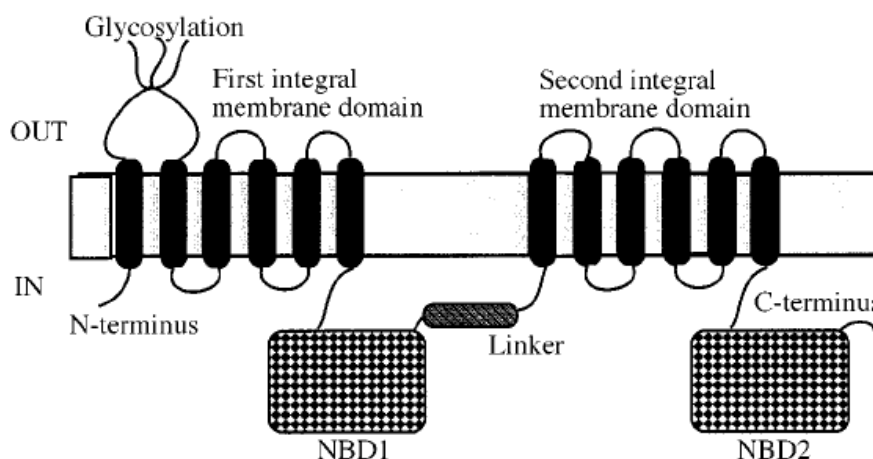


Figure 3: Topological map and domain organization of P-gp (NBD1 and NBD2 = nucleotide-binding domains) (Source: Higgins et al., 1997)

The possible model of the drug-binding domain of P-gp has been proposed to be funnel shape. This binding site has the narrow at the cytoplasmic side. The drug-substrate binding region has a diameter of 9-25 Å and is possible the high affinity site which appears large enough to accommodate two different drugs at the same time. The widest binding region is approximately 50 Å and represents either a low affinity site or the site for the release of the substrate (Figure 4) (Ambudkar, Kim, and Sauna, 2006).



Figure 4: A schematic showing the drug-substrate binding pocket of P-gp. Two drugs are depicted as simultaneously bound in the drug-binding pocket. The drug shown in orange appears to have a greater affinity for P-gp than the one depicted in red.

(Source: modified from Ambudkar et al., 2006)

Location of P-gp (Chan et al., 2004; Fardel et al., 1996; Takano et al., 2006)

The expression of P-gp has been found on the apical membrane of a variety of normal human tissues such as kidneys, liver, colon, small intestine, pancreas, placenta, and uterus. P-gp is also expressed at various blood-tissue barriers, including the blood-brain barrier, blood-testis barrier, blood-placenta barrier, and blood-ocular barrier. The overexpression of P-gp has been found in the primary and treated tumors.

P-gp function

P-gp plays a major physiological role in absorption, distribution, metabolism, and excretion of xenobiotics. The function of P-gp is to prevent the intracellular accumulation of substrates by limiting the influx into cells and facilitating the efflux out of cells. In normal tissues, P-gp has a significant role in the elimination of

xenobiotics, toxins, or some endogenous metabolites. In cancer cells, the result of P-gp function is the multidrug resistance of cancer cells to anticancer drugs and, consequently, the failure in clinical therapy (Krishna and Mayer, 2000; Mamot et al., 2003; Mayer and Shabbits, 2001; Takano et al., 2006; Sauna et al., 2001; Ozben, 2006).

Substrates of P-gp

The substrates of P-gp include many structurally and pharmacologically unrelated hydrophobic compounds (Takano et al., 2006). The common dominator identified in all P-gp substrates is an organic molecule ranging in size from less than 200 Dalton to almost 1900 Dalton (Schinkel and Jonker, 2003). The molecule contains at least two electron donor groups with a spatial separation (Seelig, 1998). Many drugs have been demonstrated to be substrates of P-gp such as anticancer agents, analgesics, HIV protease inhibitors, immunosuppressants, steroid hormones, antibiotics, calcium channel blockers, β -blockers, and cardiac glycosides. Some fluorescent dyes can also act as P-gp substrates (Table 1).

Table 1: Examples of P-gp substrates (Chan et al., 2004; Schinkel and Jonker, 2003)

Class	Representative
Antibiotics	grepafloxacin, sparfloxacin, levofloxacin, erythromycin
Anticancer drugs	
-Vinca alkaloids	vinblastine, vincristine
-Taxanes	paclitaxel, docetaxel
-Anthracyclines	doxorubicin, daunorubicin, epirubicin
-Anthracenes	bisantrone, mitoxantrone
-Epipodophyllotoxins	etoposide, teniposide
Fluorescent dyes	calcein AM, rhodamine 123, fluo 3
HIV protease inhibitors	saquinavir, ritonavir, nelfinavir, indinavir, lopinavir, amprenavir
Immunosuppressants	cyclosporin A, tacrolimus

Mechanisms of P-gp function (Varma et al., 2003; Fardel et al., 1996)

The action of P-gp occurs by the energy from ATP hydrolysis. A single catalytic cycle of P-gp occurs when two ATPs are hydrolyzed on the nucleotide binding domains. One ATP hydrolysis is associated with the efflux of drug and the other is responsible for the conformational change that resets the transporter for the next catalytic cycle (Sauna et al., 2001; Ambudkar et al., 2006).

Various models have been proposed to explain the mechanism of P-gp extrusion of xenobiotics. The P-gp substrate must partition into the lipid membrane before being extruded by P-gp. This is the rate-limiting step for the interaction of a substrate with P-gp (Seelig and Landwojtowicz, 2000). The three prevalent models that have been proposed to explain the efflux mechanism are the pore model, the flippase model, and the hydrophobic vacuum cleaner model (Figure 5). In the pore model, P-gp acts as a transmembrane pore-forming protein. The substrates interact with P-gp in cytosolic compartment and are expelled out of the cell through a protein channel. In the flippase model, the drugs, which are embedded in the inner leaflet of the plasma membrane, bind to P-gp in the membrane. They are then translocated to the outer leaflet of bilayer and diffuse into the extracellular medium (Higgins and Gottesman, 1992; Romsicki and Sharom, 2001). The hydrophobic vacuum cleaner model, which combines the features of the pore and the flippase models, is the most popular model. In this model, P-gp binds directly with the substrates in the plasma membrane and pumps them out of the cell through a protein channel (Gottesman and Pastan, 1993).

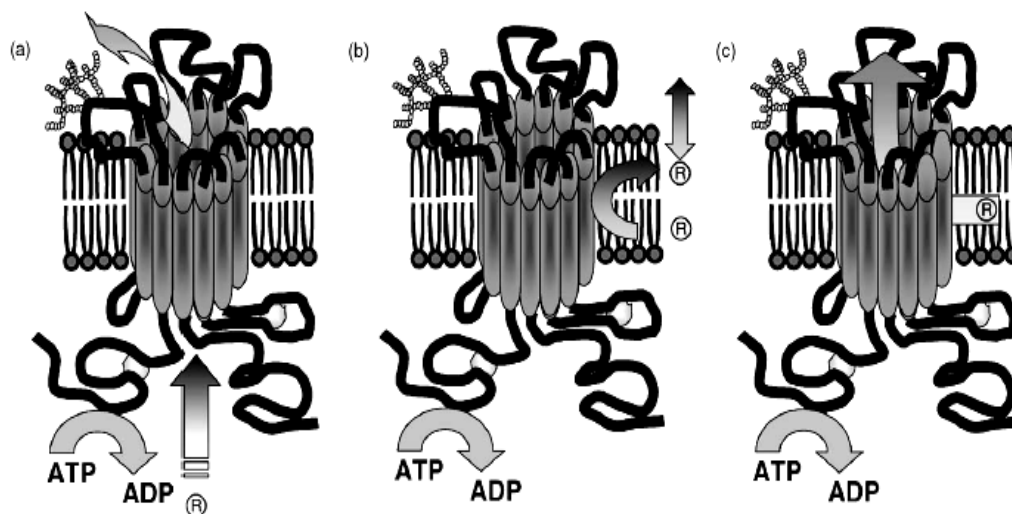


Figure 5: Models proposed to explain the possible mechanisms of drug efflux by P-gp: (a) pore model, (b) flippase model, and (c) hydrophobic vacuum cleaner model (Source: Varma et al., 2003)

P-gp screening methods (Hämmerle et al., 2000)

Several screening methods for P-gp expression and P-gp function have been established. For P-gp expression, specific monoclonal antibodies followed by Western blot analysis can be used. The presence of 170 kDa protein usually refers to the expression of P-gp in the cells. Immunofluorescence labeling study can display the expression as well as the localization of P-gp. P-gp on the plasma membrane is localized by fluorescence immunocytochemistry with specific antibodies. Presence of P-gp is detected by flow cytometric technique or directly observed under a fluorescence microscope (Gheuens et al., 1991).

P-gp functionality is evaluated *in vitro* by the transport study of P-gp substrates in the presence and absence of specific P-gp inhibitors. Substrates that are selective to P-gp are recommended for studying of P-gp function since non-selective substrates can lead to underestimation of P-gp activity (van der Sandt et al., 2000). The apparent permeability values of P-gp substrates with and without P-gp inhibitor are compared to estimate P-gp activity. A variety of P-gp substrates and P-gp inhibitors is recommended by the US FDA for evaluation of P-gp function *in vitro* (Tables 2 and 3). Fluorescent dyes such as rhodamine 123 and calcein AM have been

used as P-gp substrates by several research groups (Eneroth et al., 2001; Loetchutinat et al., 2003; Troutman and Thakker, 2003; Utoguchi et al., 2000). Other therapeutic agents including doxorubicin, epirubicin, and vinblastine are also used for this purpose (Hunter et al., 1993; Lo, 2003). Either cyclosporin A or verapamil is widely used as a specific inhibitor or a potent inhibitor, respectively (Hunter et al., 1993; Sarkadi and Müller, 1997; van der Sandt et al., 2000). Efflux ratio is a parameter often used in the study of P-gp substrates. The efflux ratio is defined as the permeability in the basolateral to apical (B-to-A) direction divided by the permeability in the apical to basolateral (A-to-B) direction. The US FDA recommends that a substance be considered a P-gp substrate when the efflux ratio of that substance across an acceptable cell culture system is over two (US FDA, 2006). A reduction in the efflux ratio to close to unity by a known P-gp inhibitor also indicates a probability of the substance being a P-gp substrate. A cell culture system is considered acceptable for investigation of P-gp functionality when it produces a minimum efflux ratio of the probe P-gp substrates (see Table 2) of two (US FDA, 2006; Faassen et al., 2003).

Table 2: Acceptable in vitro P-gp substrates (Source: US FDA, 2006)

Drug	Conc. Used (μM)	Ratio		
		Caco-2	MDCK- MDR1	LLC-PK1 MDR1
Digoxin	0.01-10	4-14	4	4
Loperamide	1-10	2-5		3.4
Quinidine	0.05	3		5
Vinblastine	0.004-10	2-18	> 9	3
Talinolol	30	26		

Table 3: In vitro P-gp inhibitors (Source: US FDA, 2006)

Inhibitor	IC ₅₀ (μM) Caco-2	Ki (μM)		
		Caco-2	MDCK- MDR1	LLC-PK1 MDR1
Cyclosporin A	1.3	0.5	2.2	1.3
Ketoconazole	1.2			5.3
LY335979	0.024			
Nelfinavir	1.4			
Quinidine	2.2	3.2	8.6	
Ritonavir	3.8			
Saquinavir	6.5			
Tacrolimus	0.74			
Valspodar (PSC833)	0.11			
Verapamil	2.1	8	15	23
Elacridar (GF120918) (GG 918)		0.4	0.4	
Reserpine		1.4	11.5	

Strategies to enhance P-gp substrate delivery

Many research groups have put much effort to inhibit the action of P-gp efflux pump and restore the intracellular concentration of drug compounds. The approaches to overcome multidrug resistance can be classified into two major categories. The first one is the modulation of P-gp function by P-gp modulators. Another approach is the avoidance of P-gp function via the use of drug carriers.

1. Modulation of P-gp function by P-gp modulators (Krishna and Mayer, 2000)

A large number of compounds known as chemosensitizers or P-gp modulators were developed to modulate P-gp function. The common properties of P-gp modulators are to be the substrate of P-gp, to display the hydrophobicity, and to contain phenyl rings in their structures. The presence of a tertiary amine side chain

also plays a major role in the reversing potential of some modulators (Fardel et al., 1996). The modulators can reverse the function of P-gp by several pathways such as interfering with ATP hydrolysis and ATPase activity, blocking P-gp binding sites, inhibiting protein kinase C activity, or altering cell membrane integrity (Varma et al., 2003; Ambudkar et al., 1999). In general, P-gp modulators have been classified into three generations.

1.1 First-generation modulators

First-generation modulators have pharmacological activities and require high doses to use as MDR reversing agent. Verapamil, the first P-gp modulator, shows the ability to enhance the intracellular accumulation of many anticancer drugs. Other calcium channel blockers such as felodipine, isradipine, nifedipine, nifedipine, bepridil, and diltiazem also exhibit this property. In addition, calmodulin antagonists, indole alkaloids, anti-malarial quinine, and anti-arrhythmic quinidine also have the MDR reversing property. The disadvantages of these first-generation modulators are their unacceptable toxicity and side effects.

1.2 Second-generation modulators

Second-generation modulators have been developed to reduce the side effects of the first-generation ones. They are more potent and less toxic. However, these modulators alter the pharmacokinetics of various anticancer drugs. Examples of the second-generation modulators include the structural analogs of verapamil (dexverapamil, emopamil, gallopamil, and R011-2933) and the non-immunosuppressant analog of cyclosporin A (PSC 833).

1.3 Third-generation modulators

Third-generation agents have been developed using structure-activity relationships. They specifically and potently inhibit P-gp efflux with the effective reversing concentration in the nanomolar range. The modulation of P-gp was achieved with low doses of these specific P-gp inhibitors such as cyclopropyldibenzosuberane LY 335979, acridonecarboxamide GF 120918, diketopiperazine XR951, and

diarylimidazole OC144-093. However, some pharmacokinetic interactions have still been observed with LY33579 and OC144-093 despite their low doses.

In order to decrease the adverse effect of P-gp modulators, researchers have employed encapsulation of the modulators in carriers such as liposomes. The encapsulation of the P-gp modulator PSC833 in liposomes considerably enhances the uptake of free epirubicin into Caco-2 cells (Lo et al., 2001).

Besides the above-mentioned chemosensitizers, other substances can also act as P-gp modulators. The lipid excipients and surfactants enlisted in lipid-based formulations are also able to modulate the activity of P-gp. These lipids comprise fatty acids, glycolipids, lipoproteins, phospholipids, and steroids (Lo, 2000; Wasan, 2007). The surfactant Tween[®] 80 and Cremophor[®] EL exert inhibition effect in Caco-2 system at a concentration below their critical micellar concentrations (Wasan, 2007). The mechanism of P-gp modulation by lipid excipients and surfactants has not been fully elucidated.

2. Avoidance of P-gp function via the use of drug carriers

A variety of drug delivery systems has been developed to overcome the multidrug resistance. Many researchers encapsulated P-gp substrates in nanoparticles such as liposomes, solid lipid nanoparticles, and polymer-based nanoparticles for this purpose. P-gp substrate-encapsulating micelles (Dabholkar et al., 2002; Zestre et al., 2006), nanospheres (Fardel et al., 1996), and polymer-lipid hybrid nanoparticles (Wong et al., 2006) are successful in delivery of the P-gp substrates to cancer cells. The most studied delivery systems to overcome multidrug resistance are liposomes. Most research groups working with liposomes focused on anticancer drugs such as cisplatin (Hwang et al., 2007), daunorubicin (Michieli et al., 1999), epirubicin (Lo, 2000), and 9-nitrocamptothecin (Chen et al., 2006). These liposomal systems result in the high intracellular accumulation of the drugs or the enhancement of their pharmacological effects such as the cytotoxicity of anticancer agents. In order to increase drug delivery efficacy, surface-modified liposomes has been also developed. These systems were designed to target the multi-drug resistant cells and/or to be long circulating. Successful surface-modified liposomal systems include transferrin receptor-targeted liposomal doxorubicin (Kobayashi et al., 2007) and pegylated

liposomal doxorubicin (Mamot et al., 2003). In contrast, the failure to reduce cancer cell resistance to anticancer drugs has been reported with some liposomal systems as well (Iffert et al., 2000). It has been proposed that drug-containing liposomes enter cells via endocytosis, thus bypassing the P-gp function on the cell membrane (Lo, 2000). Success of liposomal systems may depend largely on the liposomal composition as well as the cell type.

Encapsulation of P-gp substrates in liposomes may not always be necessary in order to enhance their delivery into the cell. Co-administration of blank liposomes with P-gp substrates may also enhance cellular uptake of the substrates. Blank dipalmitoyl phosphatidylcholine (DPPC) and dipalmitoyl phosphatidylethanolamine (DPPE) liposomes increase uptake of epirubicin from epirubicin solution into Caco-2 cells (Lo, 2000). Moreover, neutral phospholipids commonly used in liposomal membrane such as phosphatidylcholine (PC) and phosphatidylethanolamine (PE) and cholesterol have been reported to be P-gp substrates that can compete with drug for P-gp binding (Bosch et al., 1997; Romsicki and Sharom, 1999). This may result in moderation of P-gp function and an increase in uptake of P-gp substrates administered concomitantly.

Liposomes as drug carriers

Liposomes are vesicles in which an aqueous volume is entirely enclosed by a membrane composed of amphiphilic lipid molecules (usually phospholipids). They form spontaneously when these lipids are dispersed in aqueous solution. They can entrap both hydrophilic and lipophilic substances in the aqueous compartment and in the lipid bilayer, respectively. Liposomes have been used as drug delivery systems for many drugs. When liposomes are taken up into biological systems, they can interact with cells in many ways.

Interactions of liposomes with cells (New, 1997; Torchilin and Weissig, 2003)

Several interactions between liposomes and cells may occur and are subsequent with the delivery of the encapsulated compounds into the cells (Figure 6). The first interaction is adsorption. Liposomes can adsorb to the cell membrane with specific attractive forces or bind with specific receptors via ligands on the liposomal

membrane. The result of this process may occur in two ways. The adsorption may take place without or with only little internalization of the aqueous and/or the lipid components of liposomes. Alternatively, the adsorption may lead to other interactions between liposomes and cells such as contact release or fusion where significant uptake of liposomal contents is possible.

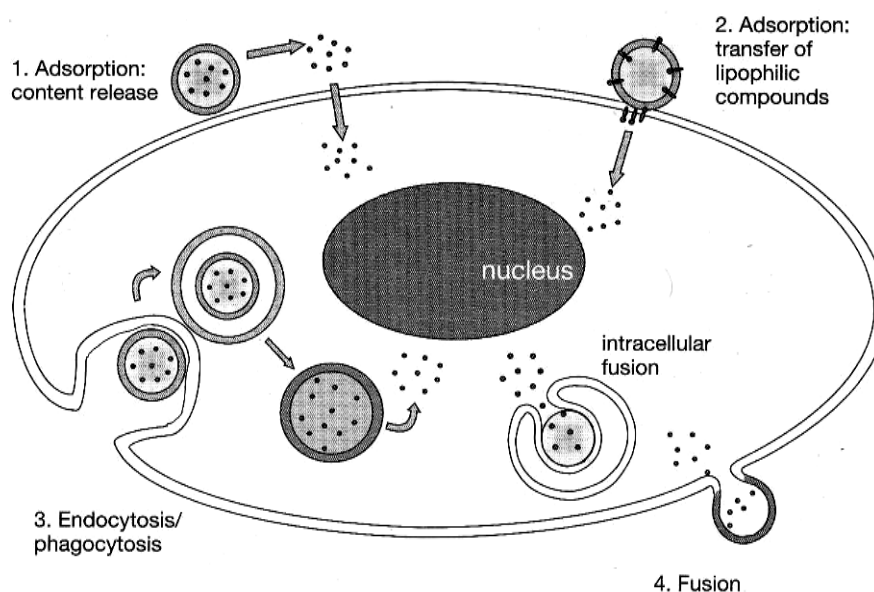


Figure 6: Possible ways by which liposomes can interact with cells and deliver their contents: 1. Adsorption of a liposome followed by release of the liposomal contents, 2. Adsorption of a liposome followed by transfer of lipophilic compounds from the liposomal bilayer to the plasma membrane, 3. Endocytosis/phagocytosis of a liposome followed by intracellular degradation of the liposome via endolysosomal pathway, and 4. Fusion of liposomal membrane with plasma membrane followed by release of liposomal contents into the cytoplasm (Source: Torchilin and Weissig, 2003)

Contact release can lead to significant uptake of liposomal contents without the liposomes being internalized. The encapsulated aqueous contents can be released in high concentration in the close vicinity of the cell membrane. These solutes may then traverse across the cell membrane due to the concentration gradient. The composition of the liposomal membrane and the physicochemical structure of the encapsulated compound are important in this process. Cell-induced leakage of solutes

from liposomes has been observed to be greater in liposomal membranes with cholesterol concentrations above 30 mole%.

Fusion may take place after the initial adsorption of liposomes to cell membrane. This process results in complete mixing of the liposomal lipid with those of the plasma membrane of the cell and the release of liposomal contents into the cytoplasm. Fusion requires specific fusion-inducing agents or fusogens. A variety of fusogens (lysolecithin, phosphatidylserine, detergents, surfactants, and analogous of virus) has been incorporated into the liposomal membrane to introduce liposome-cell fusion (Papahadjopoulos et al., 1973; Mishra et al., 2006).

Intermembrane transfer of lipid components can take place upon close approach of the phospholipid bilayer without disruption of the liposome. Lipophilic compounds may be transferred from the liposomal membrane to the cell membrane. The two membranes must come into close contact during the process of transfer.

Finally, liposomes may interact with cells and lead to endocytosis or phagocytosis of the vesicles. After binding of liposomes to cell surface, liposomes are endocytosed by invagination of the cell membrane into endosomes, which have a pH of 5 to 5.5. The endosomes then fuse with lysosomes to digest the endosomal content. The cellular digestion occurs at approximately pH 4.5. The liposomal structure is disrupted and the liposomal phospholipids are hydrolyzed to fatty acids, which can be recycled and reincorporated into host phospholipids. During liposome breakdown in the lysosomes, the aqueous contents are released. The contents will remain sequestered in the lysosomes until exocytosis occurs, particularly if they are highly charged at low pH, or they will slowly leak out of the lysosomes into the cell cytoplasm. In endocytosis, internalization of liposomes may also take place by a receptor-mediated process. Liposomes coated with low-density lipoproteins or transferrin will bind to the cell via surface receptors and will be internalized via coated pits.

Factors influencing the uptake of liposomes into cells

Several factors affecting the liposome-cell interaction that leads to the uptake of liposomes by cells have been reported. These factors include liposomal

composition, bilayer fluidity of liposomal membrane, liposome size, and cell type. The summarization is as follows.

1. Liposomal composition

The composition of lipid bilayers is an important component influencing the liposome-cell interaction. The effects of phospholipid type, specific surface protein, and liposomal surface charge on cellular uptake have been investigated. The neutral PC vesicles are incorporated into cells primarily by endocytosis, whereas negatively charged liposomes composed of phosphatidylserine (PS) and PC are taken up by a non-endocytotic pathway or fusion (Papahadjopoulos et al., 1973; Poste and Papahadjopoulos, 1976). Moreover, PC-based liposomes with PS, phosphatidylglycerol (PG), or phosphatidic acid (PA) are endocytosed into CV1 cells (Lee et al., 1992). 1,2-dioleoyl-*sn*-glycero- β -phosphatidylcholine (DOPC)-based liposomes containing either negatively or positively charged lipid are taken up into J774 cells better than the uncharged DOPC liposomes (Miller et al., 1998). The extent of positively charged liposomes composed of DOPC and 1,2-dioleoyl-3-dimethylammoniumpropanediol (DODAP) endocytosed into HeLa cells is higher than those of either neutral (DOPC) or negatively charged liposomes (DOPC:1,2-dioleoyl-*sn*-glycero-3-phosphatidylserine) (Miller et al., 1998).

2. Bilayer fluidity

The physical state of liposomes is of considerable importance in determining the pathway by which lipid vesicles are incorporated into the cultured cells. Solid charged vesicles (PS:DPPC:DSPC) and fluid neutral vesicles (PC) are incorporated into 3T3 cells almost exclusively by endocytosis. In contrast, the major incorporation pathway for fluid charged vesicles (PS/PC) is via a non-endocytotic mechanism, which involves fusion of the lipid vesicles with the plasma membrane (Poste and Papahadjopoulos, 1976). Moreover, the increasing bilayer rigidity by adding cholesterol, sphingomyelin, or monosialoganglioside to PC liposomes results in substantial reduction in the cellular uptake via endocytosis by bone marrow macrophages (Allen et al., 1991). In egg PC (EPC) and hydrogenated egg PC (HEPC)-based liposomes, the tumor accumulation of HEPC liposomes is markedly

greater than that of EPC liposomes. These accumulations correspond to their membrane fluidity, the membrane fluidity of HEPC liposomes being less than that of EPC liposomes (Uchiyama et al., 1995).

3. Size

Size of liposomes also affects the uptake of liposomes. The size of liposomes less than 200 nm shows higher accumulation of liposomes in tumors, and the maximal accumulation occurs at the diameter of around 100 nm (Uchiyama et al., 1995). Furthermore, the uptake of PC liposomes by bone marrow macrophages is increasing when liposomes are extruded through the decreasing pore-size filters (Allen et al., 1991).

4. Cell type

The uptake of liposomes also depends largely on the cell type as well as on the liposomal composition. The uptake of PC liposomes containing negatively charged lipids (PS, PG, PA) into CV1 cells, an African green monkey kidney cell line, is the same as that of the neutral PC liposomes (Lee et al., 1992). In contrast, under the same culture condition, J774 cells take up only PS liposomes (Lee et al., 1992). Additionally, J774 cells endocytose both positively charged and negatively charged liposomes better than neutral liposomes, while HeLa cells endocytose a greater extent of positively charged liposomes (Miller et al., 1998).

The effect of cell type on liposome uptake seems to be confounded by other factors. The uptake of liposomes via non-endocytotic pathways into two cancer cells (PC-3, a human prostate cancer cell line, and A-375, a malignant melanoma cell line) and two non-cancer cell lines (RACEC, a rat aortic endothelium cell, and HUVEC, a human umbilical vein endothelium cell) is similar (Kheiriloom and Ferrara, 2007). On the contrary, the mouse bone marrow macrophages from different mouse strains show some differences in the ability to take up liposomes (Allen et al., 1991).

Thus, the liposomal composition, which also governs the bilayer fluidity, and the cell type seem to play an interdigitating role in liposome-cell interaction.

Techniques used in investigation of liposome-cell interactions

In order to study liposome-cell interactions, several techniques are used to investigate the probable mechanisms. Most researchers use markers (fluorescent probes and radiolabeled probes) to discriminate the mechanisms. Some researchers use specific inhibitors to corroborate the possible mechanisms.

1. Use of fluorescent and radiolabeled markers

Fluorescent markers are widely used both as the aqueous-phase markers and as the lipid-phase markers. The aqueous-phase markers include calcein (Connor and Huang, 1985; Chu et al., 1990), sulforhodamine B (Khalil et al., 2006), carboxyfluorescein (Manconi et al., 2007), and HIPS pyranine (1-hydroxypyrene-3,6,8-trisulfonate) (Lee et al., 1992). Fluorescent phospholipids such as rhodamine-PE (Fretz et al., 2004; Lee et al., 1992; Manconi et al., 2007) and NBD-PE (Khalil et al., 2006) are often used as the lipid-phase markers. These probes are incorporated into liposomes during the liposome preparation process. After incubation of the liposomes with cells, the liposome-cell interactions are elucidated under a fluorescence microscope. The intracellular delivery pathway can be monitored by the use of confocal laser scanning microscope, which can monitor the samples in three dimensions.

The fluorescence patterns can be used to distinguish the different interactions. In adsorption, the attachment or binding of the fluorescent marker is evident around the cell membrane (Fretz et al., 2004; Manconi et al., 2007). Fusion and endocytosis display intracellular fluorescence in different patterns. Fusion of liposomes with cell membrane shows the diffuse fluorescence of the aqueous-phase marker throughout the cytoplasm with the fluorescence of the lipid-phase marker on the cell membrane (Halovati, Gyongyossy-Issa, and Acker, 2008). In contrast to fusion, endocytosis results in the entrapped fluorescent dye being located in the endosomes or the lysosomes. Cells will show punctate fluorescence (Chu et al., 1990; Connor and Huang, 1985). Furthermore, if liposomes are double-labeled with both the aqueous-phase and the lipid-phase markers with different fluorescence colors, the result will show co-localization of the two fluorescent markers. This phenomenon strongly indicates the presence of liposomes in the cells (Fretz et al., 2004; Lee et al., 1992;

Manconi et al., 2007). However, the diffuse fluorescence of the aqueous-phase marker in the cytoplasm is also seen with pH-sensitive liposomes though these liposomes are taken up by endocytosis (Chu et al., 1990; Connor and Huang, 1985). This special type of liposomes becomes highly fusion-active at an acid pH of the endosomes and/or the lysosomes. Thus, fusion between the liposomal membrane and the endosomal/lysosomal membrane occurs, leading to delivery of the aqueous-phase marker to the cytoplasm.

Self-quenching is another property of fluorescent markers that can be used to discriminate between fusion and endocytosis (New, 1997). Fluorescent dyes such as calcein or carboxyfluorescein display very little fluorescence intensity at self-quenching concentrations (at approximately 60 mM or higher). In fusion, these dyes will show the strong fluorescence after being diluted many hundred fold in the cytoplasm. In endocytosis, the dyes are concentrated in endosomes and display little fluorescence when measured by flow cytometry. However, if these cells are digested with a detergent such as Triton[®] X-100, dilution of the fluorescent dye will take place. Consequently, the increase in fluorescence intensity of the cell lysate will be evident.

To distinguish between lipid exchange and association of liposomes with cells, radiolabeled lipids are used. To monitor the uptake of liposomes by cells, the lipid marker should not exchange spontaneously and should be non-metabolizable (New, 1997). The most satisfactory group of markers for this purpose is cholesteryl alkyl ethers (Pool et al., 1982).

2. Use of specific inhibitors

Specific inhibitors of different possible mechanisms can be used to distinguish between various mechanisms of liposome-cell interactions. The biochemical effects of these inhibitors usually result in reduction or absolute inhibition of the targeted liposome-cell interaction. This technique has been used mostly to verify endocytosis of liposomes by cells. Endocytosis is an energy-dependent process. Since endocytosis involves several metabolic steps, various inhibitors, as well as combinations of inhibitors, are often used (Poste and Papahadjopoulos, 1976). The metabolic inhibitor sodium azide is widely used to inhibit cell respiration. Various concentrations (5-60 mM) of sodium azide have been used with different cell types (Khalil et al, 2006;

Palm et al., 2007; Poste and Papahadjopoulos, 1976). Sodium azide at a concentration of 10 mM under glucose-free conditions yields 90% ATP depletion in MDR1- and MRP-transfected leukemic cell lines (Essodaïgui et al., 1998). The other metabolic inhibitors that inhibit glycolysis such as deoxyglucose, sodium fluoride, and iodoacetate are often used in a combination with sodium azide (Poste and Papahadjopoulos, 1976).

The combination of respiration and glycolysis inhibitors is usually more effective in endocytosis inhibition. For example, sodium azide at 5 mM can inhibit the uptake of PC liposomes by 15% in BALB/c mouse 3T3 cells, whereas 90% inhibition can be seen when a combination of sodium azide with deoxyglucose, sodium fluoride, or iodoacetate is used (Poste and Papahadjopoulos, 1976). The uptake of octaarginine-modified liposomes into NIH 3T3 cells is also strongly inhibited by combinations of metabolic inhibitors (Khalil et al., 2006).

Cytochalasin B or cytochalasin D, which causes actin depolymerization, is also used to inhibit endocytosis. Different studies using cytochalasin B as an endocytosis inhibitor showed different degrees of inhibition, depending on concentration of the inhibitor and cell type. For example, the inhibition of uptake of polymer-lipid hybrid nanoparticles containing doxorubicin with cytochalasin B (5 µg/ml) was 20-30% in one study (Wong et al., 2006). The inhibition of peptide uptake into Chinese hamster ovarian cells in another study was rather similar (Palm et al., 2007). On the contrary, cytochalasin B (20 µg/ml) caused 80-90% inhibition of liposome uptake in 3T3 cells (Poste and Papahadjopoulos, 1976). The uptake of different liposomal formulations of Amphotericin B into J774 cells was inhibited by cytochalasin B (6 µM) at different degrees between 11-75% (Legrand, Vertut-Dou, and Bolard, 1996).

Furthermore, the incubating temperature can affect the interaction of liposomes with cells. The uptake of liposomes is significantly faster at 37 °C than at 4 °C in a murine macrophage-like cell line, J774 (Lee et al., 1992). At 4 °C, the cellular uptake is a measurement of binding without any energy-dependent process, while the uptake at 37 °C is a measurement of the total association. Thus, this

phenomenon can be used as a supplementary technique to verify the endocytosis mechanism.

Caco-2 as a cell culture model (Artursson and Borchardt, 1997; Balimane and Chong, 2005; Ferrec et al., 2001; Gan and Thakker, 1997; Sambuy et al., 2005; Xia et al., 2005)

Caco-2 is an epithelial human colon adenocarcinoma cell line. Caco-2 cells have been extensively used as a culture model to predict absorption of drug molecules. In culture process, Caco-2 cells undergo spontaneous enterocytic differentiation at 14-21 days after seeding. The cell monolayer grown on porous polycarbonate membranes exhibits several characteristics of differentiated epithelial cells similar to those of the small intestine. The most important characteristics are brush border on the apical surface, tight junctions between adjacent cells, and transporters. Several active transport systems are expressed in Caco-2 cells, including those for sugars, amino acids, dipeptides, bile acids, vitamins, and hormones. Several enzymes (e.g. aminopeptidase, alkaline phosphatase, sucrase, dipeptidyl aminopeptidase, and γ -glutamyl transpeptidase) are also found in the brush border membrane. The existence of a phase I metabolizing enzyme (CYP1A1) and phase II metabolizing enzymes (glutathione s-transferase, glucuronidase, and sulfotransferase) in this cell line has been reported. However, CYP3A, which is present in almost all intestinal cells, is very weakly expressed in Caco-2 cells. In addition, Caco-2 cells display expression of energy-dependent drug efflux pumps such as P-gp, MRP, breast-cancer resistance protein (BCRP), and lung cancer-associated resistance protein. Thus, Caco-2 cells seem to be suitable in drug absorption studies with well-defined physicochemical barrier properties. Caco-2 cells have been used to study various drug delivery systems, examples of which are displayed in Table 4.

Table 4: Examples of studies on drug delivery systems using Caco-2 cells as a model

Dosage form	Drug/marker	Reference
Biodegradable nanoparticles	rhodamine B	Cartiera et al., 2009
Block copolymer micelles	celiprolol	Huang et al., 2008
Dendrimers	doxorubicin	Ke et al., 2008
Liposomes	epirubicin	Lo, 2000
	insulin	Degim et al., 2004
Microemulsions	diclofenac	Spornath et al., 2007
Micelles	carotenoid	Sugawara et al., 2001
Poly (amidoamine) dendrimers	¹⁴ C-paclitaxel	El-Sayed et al., 2003
Poly (lactide-co-glycolide) polymer microspheres	famotidine	Degim et al., 2004

Factors influencing the characteristics of Caco-2 cells (Balimane and Chong, 2005; Sambuy et al., 2005)

Cell and culture-related factors are shown to influence the morphological and functional characteristics of Caco-2 differentiation. It is extremely difficult to compare results from different laboratories when Caco-2 cells are used as a culture model. Small differences in culturing conditions (seeding density, culturing time, cell feeding routine, and medium composition) and age of the cells (passage number) are factors that are known to produce dramatic inconsistencies in permeability values among different laboratories.

For cell-related factors, the passage number of cells influences the different functions and activity of Caco-2 cells. TEER increases in the later passages of the cell monolayer. The proliferation rate also increases in late passage cells.

In culturing condition, seeding density can affect the differentiation process since the process starts when cells reach confluence. Cell differentiation and expression of transporters depend on the culturing time. Caco-2 cell differentiation appears to follow a strict time schedule in the expression of pharmacological and biochemical characteristics of the absorptive enterocytes. The medium composition can modulate some functions of cells such as proliferation, differentiation, permeability, and morphology.

Both cell and culture-related factors have been reported to affect the expression of P-gp. When cells are trypsinized after confluence, P-gp expression decreases in the higher passages when compared with the starting passage. In contrast, the significant increase in P-gp level is observed when the cells are trypsinized before confluence. The P-gp functionality is also increased with culturing time (Anderle et al., 1998).

Liposomes and the delivery of P-gp substrates

Success in the in vitro delivery of P-gp substrates by liposomes has been reported by many research groups. Anticancer agents such as cisplatin (Hwang et al., 2007), daunorubicin (Michieli et al., 1999), doxorubicin (Kobayashi et al., 2007), epirubicin (Lo, 2000), and 9-nitrocamptothecin (Chen et al., 2006) are the most studied. The results of these studies are very promising. Some of liposomal formulations of anticancers are available commercially with improved clinical outcome (Massing and Fuxius, 2000). These products include liposomal doxorubicin and liposomal daunorubicin. However, the mechanism of liposomes in the delivery of these P-gp substrates is still unclear. One research group suggested that liposomes might act as P-gp modulator and interact with P-gp at the drug-binding site leading to the higher drug uptake (Lo, 2000). The researcher has assumed that liposomes were taken up into cells via endocytosis.

CHAPTER III

MATERIALS AND METHODS

Materials

1. Alexa Fluor[®] 488-conjugated dextran (Molecular Probes[®], USA, Cat. no. D22910)
2. Calcein (Sigma, USA, Lot no.118H0907)
3. Calcein acetoxymethyl ester (Fluka, Switzerland, Lot no. 1314931)
4. Calcium chloride (Univar, Australia, Lot no. AF407272)
5. Chloroform AR grade, (Labscan, Ireland, Lot no. 07091095)
6. Cholesterol (Sigma, USA, Lot no. 072K5313)
7. Cytochalasin B (Sigma, USA, Lot no. 076K4052)
8. Deoxyglucose (Sigma, USA, Lot no. 117K5009)
9. D-Glucose monohydrate (Univar, Australia, Lot no. AF606215)
10. Dicetylphosphate (Sigma, USA, Lot no. 10K1593)
11. Dimethyl sulphoxide (DMSO) (Sigma, USA, Lot no. 076K2321)
12. Dipalmitoyl phosphatidylcholine (Lipoid GmbH, Germany, Lot no. 563071-1/902)
13. Dulbecco's Modified Eagle's Medium (GibcoBRL, USA, Cat. no. 12800-017, Lot no. 304670, 460387)
14. EDTA ([Ethylenedinitrilo]tetraacetic acid) (Sigma, USA, Lot no. 85H00085)
15. Fetal bovine serum (Biochrom AG, USA, Lot no. 1055FF, 0087L, and 0739L)
16. Hank's balanced salt solution (Sigma, USA, Lot no. 103K83021)
17. HEPES (N-[2-Hydroxyethyl]piperazine-N'-[2-ethanesulfonic acid]) (Sigma, USA, Lot no. 21K5448)
18. L-Glutamine (GibcoBRL, USA, Lot no. 1384126)
19. Magnesium chloride (Univar, Australia, Lot no. 802452)
20. MEM non-essential amino acid (Sigma, USA, Lot no. 44K2415, 058K2362)

21. MES (2-[N-Morpholino]ethanesulfonic acid) (Sigma, USA, Lot no. 47H5704)
22. Methanol, AR grade (Merck, Germany, Lot no. K36943309)
23. MTT (Thiazolyl Blue Tetrazolium Bromide) (Sigma, USA, Lot no. 094K5312)
24. Penicillin-Streptomycin (GibcoBRL, USA, Lot no. 1354059 and 1386472)
25. Potassium chloride (Merck, Germany, Lot no. TA419536)
26. Potassium dihydrogen phosphate (Merck, Germany, Lot no. K23775573707)
27. Potassium hydroxide (Merck, Germany, Lot no. B742533049)
28. Rhodamine 123 (Sigma, USA, Lot no. 014K3689 and 017K3696)
29. Sephadex G-50 (Sigma, USA, Lot no. 115H0876)
30. Sodium azide (Fisher Scientific, UK, Lot no. 0442395)
31. Sodium bicarbonate (Carlo Erba, Italy, Lot no. Z2G569173M)
32. Sodium chloride (Merck, Germany, Lot no. K32232604)
33. Sodium hydroxide (Merck, Germany, Lot no. B0119798)
34. Soybean phosphatidylcholine (Phospholipon[®]90 Nattermann Phospholipid GmbH, Cologne, Germany, Lot no. 770991)
35. Stearylamine (Fluka, Switzerland, Lot no. 1292539)
36. Triton[®] X-100 (Sigma, USA, Lot no. 40F1535)
37. Trypan blue (Sigma, USA, Lot no. 87F50385)
38. Trypsin (Sigma, USA, Lot no. 064K7696, 016K7680)
39. α -Tocopherol (Approx. 95%, Sigma, USA, Lot no. 063K0796)
40. \pm Verapamil hydrochloride (Sigma, USA, Lot no. 062K0325)

Equipment

1. Analytical balances (AX 105 and PG403-S, Mettler Toledo, Switzerland)
2. Autoclave (Hirayama, Japan)
3. Confocal laser scanning microscope (FluoView[™] FV1000, Olympus, Japan)
4. Counting chamber (BOECO, Germany)
5. Flex-column (Kontes, USA)

6. Flow cytometer (FACS Calibur, Becton Dickinson, USA)
7. Fluorescence microplate reader (VICTOR3, Perkin Elmer, USA)
8. Fluorescence microscope (BX-FLA, Olympus, Japan)
9. Hand-held extruder (LiposoFastTM, AVESTIN, Canada)
10. Hot air oven (MEMMERT, Germany)
11. Humidified carbon dioxide incubator (Forma Scientific, USA)
12. Laminar air flow hood (BV2225, ISSCO, Thailand)
13. Light microscope (CKX41, Olympus, Japan; Axiovert 135, ZEISS, Germany)
14. Microplate reader (Anthos htl, Austria)
15. Milicell[®]-ERS potentiometer (Millipore, USA)
16. Multiwell plates (Corning, USA)
17. pH meter (Orion, USA)
18. Polycarbonate membranes (100 nm) (Millipore, USA)
19. Refrigerated centrifuge (Z383K, Hermle, Germany)
20. Rotary evaporator (R 215, Buchi, Switzerland)
21. Shaking waterbath (Memmert, Germany)
22. Sonication (Elma, Germany)
23. Sterilization filtration membranes (cellulose acetate membrane, 0.22 μm) (Corning, USA and Roseville, Michigan)
24. Transmission electron microscope (TEM Model JEM-1230, Jeol, Japan)
25. Transwell[®] insert (Corning, USA)
26. Tissue culture flasks (Corning, USA)
27. UV spectrophotometer (Model 7800, Jasco Corporation, Japan)
28. Vortex mixer (G-560E, Scientific Industries, USA)
29. Zetasizer (Zetasizer Nano series, Nano-zs, Malvern, UK)

Methods

1. Preparation of liposomes

1.1 Preparation of calcein AM-loaded liposomes

Calcein AM-loaded liposomes were prepared by the film-hydration method (New, 1997). The liposomal preparation contained soybean phosphatidylcholine (soybean PC) and cholesterol (CH) with a total lipid concentration of 35 mg/ml. The antioxidant used in the preparation was alpha-tocopherol at 0.1 mole%. The lipid phase comprised calcein AM at 2.5 μ M of liposome suspension with soybean PC and CH at a molar ratio of 7:3 for neutral liposomes. Charged liposomes contained soybean PC, CH, and either stearylamine (SA) or dicetylphosphate (DCP) at a molar ratio of 6:3:1 for positively and negatively charged liposomes, respectively. Briefly, all lipids were dissolved in chloroform and the solution was transferred to a round-bottomed flask. The organic solvent was evaporated to form a thin lipid film using a rotary evaporator. The lipid film was kept under vacuum for another 1 hour to remove all traces of the organic solvent. The thin film was hydrated with 10 mM HEPES buffer (pH 7.4) as the aqueous phase. The hydration time was at least 2.5 hours to allow liposomal vesicles to form completely. A routine check of liposomal suspension quality was carried out by inspection of the preparation under a light microscope at 400x magnification. The liposomal suspension was extruded through two-stacked 100 nm polycarbonate membranes with a hand-held extruder (LiposoFastTM, AVESTIN, Canada) for 19 cycles to reduce the liposomal size. The liposomal suspension was kept in a refrigerator at 4 °C until use.

Calcein AM-loaded liposomes with different soybean PC and CH ratios were similarly prepared. The molar ratios of soybean PC and CH were 6:4, 7:3, 8:2 and 10:0.

For the experiments to investigate the effect of phosphatidylcholine type, dipalmitoylphosphatidylcholine (DPPC) was used instead of soybean PC to prepared calcein AM-loaded DPPC liposomes. The molar ratios of DPPC and CH were 7:3 and 10:0.

1.2 Preparation of calcein-loaded liposomes

Calcein-loaded liposomes were prepared by the film-hydration method as described under Section 1.1. The liposomal preparation comprised soybean PC and CH at a molar ratio of 7:3 with a total lipid concentration of 50 mg/ml. The lipid film was hydrated with calcein solutions (20 mM or 80 mM calcein in 0.3 N NaOH, pH = 7.4-7.8). The resultant liposomal suspension was examined under an optical microscope and then extruded to reduce the liposomal size as described under Section 1.1.

Non-encapsulated calcein was removed by the gel filtration method. The liposomal suspension (400 μ l) was loaded onto a 1 x 21 cm gel bed column of Sephadex G-50 and eluted with PBS, pH 7.4. An aliquot (75 μ l) of calcein-loaded liposomes eluted from the column was dissolved in 1% Triton[®] X-100 to make 5.0 ml. The solution was further diluted to the desired concentration with phosphate buffered saline (PBS). The amount of calcein encapsulated in liposomes was determined by spectrofluorometric method using a microplate reader (VICTOR3, Perkin Elmer, USA) with the excitation wavelength of 485 nm and the emission wavelength of 535 nm. The amount of phospholipid in the preparation was determined by the standard Bartlett assay (New, 1997). The liposomal suspension was kept in a refrigerator until use. The calcein-loaded liposomal suspension that was devoid of non-encapsulated calcein was used within the same day of separation to avoid liposome leakage and bleaching of the fluorescent marker.

1.3 Preparation of liposomes labeled with 1,2 –Dioeoyl-sn-Glycero-3-Phosphoethanolamine-N-(7-nitro-2-1,3-benzoxadiazol-4-yl) (NBD-PE)

To investigate the mechanism of uptake of liposomes into Caco-2 cells, NBD-PE was used as a lipid marker to trace the existence of/to locate liposomes in the cells.

1.3.1 Liposomes labeled with NBD-PE

Blank liposomes tagged with NBD-PE were prepared using the same conditions and method as those described under Section 1.1. NBD-PE was dissolved

in chloroform and added to the lipid phase at 0.1 mole%. The total lipid concentration was 35 mg/ml.

1.3.2 Liposomes double-labeled with NBD-PE and rhodamine 123

Liposomes double-labeled with the fluorescent NBD-PE as a lipid marker and rhodamine 123 as a dual lipid/aqueous phase marker were also prepared using the film-hydration method as described under Section 1.1. NBD-PE was dissolved in chloroform and added to the preparation at 0.1 mole%. Rhodamine 123 was used at 0.1 mg/ml of liposome suspension. Rhodamine 123 was dissolved in chloroform:methanol (4:1). Both fluorescent markers were added in the lipid phase. The total lipid concentration was 7 mg/ml.

2. Characterization of the physical properties of liposomes

The surface charge and particle size of liposomes were measured by dynamic laser light scattering (Zetasizer Nano series, Nano-zs, Malvern, UK). The liposome suspension was diluted with 10 mM HEPES buffer pH 7.4 to an appropriate concentration. The experiment was done in triplicate with three batches of liposomes. The measurement was repeated 3 times for each batch.

3. Maintenance of Caco-2 cells

Caco-2 cells were cultured at 37 °C in a humidified CO₂ incubator. Cells were grown in standard Dulbecco's Modified Eagle's Medium (DMEM) supplemented with 4 mM L-glutamine, 4.5 g/ml glucose, 1.5 g/ml sodium bicarbonate, 110 mg/ml sodium pyruvate, 100 µg/ml penicillin, 100 µg/ml streptomycin, 1% MEM non-essential amino acid, and 10% fetal bovine serum. Caco-2 cells were subcultured at 70-80% confluence. Briefly, the cell monolayer was washed with 5 ml of PBS and detached by incubating with 0.25% trypsin in 1 mM EDTA solution (1.2 ml/75 cm²) for 2-3 minutes at room temperature. Trypsin solution was then removed and 10 ml of the culture medium was added to stop the action of trypsin and to disperse the cells. The dispersed cells were counted and seeded into new 75-cm² culture flasks with a cell density of 5-6 x 10⁵ cells per 15 ml in each flask.

For the experiments, cells were grown and trypsinized as described above and the cell suspension was seeded into culture plates at a concentration of 5×10^4 cells/ml (0.5 ml and 1 ml per well in 12-well and 24-well culture plates, respectively). The cell monolayer was allowed to grow for 21 days with the medium changed every 48 hours.

4. Characterization of Caco-2 monolayers

In order to use Caco-2 monolayers as a cell culture model to study drug uptake and transport, the monolayers should be validated in terms of functionality of the cells according to the specific objectives of the study. For this present study, Caco-2 monolayers ought to express P-gp efflux transporters and display endocytosis activity.

4.1 Expression of P-gp in Caco-2 monolayers

4.1.1 Transport study

The purpose of this experiment was to confirm that Caco-2 monolayers cultivated under the condition used could express functional P-gp. The cells were seeded onto the polycarbonate membranes (Transwell[®] inserts with 3- μ m pore size, 24 mm diameter) at a concentration of 2.83×10^5 cells per 4.71 cm^2 . Transwell[®] inserts (see picture in Appendix I) were measured for a baseline TEER value with a Millicell[®]-ERS potentiometer (Millipore, USA) before the cells were seeded. Cells were grown under the standard conditions for 21 days with the medium replaced every 48 hours. TEER was measured every 2 days after the monolayer had completely reached confluence. TEER values of Caco-2 monolayers were determined as follows:

$$\text{TEER}_{\text{monolayer}} = (\text{TEER}_{\text{total}} - \text{TEER}_{\text{membrane}}) \times A$$

where $\text{TEER}_{\text{monolayer}}$ = TEER of Caco-2 monolayer at the specified time ($\Omega \cdot \text{cm}^2$)

$\text{TEER}_{\text{total}}$ = Total TEER measured at the specified time

$\text{TEER}_{\text{membrane}}$ = TEER of the polycarbonate membrane measured before cell seeding

A = area of Transwell[®] insert (cm^2)

The transport of rhodamine 123 in the A-to-B and the B-to-A directions in the absence and the presence of verapamil was determined. Rhodamine 123 (20 μM) was used as a P-gp substrate and verapamil at 100 μM was used as a specific P-gp inhibitor (Sarkadi and Müller, 1997; Troutman and Thakker, 2003). In the study without verapamil, Caco-2 monolayers were rinsed with the apical buffer, pH 6.5. The monolayers were then pre-incubated with the apical buffer on the apical side and with the basolateral buffer, pH 7.4, on the basolateral side at 37 °C for 30 min. The compositions of the apical and the basolateral buffers are displayed in Appendix II. For the A-to-B transport, the buffer was replaced with rhodamine 123 in the apical buffer on the apical side. Aliquots (1 ml) of the basolateral buffer were taken every 10 min. The buffer was replaced with the same amount of the fresh medium. For the B-to-A transport, rhodamine 123 solution was placed on the basolateral side. Aliquots (0.75 ml) of the apical buffer were taken every 5 min and the buffer was replaced with the fresh one. In the experiment with verapamil, the Caco-2 monolayer was pre-incubated with 100 μM verapamil in the transport buffer (either the apical or the basolateral according to the transport direction studied) at 37 °C for 30 min. The medium was then changed to the transport buffer containing both verapamil and rhodamine 123 at 100 μM and 20 μM , respectively. Samples were collected in a similar manner to that in the experiment without verapamil. The extent of rhodamine 123 transported was quantified by spectrofluorometric method using a microplate reader with the excitation wavelength at 485 nm and the emission wavelength at 535 nm. The apparent permeability coefficients of rhodamine 123 in the A-to-B direction ($P_{\text{app, AB}}$) and in the B-to-A direction ($P_{\text{app, BA}}$) were calculated as follows:

$$P_{\text{app}} = \frac{dQ}{dt} \times \frac{1}{C_0 A}$$

where P_{app} = apparent permeability coefficient (cm/sec)

dQ/dt = the amount of rhodamine 123 appearing in the receiver
(or the donor) compartment as a function of time (nmol/sec)

A = the surface area across which the transport occurred (cm^2)

C_0 = the initial concentration in the donor compartment (μM)
(assuming sink conditions)

The efflux ratios of rhodamine 123 in the absence and in the presence of verapamil were determined and compared. The equation used to calculate the efflux ratio was as follows:

$$\text{Efflux ratio} = P_{\text{app, BA}} / P_{\text{app, AB}}$$

The efflux ratio of more than two is considered a verification of P-gp function (Faassen et al., 2003).

4.1.2 Uptake study

The purpose of this experiment was to confirm that Caco-2 monolayers cultivated under the experimental conditions used in this present study could still express functional P-gp. The uptake of both rhodamine 123 and calcein AM in the absence and the presence of verapamil was studied. Briefly, Caco-2 cells were cultivated in 24-well culture plates at a seeding density of 2.5×10^4 cells/0.5 ml/well (1.3×10^4 cells/cm²) for 21 days. Under these conditions, confluence was reached in 5-7 days. On the experiment day, cells were washed with PBS (pre-warmed at 37 °C) and pre-incubated with verapamil (100 µM) at 37 °C for 30 min. The pre-incubating medium was removed and replaced with the medium containing 100 µM verapamil and 2 µM rhodamine 123. The cells were incubated with the mixture for another 120 min. After the incubation period, cells in each well were washed 4 times with 1 ml ice-cold PBS and digested with 0.5 ml of 1% Triton[®] X-100 in PBS. The cells pre-incubated with serum-free DMEM were used as a control group. The uptake of rhodamine 123 into the cells was determined by measuring the amount of rhodamine 123 in the digested cells using a microplate reader with the excitation wavelength of 485 nm and the emission wavelength of 535 nm. The standard curve was prepared in the same medium used in the experiment. Digested untreated cells were also used for background correction. The preliminary study indicated that the presence of cells did not alter rhodamine 123 fluorescence under the conditions used. For calcein AM uptake, the cells were incubated with calcein AM (25 nM) instead of rhodamine 123. The experiment was carried out under the same conditions as those described above, with the incubation period of 60 min. The preliminary study indicated that the presence of cells and liposomal components did not alter rhodamine 123 and calcein fluorescence under the condition used.

4.2 Endocytosis activity of Caco-2 cells

The purpose of this experiment was to verify the endocytosis activity of the cell model. Alexa Fluor[®] 488-conjugated dextran (Molecular Probes[®], USA) was used as an endocytosis marker (Molecular Probes, 2006). Briefly, cells in 24-well culture plates were washed with warm PBS and pre-incubated with serum-free DMEM at 37 °C for 30 min. Then the medium was replaced with Alexa Fluor[®] 488-conjugated dextran 0.1 mg/ml in serum-free DMEM. After 90 min of the incubation period, cells were washed 4 times with 1 ml of ice-cold PBS and detached from the culture plate with 150 µl of 0.25% trypsin in 1 mM EDTA solution per well. Trypsin solution was replaced with 1 ml of ice-cold PBS and cells were triturated and transferred to centrifuge tubes. The cell suspension was centrifuged for 4 min at 1,200 rpm in a refrigerated centrifuge at 4 °C. The pellet was re-suspended and fixed with 1% formaldehyde in PBS. The measurement of Alexa Fluor[®] 488-conjugated dextran uptake was done using a flow cytometer (FACS Calibur, USA) with an argon ion laser light source. A total of 10,000 cells per sample was analyzed. The instrument was operated at 488 nm and 15 mW. Alexa fluorescence intensity was collected through a 525/42 nm band pass filter (ISCR, 2008). Cells incubated with serum-free DMEM were used as the control.

5. Uptake of calcein AM into Caco-2 cells as a function of time

The purpose of this experiment was to determine whether liposome encapsulation could increase the intracellular accumulation of the P-gp substrate calcein AM in a time-dependent manner. The experiment was done by comparing the uptake profiles of calcein AM from solution and from liposomes. Calcein AM is a specific substrate of P-gp. When the non-fluorescent calcein AM passes through cell membrane, it is converted to hydrophilic and intensely fluorescent calcein by endogenous esterases in the cell (Varma et. al., 2003). Briefly, Caco-2 cells were cultivated in 24-well culture plates at a seeding density of 2.5×10^4 cells/0.5 ml/well (1.3×10^4 cells/cm²) for 21 days. Cells were washed with pre-warmed PBS and pre-incubated with serum-free DMEM at 37 °C for 30 min. After the pre-incubation period, the medium was changed to calcein AM solution or calcein AM-loaded liposomes at a calcein AM concentration of 25 nM in serum-free DMEM at 37 °C for

30, 45, 60, 90, and 120 min. At the end of incubation period, cells in each well were washed 4 times with 1 ml ice-cold PBS and digested with 0.5 ml of 1% Triton[®] X-100 in PBS. The uptake of calcein AM was determined by measuring the amount of calcein in the cells using a microplate reader with the excitation wavelength of 485 nm and the emission wavelength of 535 nm as described under Section 4.1.2. The standard curve was prepared in 1% Triton[®] X-100 in PBS. Digested untreated cells were also used for background correction.

6. Uptake of calcein AM into Caco-2 cells as a function of concentration

The purpose of this experiment was to study whether calcein AM uptake by Caco-2 cells from solution and from calcein AM-loaded liposomes displayed any saturation in the lipid concentration range studied. The cells were washed with pre-warmed PBS and pre-incubated with the serum-free DMEM at 37 °C for 30 min. After the pre-incubation period, Caco-2 cells were incubated for 90 min with either calcein AM solution or calcein AM-loaded liposomes at the calcein AM concentration of 12.5-250 nM in serum-free DMEM (equivalent to 0.175-3.5 mg/ml of total lipid). At the end of the incubation period, cells were washed with ice-cold PBS, detached from culture plate with 0.25% trypsin in 1 mM EDTA solution, and fixed with 1% formaldehyde in PBS. The uptake of calcein AM into the cells was measured by a flow cytometer as described under Section 4.2. The fluorescence intensities were compared using appropriate controls.

7. Investigation of the possible mechanisms of liposomes in the delivery of calcein AM into Caco-2 cells

Results from Sections 5 and 6 indicated that liposomes could increase the extent of calcein AM uptake into Caco-2 cells. The purpose of this experiment was to investigate possible mechanisms of liposomes in the delivery of calcein AM into the cells.

7.1 Effect of blank liposomes on cell membrane permeability

This experiment was designed to test whether blank liposomes (PC:CH at 7:3 molar ratio) would have any effect on the cell membrane permeability that could

lead to an increase in the uptake of P-gp substrates. Calcein is a hydrophilic molecule that cannot cross the lipid bilayer of cell membrane (Manconi et al., 2007). Hence, if cell membrane permeation was changed due to effect of blank PC liposomes, calcein would pass through cell membrane leading to higher intracellular accumulation of the fluorescent dye. Both pre-treatment of the cells with blank liposomes and pre-treatment followed by co-treatment of blank liposomes and the fluorescent dye were investigated. Briefly, Caco-2 cells were washed with pre-warmed PBS. In the pre-treatment condition, Caco-2 cells were pre-incubated with either serum-free DMEM or with blank PC liposomes (0.35 mg/ml of total lipid) at 37 °C for 30 min. The pre-incubation medium was then replaced with calcein solution in serum-free DMEM at a concentration of 80 µM. The incubation was continued for 60 min at 37 °C.

In the experiment with co-treatment condition, cells were pre-treated with blank PC liposomes and then incubated in the presence of both calcein and blank PC liposomes. The measurement of calcein uptake was done as described under Section 5.

7.2 Modulation of P-gp function by liposomes

This experiment was to test whether blank liposomes could modulate P-gp function. Verapamil, a known P-gp inhibitor, was also used for comparison. Experiments with both the pre-treatment and the co-treatment conditions were carried out. The experiment was done using the same method as that described under section 7.1. Briefly, Caco-2 cells were washed with pre-warmed PBS and pre-incubated with either serum-free DMEM, blank PC liposomes (0.35 mg/ml of total lipid), or verapamil solution (100 µM) at 37 °C for 30 min. The pre-incubation medium was then replaced with calcein AM solution in serum-free DMEM at a concentration of 25 nM.

In the experiment with co-treatment condition, cells were incubated with either calcein AM only, calcein AM and blank PC liposomes, or calcein AM and verapamil at the concentrations described above. The uptake of calcein AM into Caco-2 cells was compared among the three treatments. The measurement of calcein uptake was done as described under Section 6.

7.3 Localization of cell-associated liposomes by confocal laser scanning microscopy

The aim of this study was to elucidate whether calcein AM association with cells seen in previous experiments was the result of adsorption or of internalization of liposomes. In these experiments, Caco-2 cells were seeded on the collagen-coated glass coverslips (Appendix III) in 12-well culture plates at a concentration of 5×10^4 cells/well. The cell monolayer was grown for 21 days with the medium changed every 48 hours as described under Section 3. On the experiment day, cells were washed with pre-warmed PBS and pre-incubated with serum-free DMEM at 37 °C for 30 min. The cells were then treated with various conditions as follows: (1) calcein AM solution and calcein AM-loaded liposomes (250 nM of final calcein AM concentration) (2) calcein solution and calcein-loaded liposomes (16 μ M of final calcein concentration) (3) blank liposomes labeled with NBD-PE (0.35 mg/ml of total lipid concentration) and (4) liposomes double-labeled with NBD-PE and rhodamine 123 (0.35 mg/ml total lipid concentration, 5.28 μ M of final NBD-PE concentration, and 2 μ M of final rhodamine 123 concentration). The cells treated with serum-free DMEM was used as the control group. The incubation time was 60 min in all conditions with calcein AM. In conditions with calcein and fluorescent-tagged liposomes, the incubation time was 120 min. At the end of the incubation period, cells were washed four times with ice-cold PBS and fixed with 3.7% (v/v) formaldehyde in PBS for 20 min. The coverslip with the fixed cells on its top was transferred to a glass slide and mounted with 80% (v/v) glycerol in PBS. All samples were visualized under a confocal laser scanning microscope (FluoViewTM FV1000, Olympus, Japan) equipped with argon and He-Ne green laser light sources. Representative areas were selected at random and pictures were taken using FITC and TRITC filters.

7.4 Discrimination between fusion and endocytosis by fluorescence dequenching technique

The purpose of this study was to distinguish the mechanism of internalization of liposomes between fusion and endocytosis. Calcein was used as the fluorescent marker at a self-quenching concentration (80 mM) and at a dequenching concentration (20 mM). The experiment was performed as described under Section 6.

Cells were incubated with calcein solution or calcein-loaded liposomes (0.35 mg/ml of total lipid) at 37 °C for 60 min. Cells were washed with ice-cold PBS, detached from culture plates with 0.25% trypsin in 1 mM EDTA solution, and the calcein uptake was measured by flow cytometry as described under Section 6. The uptake of calcein at the self-quenching concentration was also measured by spectrofluorometric method after cell digestion as described under Section 5.

7.5 Effect of inhibition of endocytosis on the uptake of calcein AM-loaded liposomes into Caco-2 cells

The purpose of this experiment was to verify the mechanism by which calcein AM-loaded liposomes were taken up by Caco-2 cells. If the mechanism of uptake was endocytosis, the calcein fluorescence intensity in the cells would be decreased when endocytosis was inhibited. Since endocytosis involves several metabolic steps, various inhibitors, as well as combinations of inhibitors, are often used (Poste and Papahadjopoulos, 1976). In this present study, cytochalasin B, sodium azide, sodium fluoride, deoxyglucose, and sodium iodoacetate were used either individually or in combination as previously reported in the literature (Poste and Papahadjopoulos, 1976). Cytochalasin B is an actin-depolymerizing agent, whereas the rest are metabolic inhibitors.

7.5.1 Effect of cytochalasin B on the uptake of calcein AM-loaded liposomes into Caco-2 cells

Caco-2 cells were washed with pre-warmed PBS and pre-incubated with cytochalasin B at a concentration of 1.25 or 2.50 µg/ml at 37 °C for 60 min (Chu and Lu, 2005). Cells pre-incubated with serum-free DMEM were used as the control. After 60 min, the solution was removed and cells were washed with pre-warmed PBS. The pre-incubation medium was replaced with calcein AM-loaded liposomes (0.35 mg/ml of total lipid) in serum-free DMEM, corresponding to 125 nM calcein AM. Cells were incubated at 37 °C for 90 min. The measurement of calcein AM uptake was done as described under Section 6.

A similar experiment using Alexa Fluor[®] 488-conjugated dextran instead of calcein AM-loaded liposomes was carried out as the positive control. The

concentration of Alexa Fluor[®] 488 conjugated-dextran was 0.1 mg/ml and the measurement of dextran uptake was done as described under Section 4.2.

7.5.2 Effect of metabolic inhibitors on the uptake of calcein AM-loaded liposomes into Caco-2 cells

The experiment was done using the same method as described under Section 7.5.1. Caco-2 cells were washed with pre-warmed PBS and pre-incubated with sodium azide (15-60 mM) only, sodium azide (15-60 mM) in the presence of sodium fluoride (10 mM), sodium azide (15-60 mM) in the presence of deoxyglucose (50 mM), or sodium azide (15-60 mM) in the presence of sodium iodoacetate (1-20 mM) at 37 °C for 30 min. Calcein AM-loaded liposomes were then co-incubated with these inhibitors at 37 °C for 90 min. The measurement of calcein AM uptake was done as described under Section 6.

A similar experiment using Alexa Fluor[®] 488-conjugated dextran instead of calcein AM-loaded liposomes was used as the positive control. A concentration of Alexa Fluor[®] 488-conjugated dextran was 0.1 mg/ml and the measurement of dextran uptake was done as described under Section 4.2.

7.5.3 Effect of temperature on uptake of calcein AM by Caco-2 cells

The purpose of this experiment was to determine whether liposome uptake by Caco-2 cells was a temperature-dependent process. The extents of cellular uptake of calcein AM from calcein AM solution and calcein AM-loaded liposomes at 37 °C and 4 °C were compared. The experiment was performed as described under Section 6. Caco-2 cells were washed and pre-incubated with serum-free DMEM at 37 °C or 4 °C for 30 min. The pre-incubation medium was replaced with calcein AM solution or calcein AM-loaded liposomes (125 nM of calcein AM) pre-warmed at the corresponding temperatures. The cells were further incubated at 37 °C and 4 °C for 90 min. At the end of the incubation period, cells were washed with ice-cold PBS and detached from culture plate with 0.25% trypsin in 1 mM EDTA solution. Calcein AM uptake was measured as described under Section 6.

8. Effect of liposomal composition on calcein AM uptake into Caco-2 cells

The purpose of this study was to investigate whether different liposomal compositions would still result in increasing the delivery of P-gp substrate calcein AM into Caco-2 cells. The extents of calcein AM uptake into Caco-2 cells were compared among liposomes with different compositions using calcein AM solution as the control group.

8.1 Effect of charge-imposing lipid on calcein AM uptake into Caco-2 cells

The objective of this experiment was to compare the uptake of calcein AM from neutral, positively charged, and negatively charged liposomes. Calcein AM solution was used as the control. The liposomal compositions and the preparation method were described under Section 1.1. The experiment was carried out using the same method as that described under Section 5 with an incubation period of 90 min.

8.2 Effect of cholesterol content on calcein AM uptake into Caco-2 cells

The effect of cholesterol content on calcein AM uptake into Caco-2 cells was studied with neutral liposomes since they were most efficient in delivering calcein AM to Caco-2 cells. In this experiment, the extents of calcein AM uptake from neutral liposomes with different molar ratios of soybean PC and CH were compared. The four formulations of liposomes (PC:CH at molar ratios of 6:4, 7:3, 8:2, and 10:0) were prepared as described under Section 1.1 and the study was performed using the same method as that described under Section 5 with an incubation period of 90 min.

8.3 Effect of phosphatidylcholine type on calcein AM uptake into Caco-2 cells

The purpose of this experiment was to determine whether the difference in type, and thus the transition temperatures, of phosphatidylcholine would affect the uptake of calcein AM from liposomes into Caco-2 cells. The neutral soybean PC-based liposomes and DPPC-based liposomes at PC:CH ratios of 7:3 and 10:0 were prepared as described under Section 1.1. The experiment was carried out under the same condition as that described under Section 5 with an incubation period of 90 min.

9. Cell viability study (Freshney, 2005)

The aim of this study was to estimate the possibility that the relatively lower extents of cell-associated calcein AM from charged liposomes seen in the previous experiments might result from the compromised cell viability rather than from the extent of liposome uptake. In the living cells, MTT is taken up by the cells and is reduced to formazan crystals by mitochondrial enzymes. The reduction of MTT cannot take place in damaged cells with impaired mitochondrial function. The extent of formazan production is proportional to the amount of viable cells. Caco-2 cells were treated with calcein AM-loaded liposomes (either neutral, positively charged, or negatively charged) as described under Section 8.1. Cells treated with serum-free DMEM were used as the control group. After the treatment period of 90 min, the treatment medium was removed and 0.5 ml of MTT solution (0.4 mg/ml in serum-free DMEM) was added. Cells were further incubated for 4 hours at 37 °C. After MTT solution was removed, the formazan crystals in the cells were dissolved in DMSO with constant shaking. The solution was diluted to an appropriate concentration and the amount of formazan production was determined using a microplate reader at 570 nm with a reference wavelength of 620 nm. Cell viability was calculated as the percentage of the control.

10. Statistical analysis

All experiments were carried out at least in triplicate. In each experiment, all data were presented as means \pm SEM (standard error of the mean) or means \pm SD (standard deviation) as appropriate. If Levene's test of equity of error of variances showed that the distribution of data did not significantly deviate from normality, the analysis of variance (ANOVA) was used at $\alpha = 0.05$. Tukey HSD was used as the post hoc multiple comparison test.

CHAPTER IV

RESULTS AND DISCUSSION

1. Characterization of the physical properties of liposomes

As shown in Table 5, the size of liposomes depended on their compositions. The mean diameters were similar between blank neutral liposomes and calcein AM-loaded neutral liposomes (123.4 ± 3.60 and 123.8 ± 5.69 nm). These results indicate that the addition of calcein AM did not affect the size of neutral liposomes. For calcein AM-loaded liposomes, the mean diameters of positively charged and negatively charged liposomes were significantly smaller than that of neutral liposomes ($p < 0.05$). Thus, the presence of a charged lipid, either SA or DCP, seemed to affect the size of calcein AM-loaded liposomes. In addition, the vesicle size was in good agreement with the physical appearances of the liposomal suspensions. The suspension containing the liposomes of smaller size was more translucent than the suspension containing the bigger ones (Figure 7). These results are in good agreement with the established effect of surface charge on bilayer curvature and liposomal size (Kraayenhof et al., 1996).

Table 5: Mean diameters and zeta potential values of blank neutral liposomes and calcein AM-loaded liposomes. Data are shown as mean \pm SD ($n = 3$).

Formulation	Mean diameter (nm)	Zeta potential (mV)
Blank neutral liposomes	123.4 ± 3.60	-7.99 ± 1.19
Calcein AM-loaded neutral liposomes	123.8 ± 5.69	-8.17 ± 1.13
Calcein AM-loaded positively charged liposomes	115.3 ± 1.41	43.24 ± 3.35
Calcein AM-loaded negatively charged liposomes	97.2 ± 6.15	-45.49 ± 5.97



Figure 7: Physical appearances of liposomal preparations: blank = blank PC liposomes, neutral = calcein AM-loaded neutral liposomes, positive = calcein AM-loaded positively charged liposomes, and negative = calcein AM-loaded negatively charged liposomes

The zeta potential values of the blank neutral liposomes and calcein AM-loaded neutral liposomes were similar. Incorporation of calcein AM did not alter the surface charge of neutral liposomes because calcein AM is a neutral molecule (Sigma-Aldrich, 2009). Both types of liposomes carried slightly negative surface potentials (Table 5). The negative surface charge of neutral liposomes may be due to the charged impurity in phospholipids used for preparation (Pincet, Cribier, and Perez, 1999) and/or the hydrolytic product of phospholipids (Sætern et al., 2005). The zeta potential of charged liposomes displayed negative or positive value according to the net charge of the charge-imposing lipid (DCP or SA) used in the preparation. These results confirm that the surface charge of liposomal formulation could be modified by the liposomal composition.

2. Characterization of Caco-2 monolayers

2.1 Integrity of Caco-2 monolayers

TEER is often used as a parameter to verify integrity of cell culture monolayers in most transport studies (Faassen et al., 2003; Lentz et al., 2000; Lo, 2000; Ward et al., 2000; Yamashita et al., 2000). In this present study, TEER values were measured every 2 days as shown in Figure 8. TEER values increased with the culture time and the average TEER value at day 21 was $840 \pm 67 \Omega \cdot \text{cm}^2$. This result agrees with previous research where TEER values of Caco-2 monolayers at 21 days

were in the range of 300-1,400 $\Omega\cdot\text{cm}^2$ (Lentz et al., 2000; van der Sandt et al., 2000; Ward et al., 2000). Generally, it is accepted that Caco-2 monolayers are suitable for transport study when TEER values exceed 300 $\Omega\cdot\text{cm}^2$ at 21 days after seeding (Hunter et al., 1993; Lo, 2000; Troutman and Thakker, 2003). Thus, the high TEER value in this study indicated that Caco-2 monolayers were tight enough to use in transport study.

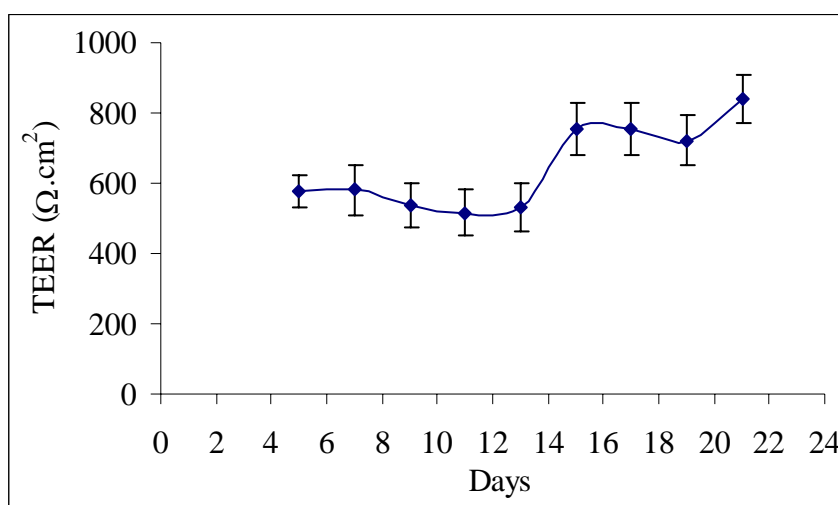


Figure 8: TEER values of Caco-2 monolayers as a function of time. Data are shown as mean \pm SD (n = 6).

2.2 Expression of P-gp in Caco-2 monolayers

2.2.1 Transport study

The permeability data of rhodamine 123 across Caco-2 monolayers in the absence and the presence of verapamil are shown in Figure 9. In the A-to-B direction, verapamil slightly increased the transport of rhodamine 123. The average $P_{\text{app, AB}}$ value of rhodamine 123 increased from $4.06 \pm 0.01 \times 10^{-6}$ cm/sec to $5.12 \pm 0.66 \times 10^{-6}$ cm/sec. On the other hand, the average $P_{\text{app, BA}}$ was considerably reduced in the B-to-A direction. The average $P_{\text{app, BA}}$ value of rhodamine 123 was significantly reduced from $35.6 \pm 7.24 \times 10^{-6}$ cm/sec to $11.1 \pm 1.47 \times 10^{-6}$ cm/sec ($p < 0.05$). The efflux ratio in the absence and in the presence of verapamil was 8.75 and 2.16, respectively (Table 6). At the end of the experiment, the TEER value slightly decreased. The TEER values before and at the end of the experiment were 840 ± 67

and $765 \pm 55 \Omega \cdot \text{cm}^2$, respectively. However, the TEER value at the end of the experiment was still much higher than the accepted TEER value for the transporter study. Thus, the integrity of Caco-2 monolayers was preserved throughout the experiment.

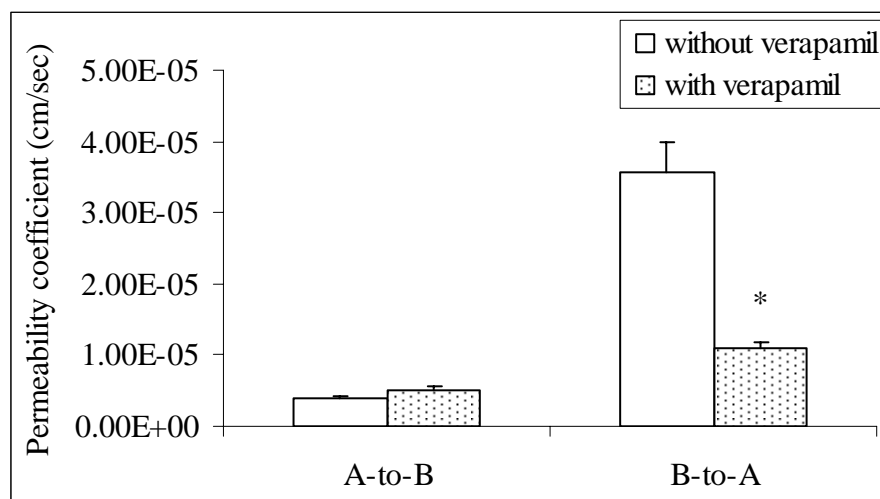


Figure 9: Absorptive (A-to-B) and secretory (B-to-A) permeability coefficients of rhodamine 123 across Caco-2 monolayers in the absence and in the presence of verapamil. Data are shown as mean \pm SEM (n = 3).

*p < 0.05 compared with the secretory permeability coefficient of rhodamine 123 without verapamil

Table 6: Apparent permeability coefficients of rhodamine 123 and the efflux activity of P-gp in the absorptive and the secretory directions across Caco-2 monolayers in the absence and in the presence of verapamil. Data are shown as mean \pm SEM (n = 3).

Treatment	$P_{app, AB} \times 10^{-6}$ (cm/s)	$P_{app, BA} \times 10^{-6}$ (cm/s)	Efflux ratio $P_{app, BA} / P_{app, AB}$
Rhodamine123 (20 μ M)	4.06 ± 0.01	35.6 ± 4.18	8.75
Rhodamine123 (20 μ M) +Verapamil (100 μ M)	5.12 ± 0.38	11.1 ± 0.84	2.16

Many studies show that the transport of P-gp substrate in the A-to-B direction markedly increases when P-gp function is inhibited (Anderle et al., 1998; Hämmerle et al., 2000; Hunter et al., 1993; Lukanawonakul, 2005). In this study, only a little effect of verapamil on rhodamine 123 transport in the A-to-B direction was seen. Rhodamine 123 is widely used as a specific P-gp substrate (Loetchutinat et al., 2003; Troutman and Thakker, 2003). Some authors considered rhodamine 123 a specific fluorescent P-gp substrate to determine the function of P-gp (Annaert et al., 2001; Deng et al., 2007). However, transport of rhodamine 123 may also occur under the influence of other efflux transporters. Rhodamine 123 is also a known substrate of MRP and BCRP (Honjo et al., 2001). All three efflux transporters have been found in Caco-2 cells (Gan and Thakker, 1997; Xia et al., 2005). Therefore, the net transport of rhodamine 123 across Caco-2 monolayers is under the influence of complex roles of at least three transporter systems. While verapamil, a potent P-gp inhibitor, can inhibit the function of both P-gp and MRP (Crivellato et al., 2002), it is not an effective inhibitor for BCRP (Zhang et al., 2005). This might explain partly why the $P_{app, AB}$ of rhodamine 123 did not dramatically increase in the presence of verapamil. In addition, the transport pathway of rhodamine 123 via the paracellular route might undermine the inhibitory effect of verapamil. Troutman and Thakker (2003) found that the absorptive transport of both rhodamine 123 and doxorubicin mainly occurred by the paracellular route. Thus, in their study, inhibition of the efflux function on the apical side by the specific inhibitor GW918 inserted only little effect on overall transport of both substrates. Lower TEER values lead to higher permeability of compounds via the paracellular route (Daugherty and Mrsny, 1999). The effect of verapamil on rhodamine 123 transport across Caco-2 monolayers was reported to be much more pronounced when the TEER value was higher than $1000 \Omega \cdot \text{cm}^2$ (Lukanawonakul, 2005).

The high efflux ratio of 8.75 in the absence of verapamil could indicate that the functional P-gp was expressed on the apical side of cell membrane under the culture conditions used in this study. Thus, these monolayers were suitable for the use as a cell culture model to study the effect of liposomes on P-gp function. P-gp function is verified when the efflux ratio is more than two (Faassen et al., 2003). The efflux ratio values from many research groups were reported to be varied widely,

from 2.3 to more than 10 fold (Lo, 2003; Hunter et al., 1993; Troutman and Thakker, 2003). The different efflux ratios may represent the difference in P-gp levels among laboratories. Andrerle and co-workers (1998) found that the level of P-gp expression was affected by the culturing time and other conditions such as passage number, composition of the medium, use of antibiotics, and sub-culturing protocol.

2.2.2 Uptake study

The uptake of the P-gp substrates rhodamine 123 and calcein AM has also been used to evaluate the functional P-gp (Eneroth et al., 2001; Loetchutinat et al., 2003; Troutman and Thakker, 2003; Utoguchi et al., 2000). The intracellular accumulation of these substrates results from the overall effect of both the influx and the efflux transport. Under the influence of verapamil, the uptake of both rhodamine 123 and calcein AM was increased with the reverse ratios of 1.82 and 1.52, respectively (Table 7). Other studies reported comparable reverse ratios with rhodamine 123 and calcein AM in the presence of verapamil (Utoguchi et al., 2000; Zastre et al., 2002). These results confirmed that the Caco-2 cells cultured under the uptake condition used for experimentation in this study also expressed functional P-gp.

Table 7: Uptake of rhodamine 123 and calcein AM from solutions in the absence and in the presence of 100 μ M verapamil. Data are shown as mean \pm SEM (n = 8, 6).

Treatment	Uptake of substrate (mole \times hr ⁻¹ \times 10 ⁻¹²)		Reverse ratio
	Without verapamil	With verapamil	
Rhodamine123 (2 μ M)	10.48 \pm 0.66	19.04 \pm 1.46	1.82
Calcein AM (25 nM)	1.40 \pm 0.28	2.12 \pm 0.27	1.52

2.3 Endocytosis activity of Caco-2 cells

Alexa Fluor[®] 488-conjugated dextran is a known endocytosis marker (Molecular Probes, 2006). The endocytosis activity has been appraised from the uptake of fluorescent dextrans by flow cytometry or fluorescence microscopy (Li, Greenwood, and Glunde, 2008; Magalhães et al., 2005; Schnatwinkel et al., 2004; Voronina et al., 2007). Figure 10 shows the histograms of fluorescence intensity from Caco-2 cells incubated with Alexa Fluor[®] 488-conjugated dextran and with serum-free DMEM (the control). In the overlay of fluorescence histograms, the high fluorescence intensity from Caco-2 cells incubated with Alexa Fluor[®] 488-conjugated dextran indicated that the Alexa Fluor[®] 488-conjugated dextran was endocytosed into the cells (Molecular Probes, 2006). The fluorescence intensity value of Alexa Fluor[®] 488-conjugated dextran uptake was significantly and markedly (more than 4 fold) higher than that of the control group ($p < 0.05$) (Table 8). This result indicated that Caco-2 cells displayed sufficient endocytosis activity and, thus, were suitable for the use as a cell culture model for later experiments.

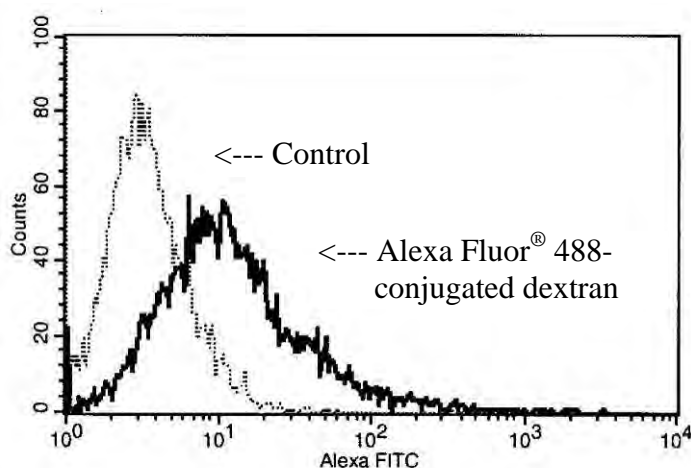


Figure 10: Overlay of fluorescence histograms from Caco-2 cells incubated with Alexa Fluor[®] 488-conjugated dextran and serum-free DMEM (Control)

Table 8: Fluorescence intensity from Caco-2 cells incubated with Alexa Fluor[®] 488-conjugated dextran and serum-free DMEM (Control). Data are shown as mean \pm SEM (n = 3).

Treatment	Fluorescence intensity
Control	3.94 \pm 0.59
Alexa Fluor [®] 488-conjugated dextran	18.61 \pm 3.69

3. Uptake of calcein AM into Caco-2 cells as a function of time

Accumulation of calcein AM in Caco-2 cells from calcein AM-loaded liposomes was higher than that from calcein AM solution at all data points along the incubation period. The difference between calcein AM uptake from liposomes and from solution increased with the increasing incubation time. Calcein AM was taken up from liposomes in a time-dependent manner from the beginning. In contrast, the uptake of calcein AM from solution was relatively constant during the first 60 min and slightly increased thereafter (Figure 11), which might be attributed to the saturation of P-gp function. A similar scenario has been reported with the in vitro absorption of celiprolol, which is a substrate of the OAT-A transporter (Kato et al., 2008).

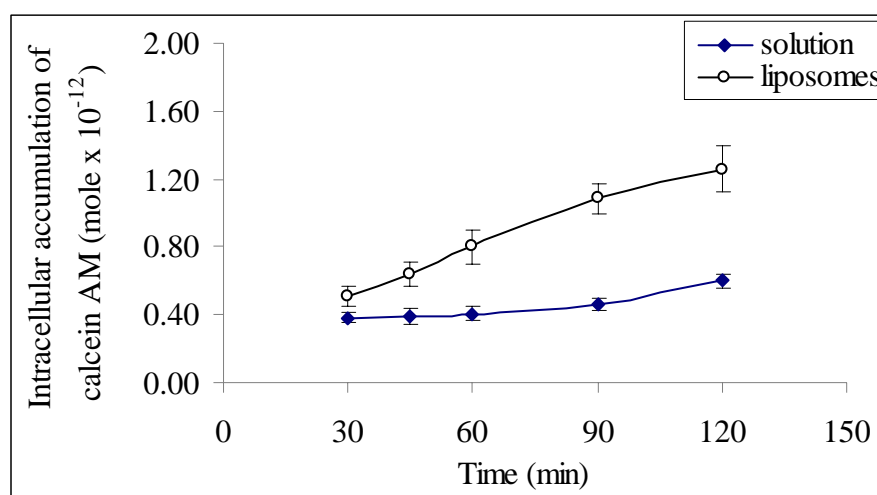


Figure 11: Calcein AM uptake profiles from calcein AM solution and calcein AM-loaded liposomes. Data are shown as mean \pm SEM (n = 4).

Other researchers have also reported the role of liposomes in increasing P-gp substrate uptake into cells. Liposomes can enhance cellular uptake of anticancers such as epirubicin into Caco-2 cells (Lo, 2000) and enhance cytotoxicity of the anticancer daunorubicin (as Daunoxome[®]) in two types of leukemia cells (Michieli et al., 1999). Moreover, liposomes can enhance the transport of HIV protease inhibitor drugs (indinavir and saquinavir) from the apical side to the basolateral side of Caco-2 monolayers (Kapitza et al., 2007). In contrast, liposomes fail to enhance the uptake of drugs into cells in some certain cases. For example, liposomes fail to enhance cytotoxicity of daunorubicin in two types of breast cancer cells (Iffert et al., 2000) and fail to enhance accumulation of doxorubicin in lung cancer cells (Kobayashi et al., 2007). These different results might be attributed in part to the different types of cells used in the studies as well as the difference in liposomal preparations.

4. Uptake of calcein AM into Caco-2 cells as a function of concentration

For carrier-mediated processes, rate of drug absorption increases with drug concentration until the carrier molecules are completely saturated (Shargel et al., 2005). Generally, the concentration of drug used in the uptake study should be in the range well below the concentration where saturation of carriers occurs to avoid the decrease in uptake efficiency. Figure 12 shows the concentration-dependent uptake of calcein AM into Caco-2 cells from calcein AM solution and calcein AM-loaded liposomes. The extent of calcein AM uptake from liposomes was linear in the range of 12.5 to 250 nM of calcein AM (equivalent to 0.175 to 3.5 mg/ml of total lipid concentration) and higher than that from solution at all data points. The data indicated that the saturation of liposome uptake by Caco-2 cells did not occur at the liposome concentrations used in the study. In other studies, the saturation of liposome uptake was observed in the mouse bone marrow macrophages, J774 cells, and Caco-2 cells at different total lipid concentrations, depending on cell type and cell density (Allen et al., 1991; Legrand et al., 1996; Lukanawonakul, 2005).

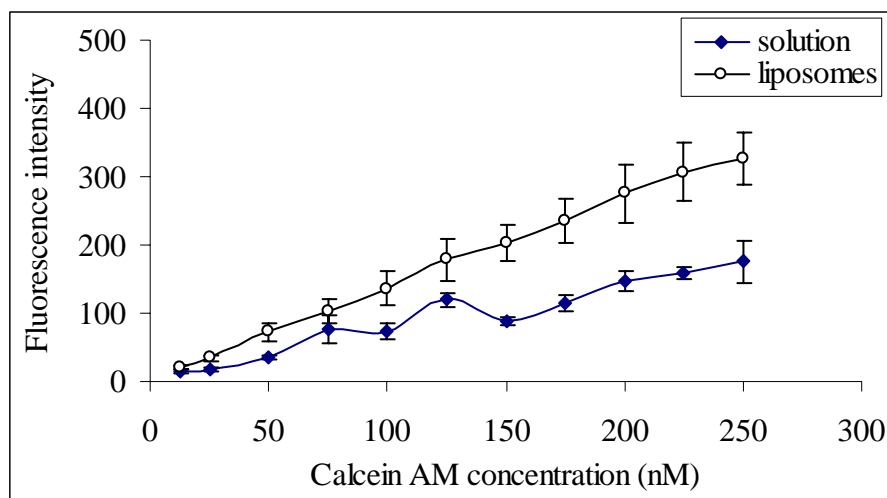


Figure 12: Calcein AM uptake from calcein AM solution and calcein AM-loaded liposomes at various concentrations. Data are shown as mean \pm SEM (n = 3).

However, it is worth noting that, for compounds that rapidly cross cell membrane by passive diffusion, liposomes might be useful for intracellular delivery only at low doses. With high concentration gradients, the passive diffusion may occur at such a high rate that it can overcome other specialized transport processes, especially those saturable ones. In the preliminary study, uptake of calcein AM from solution was higher than that from neutral liposomes at 2 μ M of calcein AM. The cumulative amounts of calcein in Caco-2 cells were 38.14-46.03 and 4.67-4.85 pmole/mg protein from solution and from liposomes, respectively.

5. Investigation of the possible mechanisms of liposomes in the delivery of calcein AM into Caco-2 cells

5.1 Effect of blank liposomes on cell membrane permeability

Liposomes are composed of phospholipids that are surface active (Nikolova and Jones, 1998; Uchiyama, Yui, and Sawada, 2004). Liposomes can interact with cells and perturb the cell membrane. This effect of liposomes on cell membrane permeability can lead to the high uptake of substances into cells (Fang et al., 2003; Uchiyama et al., 2004). Fluidizing of the cell membrane lipid bilayer is one of the methods that have been used to increase drug permeation into cells (Daugherty and Mrsny, 1999). The permeabilities of many compounds (such as mannitol, furosemide, atenolol, and acyclovir) into Caco-2 cells are increased by sodium lauryl

sulfate (Rege et al., 2001). Tween[®] 80 and Cremophor[®] EL are known to increase drug permeation into cells by increasing cell membrane fluidity (Rege, Kao, and Polli, 2002).

To prove this mechanism, Caco-2 cells were pre-treated with blank liposomes followed by calcein solution (the pre-treatment condition). Co-incubation of the cells with both liposomes and calcein solution after pre-treatment with only blank liposomes (the co-treatment condition) was also studied. The extents of calcein uptake from all conditions studied were not different ($p > 0.05$) (Figure 13). The results indicate that blank liposomes did not affect cell membrane permeability. The enhancement of calcein AM uptake into Caco-2 cells by liposomes seen in Sections 3 and 4 was not likely to be due to changes in cell membrane permeability.

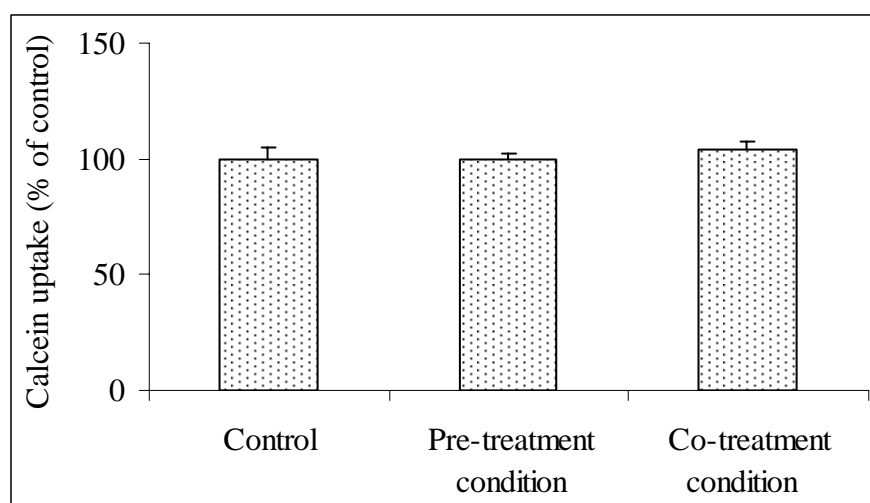


Figure 13: Calcein uptake into Caco-2 cells from calcein solution with blank liposomes in the pre-treatment and the co-treatment conditions. Data are shown as mean \pm SEM ($n = 3$).

5.2 Modulation of P-gp function by liposomes

Figure 14 reveals that the extents of calcein AM uptake in the pre-treatment and in the co-treatment conditions with blank liposomes were not different from that of the control group ($p > 0.05$). These results indicate that blank soybean PC liposomes did not modulate P-gp function under the experimental condition used. In contrast to this finding, either blank DPPC or blank DPPE liposomes can enhance

epirubicin uptake from solution into Caco-2 cells, probably by competing with the drug in binding with P-gp (Lo, 2000). Liposomes composed of egg PC tagged with either 40% NBD-PE or 40% NBD-PC also behave as substrates for P-gp in two multidrug-resistance cell lines transfected with human P-gp (Bosch, et. al., 1997). The different results seen might be attributed to the differences in the type and degree of fatty acid saturation in acyl chains of these lipids. In addition, the difference in the binding affinity between epirubicin and calcein AM with the binding sites on P-gp relative to that of the phospholipids could also be responsible.

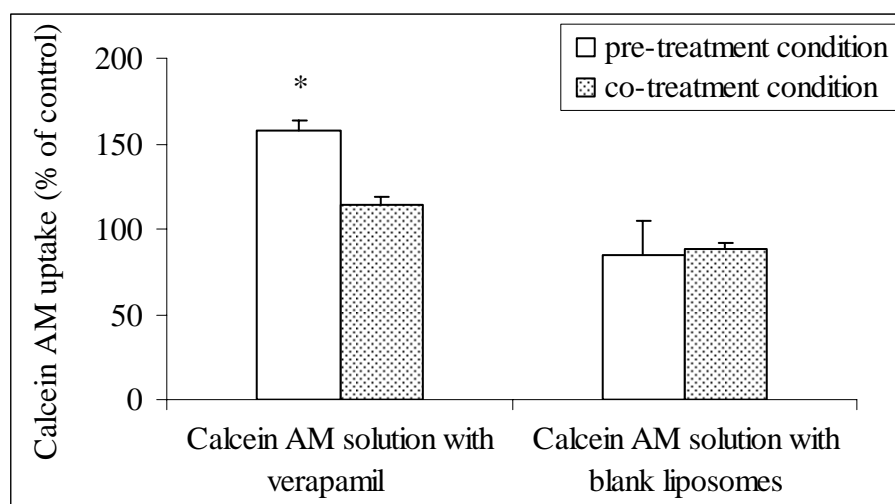


Figure 14: Calcein AM uptake from calcein AM solution with either verapamil or blank liposomes in the pre-treatment and the co-treatment conditions. Data are shown as mean \pm SEM (n = 3).

*p < 0.05 compared with control

The treatments with verapamil were used as the positive control group in this study. Modulation of P-gp function by verapamil was seen only in the pre-treatment condition (Figure 14, p < 0.05). The inhibition of calcein AM efflux by verapamil may occur via a non-competitive process. Eneroth and co-workers (2001) demonstrated that calcein AM and verapamil might bind to different binding sites located on P-gp. Unexpectedly, the uptake of calcein AM in the presence of verapamil under the co-treatment condition was not different from that of the control group (p > 0.05). In the co-treatment condition, calcein AM became in direct contact with

verapamil. It was possible that the two compounds might interact via a hydrophobic interaction. This could result in much less free calcein AM available for penetration into the cells since the complex formed might be too big to cross the cell membrane. However, this scenario was not further verified in this study.

5.3 Localization of cell-associated liposomes by confocal laser scanning microscopy

The images from the confocal laser scanning microscopy of the liposome uptake studies are shown in Figure 15. The fluorescence pattern can be used to identify the liposome-cell interaction (New, 1997). The fluorescence images (at 4-8 μm below the apical surface of the cells) of liposomes labeled with NBD-PE showed punctate NBD fluorescence in the cytoplasm (Figure 15-B). This result indicates the internalization of liposomes. The punctate appearance was consistent with the hypothesis that liposomes were confined within a specific compartment of the cells, which is most likely to be endosomes or lysosomes, after endocytosis. In the calcein AM uptake studies, the fluorescence images showed both diffuse and punctate calcein fluorescence in the cells. These fluorescence patterns were seen in the uptake of calcein AM from both solution and liposomes (Figures 15-C and 15-D). The higher fluorescence intensity of calcein AM uptake from liposomes (Figure 15-D) agrees well with the previous experiments in Sections 3 and 4 that calcein AM uptake from liposomes was better than that from solution. The fluorescence images were consistent with endocytosis of calcein AM-loaded liposomes into the cells. The diffuse fluorescence pattern that was also evident may be due to the diffusion of calcein AM from endosomes into the cytoplasm or the fusion of some liposomes with the endocytic-endosomal compartment. The diffusion of calcein AM across the endosomal membrane was possible since calcein AM is hydrophobic with a log P of 8 (Sigma-Aldrich, 2009). Manconi and co-workers (2007) observed the fusion of liposomes with endosomes in a previous study. Liposomes comprising soybean lecithin of 80% and 90% purity fused with the endocytic-endosomal compartment after endocytosis by HeLa cells. In this present study, soybean PC of 90% purity (as Phospholipon[®] 90) was also used. However, this mechanism seemed to be negligible in Caco-2 cells since the diffuse fluorescence pattern was not seen with calcein-loaded

liposomes (see Figure 15-F). It should also be noted that the punctate pattern was also seen with calcein AM solution. This observation was consistent with the cellular uptake mechanisms of calcein AM previously reported. Calcein AM can enter cells by both passive diffusion and fluid-phase endocytosis (Tenopoulou et al., 2007). After the fluid-phase endocytosis, it is hydrolyzed to calcein by lysosomal esterases, resulting in the punctate fluorescence as seen in Figure 15-C.

When the water-soluble calcein was used as a liposomal aqueous phase marker, the fluorescence image of calcein-loaded liposome uptake shows only the punctate fluorescence (Figure 15-F). In contrast, the incubation of Caco-2 cells with calcein solution did not result in any fluorescence in the cells (Figures 15-E and 15-F). These results agree well with the results seen with calcein AM liposomes above and could be used to confirm that the uptake of liposomes occurred via endocytosis. Moreover, since the diffuse calcein fluorescence was not observed with calcein-loaded liposomes, fusion of the liposomes with cell membrane was not likely to occur. This observation also ruled out the possibility of liposome fusion with endosomes/lysosomes (Chu et al., 1990; Connor and Huang, 1985) as discussed above.

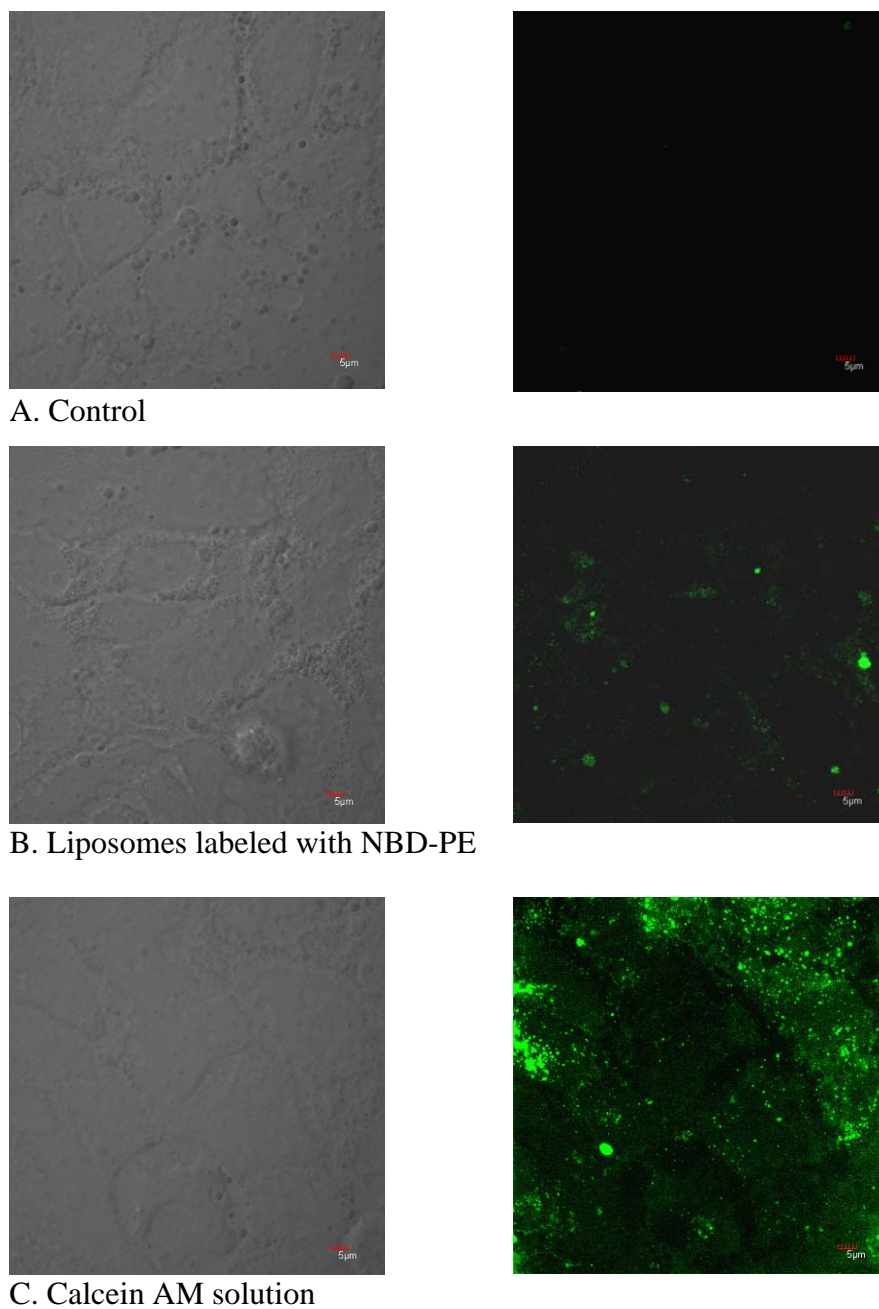


Figure 15: CLSM images (with bright field images on the left panel and fluorescence field images on the right panel) of Caco-2 cells treated with various conditions: (A) control, (B) liposomes labeled with NBD-PE (0.35 mg/ml of total lipid concentration), (C and D) calcein AM solution and calcein AM-loaded liposomes (250 nM of final calcein AM concentration), (E and F) calcein solution and calcein-loaded liposomes (16 μ M of final calcein concentration)

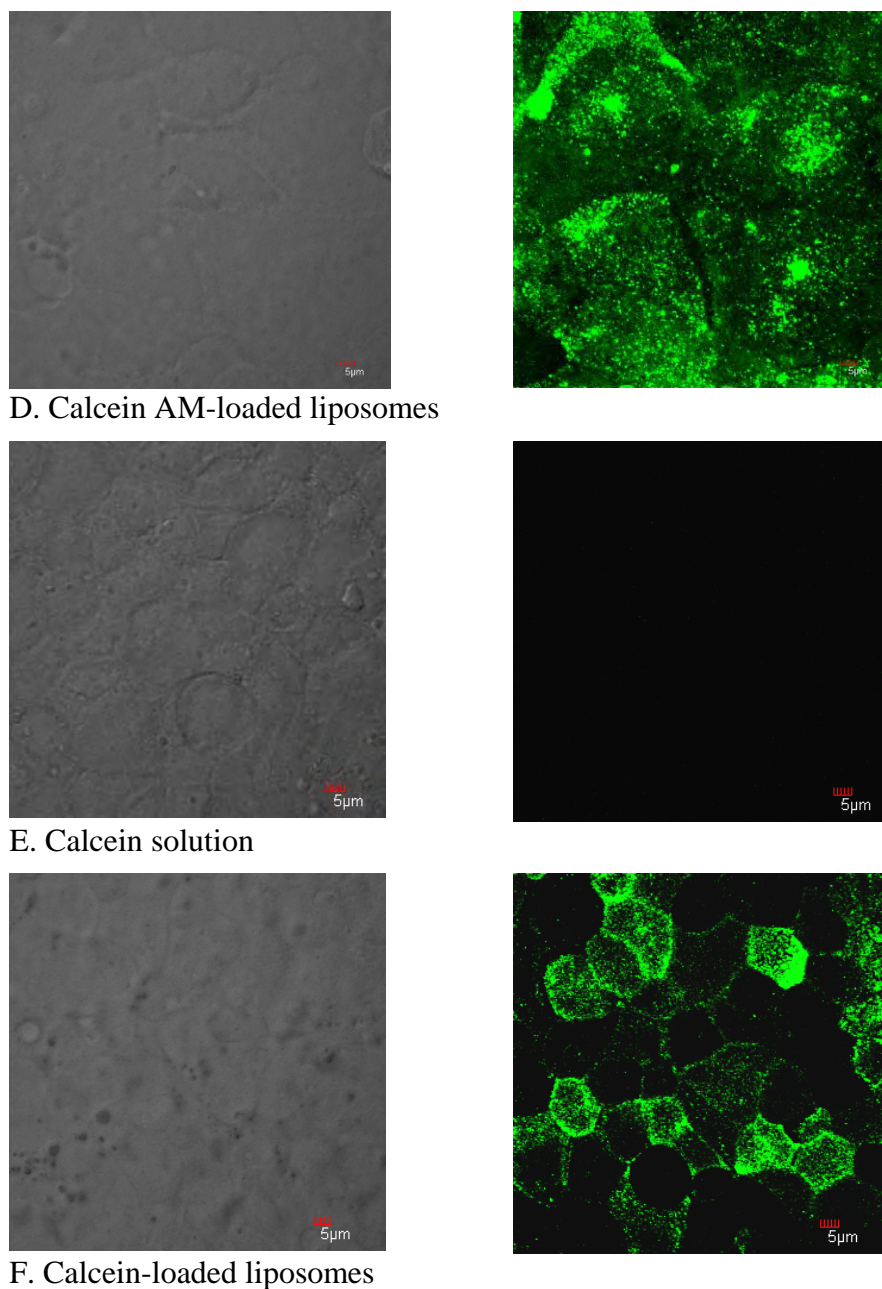
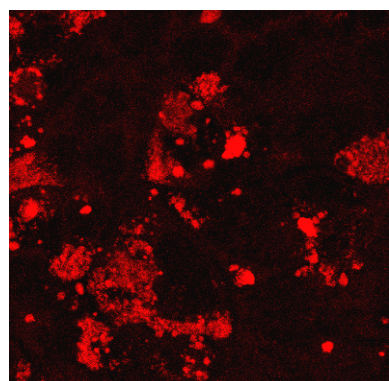
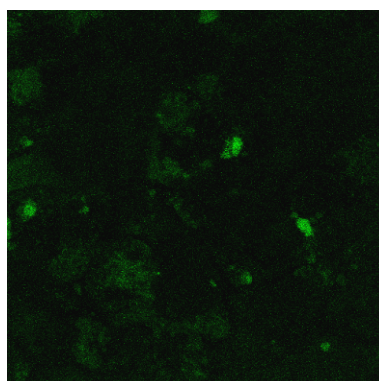


Figure 15 (continue): CLSM images (with bright field images on the left panel and fluorescence field images on the right panel) of Caco-2 cells treated with various conditions: (A) control, (B) liposomes labeled with NBD-PE (0.35 mg/ml of total lipid concentration), (C and D) calcein AM solution and calcein AM-loaded liposomes (250 nM of final calcein AM concentration), (E and F) calcein solution and calcein-loaded liposomes (16 μM of final calcein concentration)

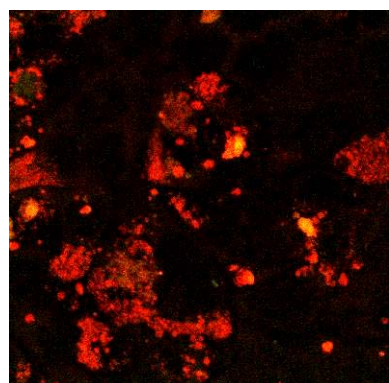
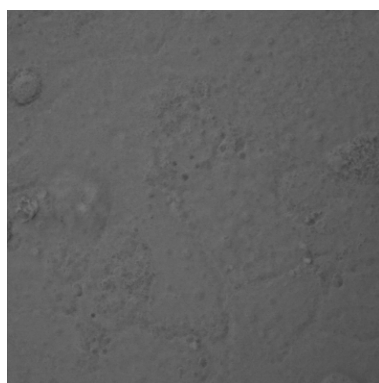
The co-localization of the lipid phase and the aqueous phase fluorescent markers of liposomes in various cells has been used as the acceptance criteria to indicate endocytosis of liposomes (Cryan et al., 2006; Fretz et al., 2004; Khalil et al., 2006; Manconi et al., 2007). In this present study, the fluorescence double-labeled liposomes were also used to verify the mechanism of liposome-cell interaction. The fluorescence images of Caco-2 cells incubated with double-labeled liposomes for 120 min are shown in Figure 16. The red fluorescence of rhodamine 123 was found distributed throughout the cells. The green fluorescence of NBD, the lipid phase marker, was also seen throughout the cells. The overlay fluorescence image of rhodamine 123 and NBD fluorescence clearly shows the co-localization of both fluorescent markers in the cells. This co-localization indicated that the soybean PC-based liposomes used in this present study entered the cells intact and could successfully carry their cargo into the cells with them. This result thus strongly supported the endocytosis mechanism. The result also indicated that fusion was not the main mechanism of the uptake of calcein AM-loaded liposomes into Caco-2 cells. If fusion had been the main mechanism, the lipid marker would have been seen only on the cell membrane, not inside the cells. The double-labeled technique was used to demonstrate fusion of DPPC liposomes with human red blood cells (Holovati, Gyongyossy-Issa, and Acker, 2008). In that study, the water-soluble carboxyfluorescein was located in the cytoplasm, whereas the lipid marker rhodamine B chloride incorporated itself into the red blood cell membrane.



A. Rhodamine fluorescence image



B. NBD fluorescence image

C. Overlay fluorescence image
of A and B

D. Bright-field image

Figure 16: CLSM images of Caco-2 cells treated with liposomes double-labeled with NBD-PE and rhodamine 123 (0.35 mg/ml total lipid concentration, 5.28 μ M of final NBD-PE concentration, and 2 μ M of final rhodamine 123 concentration). The pictures were taken using FITC and TRITC filters for NBD and rhodamine 123, respectively.

5.4 Discrimination between fusion and endocytosis mechanism by fluorescence dequenching technique

The fluorescence intensities of calcein from the uptake of calcein solution and calcein-loaded liposomes into Caco-2 cells are shown in Table 9. The extent of calcein uptake into Caco-2 cells was measured by flow cytometry. At a dequenching concentration of calcein (20 mM of calcein encapsulated in liposomes), the uptake of calcein from liposomes was significantly higher than that from solution ($p < 0.05$). In contrast, the uptake of calcein at a self-quenching concentration (80 mM of calcein encapsulated in liposomes) from liposomes was significantly lower than that from solution ($p < 0.05$). These results also confirm that liposomes were taken up into Caco-2 cells by endocytosis and not by fusion. In the fusion mechanism, calcein at a self-quenching concentration in liposomes will show strong fluorescence after being diluted many hundred fold in the cytoplasm (New, 1997). This technique has been used successfully to discriminate fusion from endocytosis. For example, the strong fluorescence diffuse throughout the cytoplasm was observed after the uptake of pH-sensitive liposomes by L929 cells, A31 cells, RAW264.7 cells, and P388D1 cells via endocytosis followed by liposomes fusion with the lysosomal membrane (Chu et al., 1990; Connor and Huang, 1985). On the contrary, the uptake of liposomes via endocytosis without subsequent fusion showed little or no diffuse fluorescence in the cytoplasm (Chu et al., 1990; Connor and Huang, 1985).

Table 9: Fluorescence intensity of calcein from the uptake of calcein solution and calcein-loaded liposomes into Caco-2 cells by flow cytometry. Data are shown as mean \pm SEM (n = 4).

	Fluorescence intensity	
	Treatment with calcein at a dequenching concentration	Treatment with calcein at a self-quenching concentration
Solution	60.42 \pm 6.01	261.72 \pm 26.68
Liposomes	195.32 \pm 24.98	81.70 \pm 2.37

To further confirm the endocytosis mechanism, after Caco-2 cells were treated with calcein solution and calcein-loaded liposomes at the self-quenching concentration, cells were digested with 1% Triton[®] X-100 and the amount of calcein in the cells was measured by spectrofluorometric method. In contrast to the result by flow cytometry, the extent of calcein uptake into Caco-2 cells from liposomes was significantly higher than that from solution ($p < 0.05$) (Figure 17). When calcein-loaded liposomes were endocytosed into the cells, the fluorescence intensity measured by flow cytometry was low since calcein was confined in the endosomes/lysosomes. After the cells were digested, calcein trapped in the endosomes/lysosomes was released and diluted several fold in the medium. Therefore, the fluorescence intensity from liposome treatment markedly increased.

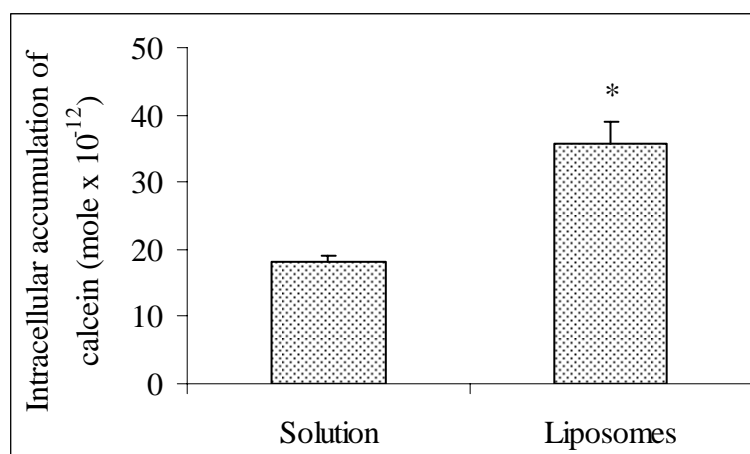


Figure 17: Intracellular accumulation of calcein from calcein solution and calcein - loaded liposomes (80 μ M of calcein) determined by spectrofluorometric method. Data are shown as mean \pm SEM (n = 3).

* $p < 0.05$ compared with calcein solution

5.5 Effect of inhibition of endocytosis on the uptake of calcein AM-loaded liposomes into Caco-2 cells

5.5.1 Effect of cytochalasin B on the uptake of calcein AM-loaded liposomes into Caco-2 cells

Pre-treatment of Caco-2 cells with cytochalasin B at 5 $\mu\text{g/ml}$ was reported to damage the tight junction (Ma et al., 2000). In the preliminary study, cytochalasin B at 5 $\mu\text{g/ml}$ also changed the morphology of Caco-2 cells markedly. Thus, only the pre-treatment condition was used in this study with concentrations of cytochalasin B below 5 $\mu\text{g/ml}$ (at 1.25 and 2.5 $\mu\text{g/ml}$). Figure 18 shows the uptake of calcein AM from calcein AM-loaded liposomes after pre-treatment with cytochalasin B at 1.25 and 2.5 $\mu\text{g/ml}$ for 60 min. The extent of calcein AM uptake into Caco-2 cells was not significantly different from that of the control group ($p > 0.05$). Both concentrations of cytochalasin B did not have any effect on the uptake of calcein AM from liposomes. Thus, the endocytosis process in Caco-2 cells could not be inhibited by cytochalasin B under the experimental condition used.

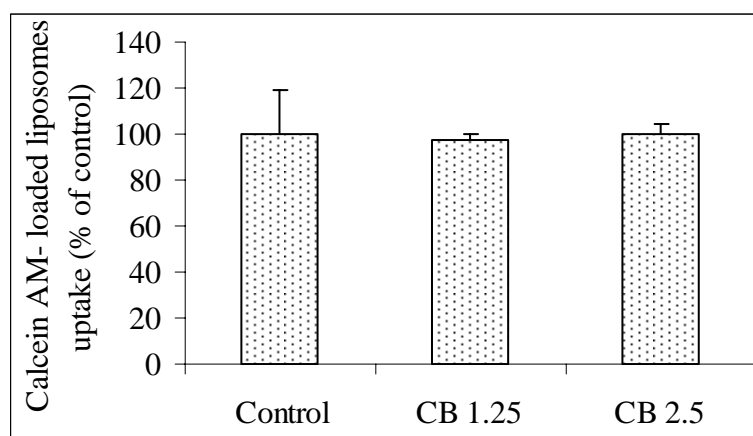


Figure 18: Uptake of calcein AM from calcein AM-loaded liposomes into Caco-2 cells after pre-treatment with cytochalasin B at 1.25 $\mu\text{g/ml}$ (CB 1.25) and 2.5 $\mu\text{g/ml}$ (CB 2.5) for 60 min. Data are shown as mean \pm SEM ($n = 3$).

In addition, the inhibition of uptake of liposomes labeled with NBD-PE and calcein-loaded liposomes by cytochalasin B was also studied. Cytochalasin B slightly inhibited the vesicle uptake (Figures 19 and 20). No significant inhibition of both the liposomal lipid marker and the aqueous phase marker was seen. This result confirmed the evidence seen with calcein AM-loaded liposomes.

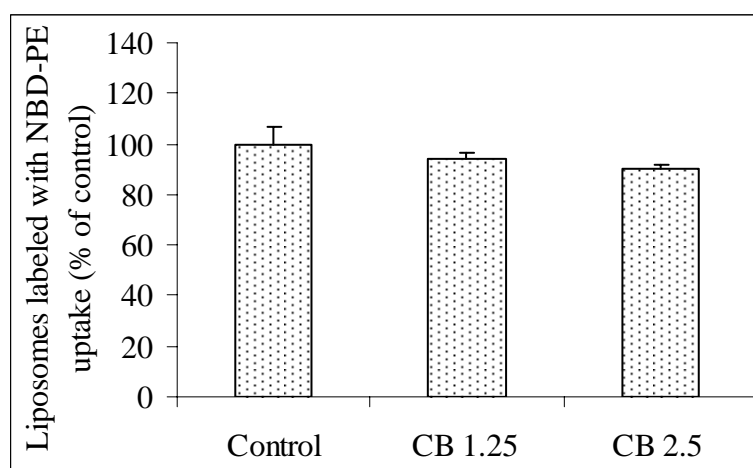


Figure 19: Uptake of liposomes labeled with NBD-PE into Caco-2 cells after pre-treatment with cytochalasin B at 1.25 $\mu\text{g/ml}$ (CB 1.25) and 2.5 $\mu\text{g/ml}$ (CB 2.5) for 60 min. Data are shown as mean \pm SEM (n = 3).

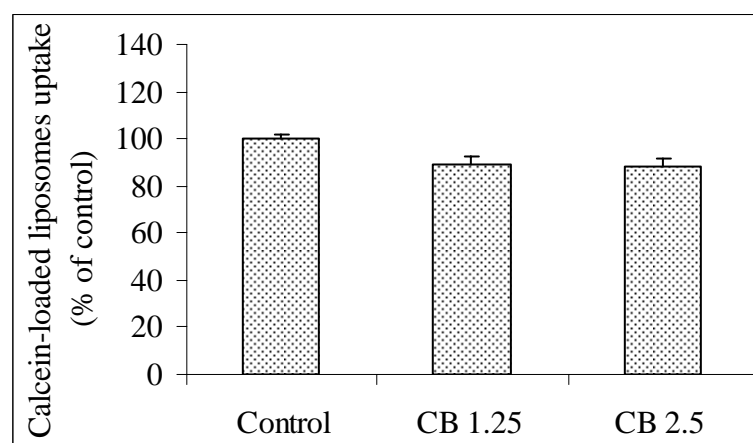


Figure 20: Uptake of calcein from calcein-loaded liposomes into Caco-2 cells after pre-treatment with cytochalasin B at 1.25 $\mu\text{g/ml}$ (CB 1.25) and 2.5 $\mu\text{g/ml}$ (CB 2.5) for 60 min. Data are shown as mean \pm SEM (n = 3).

Cytochalasin B inhibits endocytosis via actin depolymerization (Watson, Jones, and Stephens, 2005). It has been used as an endocytosis inhibitor to inhibit uptake of a wide range of materials into cells. Inhibition of liposome uptake by cytochalasin B and metabolic inhibitors has been used to verify endocytosis of liposomes by various cells (Legrand et al., 1996; Palm et al., 2007; Poste and Papahadjopoulos, 1976; Wong et al., 2006). The extent of inhibition of endocytosis process with endocytosis inhibitors varies and depends on several factors. These factors include cell type, experimental condition, and type of inhibitor(s) as well as concentration used. For example, in 3T3 cells, cytochalasin B (20 $\mu\text{g}/\text{ml}$) caused a marked inhibition (up to 90%) in the uptake of solid charged vesicles and fluid neutral vesicles (Poste and Papahadjopoulos, 1976). Smaller degrees of inhibition were seen in some other studies. Cytochalasin B at a concentration of 5 $\mu\text{g}/\text{ml}$ inhibited the uptake of liposomes and vesosomes in J774A.1 cells by 50% (Mishra et al., 2006) and the endocytosis of liposome-DNA complexes in RTE cells was 50% inhibited (Matsui et al., 1997). The amphotericin B liposome uptake was inhibited with cytochalasin B (6 μM) by 62-75% (Legrand et al., 1996). Cytochalasin B at the same concentration as that used in this present study (2.5 $\mu\text{g}/\text{ml}$) significantly decreased the uptake of human growth hormone in perfused rat kidneys (Kau and Maack, 1986) and inhibited glucose transport by more than 85% in J774A.1 macrophages (Echevarria and Verkman, 1992).

Alexa Fluor[®] 488-conjugated dextran, an endocytosis marker, was used to validate the inhibitory effectiveness of cytochalasin B in Caco-2 cells. The fluorescence intensities from dextran uptake of the control group and the treatment with cytochalasin B were 22.91 and 36.88 relative fluorescence units, respectively (Figure 21). The result reveals that cytochalasin B at 2.5 $\mu\text{g}/\text{ml}$ was unable to inhibit endocytosis in Caco-2 cells. Therefore, the use of cytochalasin B as an endocytosis inhibitor in this study could not corroborate the endocytosis mechanism.

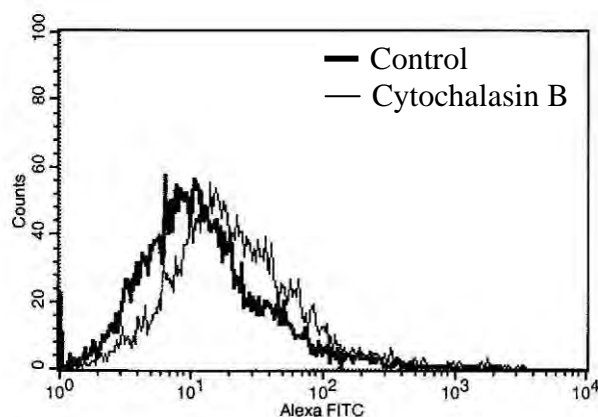


Figure 21: Fluorescence histograms from Caco-2 cells incubated with Alexa Fluor[®] 488-conjugated dextran after pre-treatment with cytochalasin B at 2.5 $\mu\text{g/ml}$ (Cytochalasin B) and with DMEM (Control)

5.5.2 Effect of metabolic inhibitors on the uptake of calcein AM-loaded liposomes into Caco-2 cells

The efficiency of selected metabolic inhibitors in inhibiting endocytosis in Caco-2 cells was further evaluated using Alexa Fluor[®] 488-conjugated dextran as the endocytosis marker. The fluorescence histograms of the uptake of Alexa Fluor[®] 488-conjugated dextran with sodium azide and with sodium azide in the presence of sodium fluoride were not different from that of the control group (Figures 22-A and 22-B). The decrease in dextran uptake was seen in the condition using sodium azide with deoxyglucose as the inhibitors (Figure 22-C). An effort to use the combination of sodium azide and sodium iodoacetate to inhibit the endocytosis was also made, but severe toxicity to the cells was observed. After 90 min of the incubation period, Caco-2 cells were detached from the culture plates. The limited inhibitory effect of these metabolic inhibitors on endocytosis activity of Caco-2 cells indicated that these metabolic inhibitors at the concentrations reported in the literature were not adequate for Caco-2 cells. Since the conditions in the literature were those used with other cells, not Caco-2 cells, this result might also indicate the discrepancy in responses to metabolic inhibitors due to the cell type. No report on effective endocytosis inhibition in Caco-2 cells was available at the time of this present study. Most research on endocytosis inhibition was aimed at phagocytotic cells, mostly the macrophages.

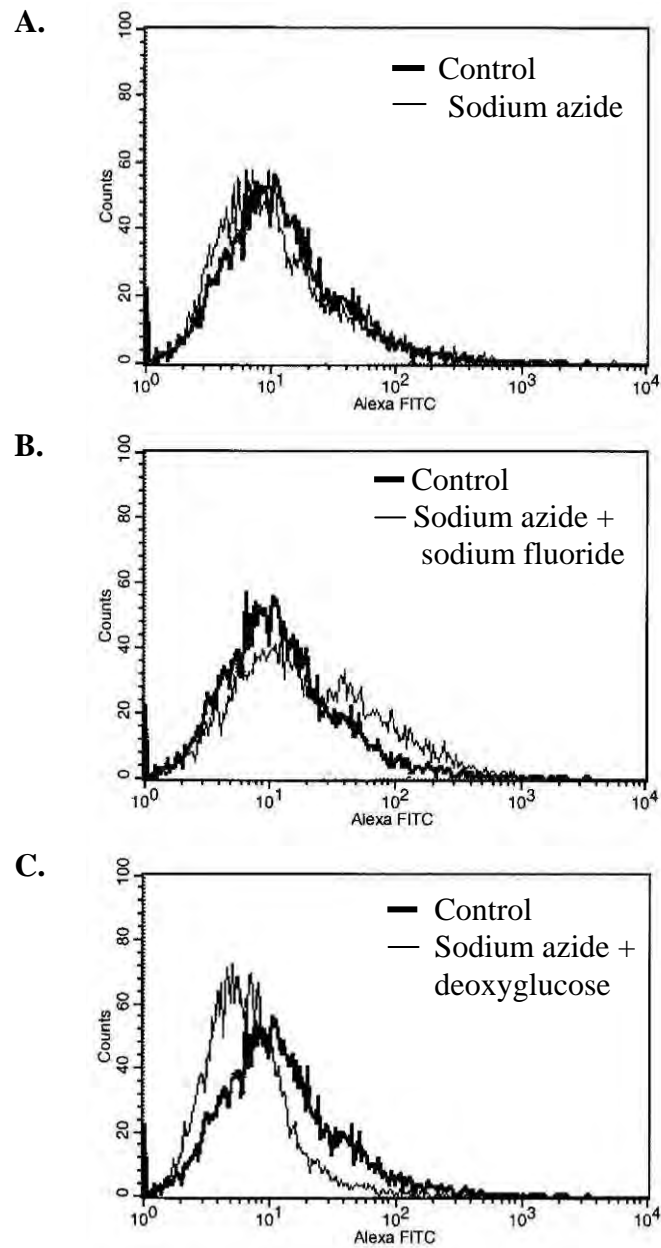


Figure 22: Fluorescence histograms from Caco-2 cells incubated with Alexa Fluor[®] 488-conjugated dextran in the presence of various metabolic inhibitors: (A) sodium azide 15 mM, (B) sodium azide 15 mM + sodium fluoride 10 mM, and (C) sodium azide 15 mM + deoxyglucose 50 mM. Cells incubated with the fluorescent dextran in the absence of metabolic inhibitor were used as the control group.

The extents of uptake of calcein AM-loaded liposomes and Alexa Fluor[®] 488-conjugated dextran into Caco-2 indicate that complete inhibition of endocytosis could not be achieved in all treatments (Table 10). However, the results still supported the endocytosis mechanism in calcein AM-loaded liposome uptake into Caco-2 cells due to the similar trend of inhibition to that of the positive control Alexa Fluor[®] 488-conjugated dextran by these metabolic inhibitors. The difference in the extents of inhibition might be due partly to the different concentrations of the liposomes and the dextran used in the study. The maximum inhibition was seen in the treatment condition using the combination of respiratory inhibitor and glycolysis inhibitor (sodium azide and deoxyglucose). The use of only sodium azide showed moderate inhibition. The minimum inhibitory effect was observed when sodium azide and sodium fluoride were concomitantly used. Deoxyglucose increased the efficiency of sodium azide. Unexpectedly, the presence of sodium fluoride seemed to attenuate, rather than to potentiate, the effect of sodium azide. The reason behind this observation was not further investigated.

In the uptake of calcein AM-loaded liposomes, the maximum effect of endocytosis inhibition occurred at 60 mM of sodium azide with 50 mM deoxyglucose. The efficiency of sodium azide was not concentration dependent in all conditions, regardless of whether it was used alone or in combination with other compounds. The extent of endocytosis inhibition by metabolic inhibitors is again likely to depend on the cell type, experimental condition, and type of inhibitor(s) as well as concentration used. In a previous study, sodium azide only inserted minimal effect on the uptake of egg PC liposomes into 3T3 cells. In contrast, the combination of sodium azide with either sodium fluoride or deoxyglucose could inhibit the endocytosis in 3T3 cells up to 90% (Poste and Papahadjopoulos, 1976).

Table 10: Uptake of calcein AM-loaded liposomes and Alexa Fluor[®] 488-conjugated dextran into Caco-2 cells in the presence of various metabolic inhibitors. Data are shown as mean \pm SEM (n = 3-6).

Treatment	Calcein AM-loaded liposome uptake (% of control)	Alexa Fluor [®] 488-conjugated dextran uptake (% of control)
Control	100.0 \pm 11.2	100.0 \pm 19.8
Sodium azide 15 mM	70.78 \pm 3.81	97.57 \pm 13.1
Sodium azide 30 mM	70.12 \pm 4.65	ND
Sodium azide 60 mM	59.86 \pm 1.98	ND
Sodium fluoride 10 mM		
+ Sodium azide 15 mM	80.06 \pm 6.27	168.4 \pm 6.27
+ Sodium azide 30 mM	83.56 \pm 9.32	ND
+ Sodium azide 60 mM	70.89 \pm 4.37	ND
Deoxyglucose 50 mM		
+ Sodium azide 15 mM	66.29 \pm 12.5	43.10 \pm 2.49
+ Sodium azide 30 mM	65.63 \pm 11.9	ND
+ Sodium azide 60 mM	54.49 \pm 2.56	ND

ND = not determined

5.5.3 Effect of temperature on calcein AM uptake into Caco-2 cells

Effect of temperature is often used to identify energy-dependent, carrier-mediated processes (Lee et al., 1992; Mamdouh et al., 1996). The approach was used in the present study to substantiate endocytosis of calcein AM-loaded liposomes into Caco-2 cells. At 4 °C, the extents of calcein AM uptake from both calcein AM solution and calcein AM-loaded liposomes were reduced by approximately 60% when compared to the uptake at 37 °C (Figure 23). The marked effect of temperature on the uptake of calcein AM solution and calcein AM-loaded liposomes strongly supported an energy-dependent, carrier-mediated process. Thus, the result verified the endocytosis of calcein AM-loaded liposomes, whereas fluid-phase endocytosis might be responsible for the uptake of calcein AM solution (Tenopoulou et al, 2007). Adsorption of liposomes on the cell membrane was excluded since the flow

cytometric technique used would not detect any non-fluorescent calcein AM that was not internalized.

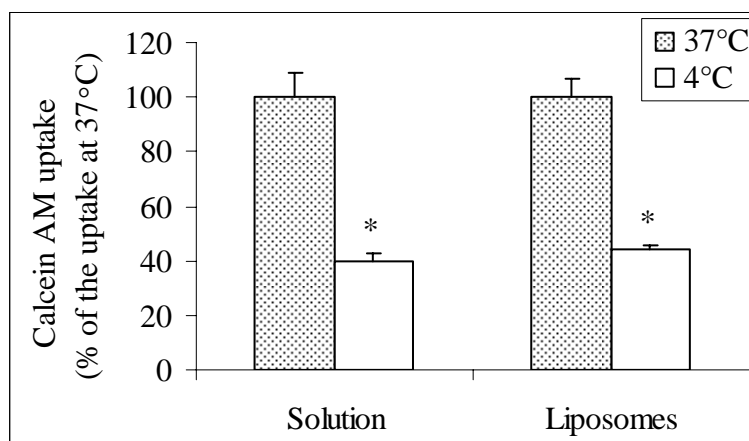


Figure 23: Intracellular accumulation of calcein AM in Caco-2 cells incubated with calcein AM solution and calcein AM-loaded liposomes at 37 °C and 4 °C. Data are shown as mean \pm SEM (n = 4).

*p < 0.05 compared with the uptake at 37 °C

Liposome uptake at 37 °C usually represents the combination of vesicular adsorption to cell surface and active cellular endocytosis. Since endocytosis is inhibited at 4 °C, the difference between cellular liposome association at 37 °C and 4 °C is a measure for the extent of liposome internalization by endocytosis (Mamdouh et al., 1996; Torchilin and Weissig, 2003). Although liposome-cell fusion can occur at low temperature (Knoll et al., 1988), the endocytosis was probably the main mechanism of the internalization of calcein AM-loaded liposomes since fusion had already been ruled out by the CLSM and the fluorescence dequenching techniques as discussed under Section 5.3 and 5.4. Several other studies also used the temperature effect as a means to verify that endocytosis was the major mechanism of liposome uptake into cells. The uptake of liposomes into mouse bone marrow macrophages, Calu-3 cells, L1210 cells, PC-3 cells, A 375 cells, and Caco-2 cells was considerably reduced at 4 °C (Allen et al., 1991; Cryan et al., 2006; Jansons et al., 1978; Kheirloomoom and Ferrara, 2007; Lukanawonakul, 2005).

However, it should be noted that the reduced uptake seen at low temperatures may not result from only the endocytosis inhibition. Low temperatures also affect membrane fluidity and the activity of enzymes in the cells (Kawakami, Nishihara, and Hirano, 1999; Mamdouh et al., 1996; Somero, 1978). In this study, calcein, a product of enzyme hydrolysis, was monitored. The lower uptake might also be attributed partly to the lower esterase activity in the cells at the lower temperature.

6. Effect of liposomal composition on calcein AM uptake into Caco-2 cells

6.1 Effect of charge-imposing lipid on calcein AM uptake into Caco-2 cells

Effect of charge-imposing lipid on liposome-cell interaction is well established (Lee et al., 1992; Miller et al., 1998; Papahadjopoulos et al., 1973; Poste and Papahadjopoulos, 1976). In this present study, calcein AM uptake from neutral, negatively charged, and positively charged liposomes into Caco-2 cells is shown in Figure 24. The extents of total calcein AM uptake from neutral liposomes and negatively charged liposomes in 90 min were $1.02 \pm 0.09 \times 10^{-12}$ mole and $0.93 \pm 0.18 \times 10^{-12}$ mole, respectively. Calcein AM from both types of liposomes was taken up by Caco-2 cells more efficiently than that from calcein AM solution. On the other hand, positively charged liposomes delivered only $0.11 \pm 0.08 \times 10^{-12}$ mole of calcein AM into the cells and, thus, failed to enhance the calcein AM uptake when compared with calcein AM solution. The ability to enhance the delivery of calcein AM by the neutral liposomes was also seen with another P-gp substrate, rhodamine 123 (Lukanawonakul, 2005). On the other hand, positively charged liposomes reduced the cellular uptake of both calcein AM in this present study and rhodamine 123 in the previous study by Lukanawonakul (2005), probably by a strong binding between the positively charged liposomes with the negatively charged Caco-2 cells (Manconi et al., 2007). In this study, negatively charged liposomes enhanced cellular uptake of calcein AM into Caco-2 cells. On the contrary, the uptake into Caco-2 cells of rhodamine 123 was reduced by negatively charged liposomes (Lukanawonakul, 2005). These results indicated that the different molecules incorporated into the liposomal bilayer might affect the properties of the liposomal membrane, and, thus, the liposome-cell interaction. Since rhodamine 123 possesses positive net charge on its molecule, it might affect the net surface charge of liposomes. An attempt to

measure the surface charge of rhodamine 123-loaded liposomes had been made in this present study without success due to the charring of these rhodamine 123-containing liposomal preparations by the laser beam.

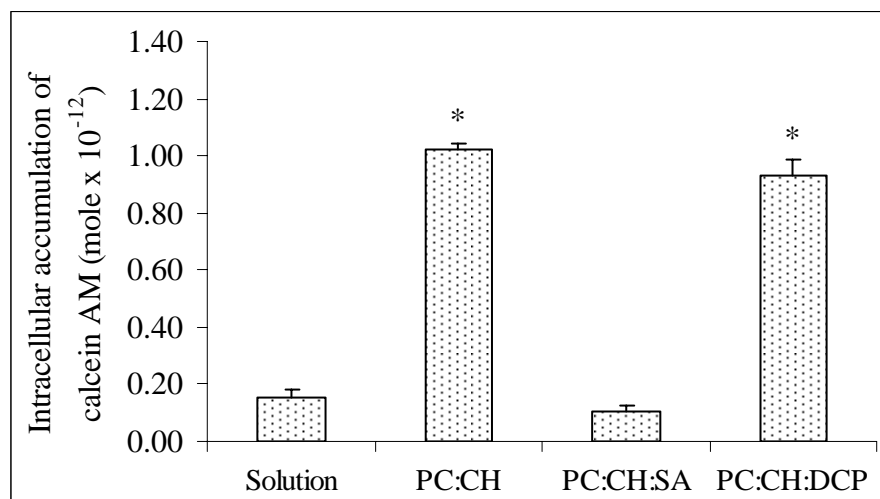


Figure 24: Intracellular accumulation of calcein AM from calcein AM solution, calcein AM-loaded neutral (PC:CH), positively charged (PC:CH:SA), and negatively charged (PC:CH:DCP) liposomes. Data are shown as mean \pm SEM (n = 3). *p < 0.05 compared with calcein AM solution

6.2 Effect of cholesterol content on calcein AM uptake into Caco-2 cells

Figure 25 shows the uptake of calcein AM from neutral liposomes comprising soybean PC and CH at different molar ratios (6:4, 7:3, 8:2, and 10:0). The calcein AM uptake from all neutral liposome formulations, regardless of CH content, was significantly better than that from solution (p < 0.05). Inclusion of CH significantly reduced calcein AM uptake from neutral liposomes (p < 0.05). The difference in calcein AM uptake was not seen among CH-containing liposomes (p > 0.05).

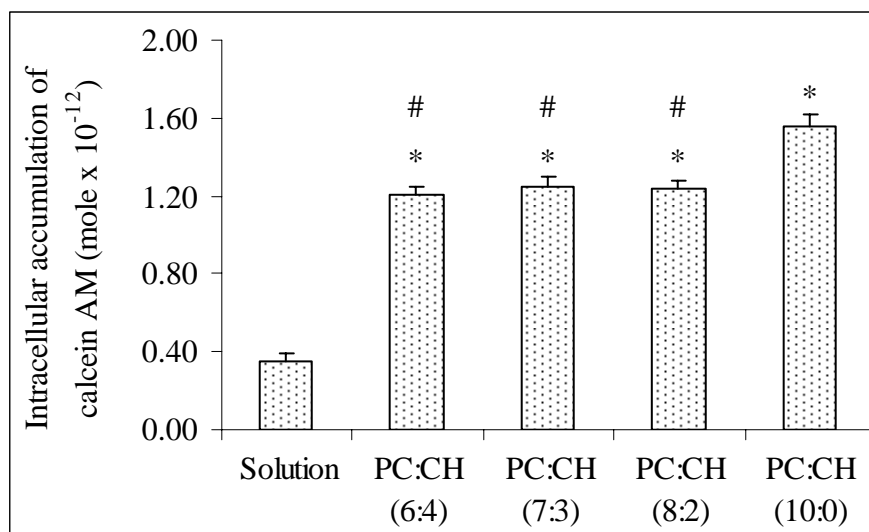


Figure 25: Intracellular accumulation of calcein AM from calcein AM solution, calcein AM-loaded neutral liposomes with the different PC:CH ratios. Data are shown as mean \pm SEM (n = 4).

*p < 0.05 compared with calcein AM solution

#p < 0.05 compared with calcein AM-loaded liposomes (PC:CH =10:0)

CH might insert its effect on cellular liposome uptake in many ways. It can interact with P-gp or modulate the P-gp function, resulting in higher P-gp substrate uptake (Tessner and Stenson, 2000; Wang, et al., 2000). Its incorporation into liposomal bilayers leads to major changes in the properties of the vesicles including membrane fluidity. At a temperature higher than the transition temperature of soybean PC, the presence of CH in liposomes causes the liposomal membrane to condense and, consequently, the fluidity of the liposomal membrane decrease (New, 1997). These changes may affect the liposome-cell interaction and lead to the differences in drug delivery efficiency. Other research groups have also reported the effect of CH inclusion in liposomal membrane seen in this study. Inclusion of CH reduces liposome uptake by macrophages and the presence of CH (0-50 mole%) reduces the liposome uptake in a dose-dependent manner (Allen et al., 1991). The effect of the different amounts of CH in liposomes was not seen with the calcein AM-loaded liposomes in this study. CH, in the form of micelles, is known to interact with P-gp resulting in increased P-gp substrate uptake by the cells (Tessner and Stenson, 2000;

Wang et al., 2000). Such P-gp modulating effect of CH was not seen in this study. It was possible that in this present study CH was tightly bound to the liposomal membrane and could not gain an access to its P-gp binding sites due to the relatively large size of liposomes. However, though this present study indicated that CH decreased the effect of liposomes in the delivery of the P-gp substrate calcein AM, inclusion of CH in liposomes might still be necessary for the stability of liposomes in the biological environment.

6.3 Effect of phosphatidylcholine type on calcein AM uptake into Caco-2 cells

When soybean PC in liposomes was replaced by DPPC, the uptake of calcein AM into Caco-2 cells was much reduced (Figure 26). The same finding was seen with both CH-riched and CH-free liposomes. A previous study reported that DPPC liposomes could increase uptake of epirubicin, a P-gp substrate, into Caco-2 cells (Lo, 2000). The enhanced uptake of calcein AM into Caco-2 cells was also seen in this present study. Soybean PC-based liposomes seemed to be much better than DPPC-based liposomes for calcein AM delivery.

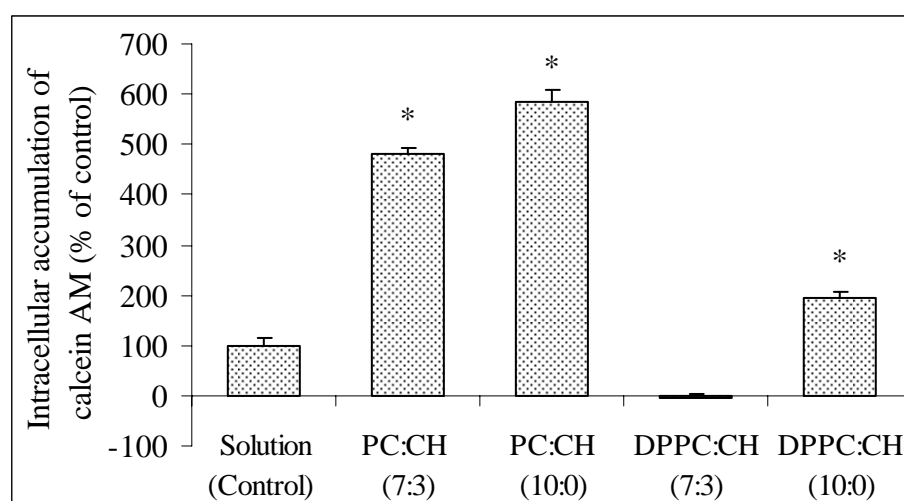


Figure 26: Intracellular accumulation of calcein AM from calcein AM solution, calcein AM-loaded neutral liposomes with either soybean PC or DPPC and CH at 7:3 and 10:0 molar ratios. Data are shown as mean \pm SEM (n = 4).

*p < 0.05 compared with calcein AM solution

DPPC and soybean PC have the same choline head group and the transition temperatures are at 41.5 °C and -15 ± 10 °C, respectively (Cevc, 1993). At the incubation temperature of 37 °C, DPPC liposomes were in the gel state, while soybean PC-based liposomes were in the liquid-crystalline state. Rigidity of bilayer is known to affect liposome-cell interaction (Allen et al., 1991; Poste and Papahadjopoulos, 1976; Uchiyama et al., 1995). Liposomes in liquid-crystalline state are more efficiently taken up by several cells such as J774 cells and HeLa cells (Manconi et al., 2007; Poste and Papahadjopoulos, 1976). The results of this study are in good agreement with previous studies. The higher uptake of soybean PC liposomes when compared to DPPC liposomes has also been reported in the literature. When the different phosphatidylcholine types were compared, the efficiency of DPPC liposomes in delivery of liposomal content into HeLa cells was less than that of soybean lecithin liposomes (Manconi et al., 2007). It should also be noted that DPPC liposomes with 30% CH content failed totally to deliver calcein AM to Caco-2 cells.

7. Cell viability study

Positively charged compounds including SA are usually regarded as toxic to the cells (Senior, Trimble, and Maskiewicz, 1991). To verify that the lower uptake of calcein AM from positively charged liposomes by Caco-2 cells was not caused by the lower amount of viable cells due to liposome toxicity, cell viability study was performed. The cytotoxicity data of calcein AM solution, calcein AM-loaded neutral (PC:CH), positively charged (PC:CH:SA), and negatively charged (PC:CH:DCP) liposomes are shown in Figure 27. In all liposome treatments, the cell viability was approximately 90% of that of the control ($94.0 \pm 1.24\%$, $88.9 \pm 1.26\%$, and $95.3 \pm 2.99\%$ from neutral, negatively charged, and positively charged liposomes, respectively). The results indicate that calcein AM solution and liposomes of all types studied were not toxic to Caco-2 cells at the concentrations used. Thus, the lower uptake of calcein AM from the positively charged liposomes described under Section 6.1 was not due to the toxicity of liposomes to the cells.

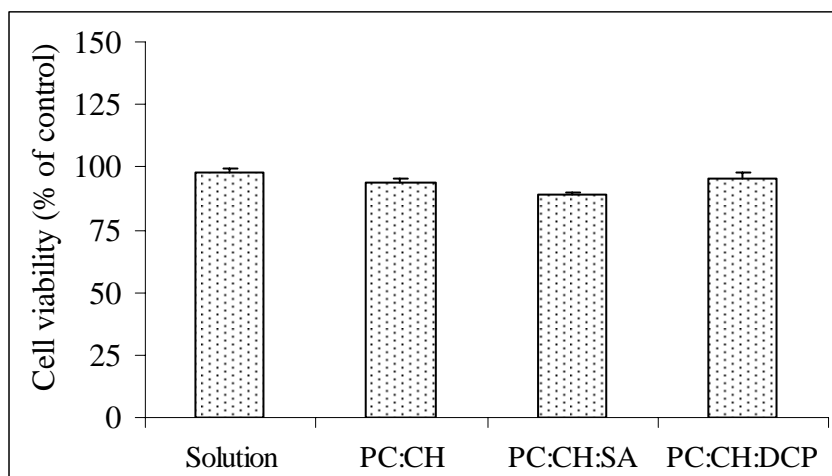


Figure 27: Cytotoxicity of calcein AM solution, calcein AM-loaded neutral (PC:CH), positively charged (PC:CH:SA), and negatively charged (PC:CH:DCP) liposomes to Caco-2 cells. Data are shown as mean \pm SEM (n = 3).

CHAPTER V

CONCLUSIONS

In this study, the probable mechanisms by which liposomes enhance delivery of P-gp substrates into Caco-2 cells was investigated with calcein AM as a model P-gp substrate. The effects of liposomal formulation factors on the delivery of P-gp substrates into the cells were also studied.

The uptake studies showed the higher calcein AM uptake from neutral PC liposomes than that from solution. The extent of calcein AM uptake from liposomes was liposomal concentration and time dependent with no saturation seen in the concentration range studied. The results from confocal laser scanning microscopy and fluorescence dequenching technique studies were used to identify the most probable mechanism of liposome uptake by Caco-2 cells. The fluorescence pattern and intensity from these experiments fitted well with that of endocytosis. Both the use of endocytosis inhibitors and the effect of temperature also provided the results that supported endocytosis of liposomes into Caco-2 cells. On the other hand, the effect of blank liposomes on cell membrane permeability and P-gp function was not seen. The result indicated that the enhancement of calcein AM uptake from liposomes did not occur via the changing in cell membrane permeability and/or modulating of P-gp function by liposomes. Thus, endocytosis was likely to be the main mechanism by which liposomes enhanced the calcein AM uptake into Caco-2 cells.

When liposomes with different compositions were used to deliver the P-gp substrate, the result showed that calcein AM from both neutral and negatively charged liposomes was taken up by Caco-2 cells similarly and more efficiently than that from calcein AM solution. Positively charged liposomes failed to deliver calcein AM to the cells. The presence of 20-40 mole% of cholesterol in PC liposomes significantly reduced calcein AM uptake into Caco-2 cells. In addition, soybean PC liposomes, both with or without cholesterol, could increase the cellular uptake of calcein AM better than DPPC liposomes did.

In conclusion, the overall results indicated that the enhanced uptake of the P-gp substrate calcein AM into Caco-2 cells occurred via endocytosis. The liposomal

compositions (inclusion of charged lipids, cholesterol content, and type of phosphatidylcholine) played a significant role in the delivery of calcein AM into the cells. Therefore, the development of successful liposomal delivery systems for P-gp substrates should be based on both endocytosis mechanism and the effects of liposomal composition.

However, charged lipids seemed to exert a strong effect on calcein AM uptake in a different way from that seen with a positively charged P-gp substrate in a previous study. The physicochemical properties of P-gp substrates might also affect liposome-cell interactions, leading to a different uptake mechanism. Thus, the investigation involving P-gp substrates with different surface charges and/or different aqueous solubilities should also be carried out. On the other hand, modification of the liposomal composition to promote liposome-cell interactions via other mechanisms might also result in liposome uptake that could also bypass the P-gp function. Such an approach might be worth trying for wider application of liposomes in cellular delivery of P-gp substrates. For example, inclusion of a fusogen into liposomal membrane might promote fusion that could lead to enhanced cellular delivery of P-gp substrates with relatively high aqueous solubility.

REFERENCES

- Allen, T. M., Austin, G. A., Chonn, A., Lin, L., and Lee, K. C. 1991. Uptake of liposomes by cultured mouse bone marrow macrophages: influence of liposome composition and size. Biochimica et Biophysica Acta (BBA) - Biomembranes 1061 (1): 56-64.
- Ambudkar, S. V., Kim, I.-W., and Sauna, Z. E. 2006. The power of the pump: Mechanisms of action of P-glycoprotein (ABCB1). European Journal of Pharmaceutical Sciences 27 (5): 392-400.
- Anderle, P., Niederer, E., Rubas, W., Hilgendorf, C., Spahn-Langguth, H., Wunderli-Allenspach, H., et al. 1998. P-glycoprotein (P-gp) mediated efflux in Caco-2 cell monolayers: The influence of culturing conditions and drug exposure on P-gp expression levels. Journal of Pharmaceutical Sciences 87 (6): 757-762.
- Annaert, P. P., Turncliff, R. Z., Booth, C. L., Thakker, D. R., and Brouwer, K. L. R. 2001. P-glycoprotein-mediated in vitro biliary excretion in sandwich-cultured rat hepatocytes. Drug Metabolism and Disposition 29 (10): 1277-1283.
- Artursson, P. and Borchardt, R. T. 1997. Intestinal drug absorption and metabolism in cell cultures: Caco-2 and beyond. Pharmaceutical Research 14 (12): 1655-1658.
- Avanti Polar Lipids. DPPC [online]. Available from: www.avantilipids.com [2008, May 1]
- Balimane, P. V. and Chong, S. 2005. Cell culture-based models for intestinal permeability: A critique. Drug Discovery Today 10 (5): 335-343.
- Bosch, I., Dunussi-Joannopoulos, K., Wu, R.-L., Furlong, S. T., and Croop, J. 1997. Phosphatidylcholine and phosphatidylethanolamine behave as substrates of the human MDR1 P-glycoprotein. Biochemistry 36 (19): 5685-5694.
- Cartiera, M. S., Johnson, K. M., Rajendran, V., Caplan, M. J., and Saltzman, W. M. 2009. The uptake and intracellular fate of PLGA nanoparticles in epithelial cells. Biomaterials 30 (14): 2790-2798.
- Cevc, G. 1993. Phospholipids Handbook. Germany: Marcel Dekker, Inc.

- Chan, L. M. S., Lowes, S., and Hirst, B. H. 2004. The ABCs of drug transport in intestine and liver: efflux proteins limiting drug absorption and bioavailability. European Journal of Pharmaceutical Sciences 21 (1): 25-51.
- Chen, J., Ping, Q. N., Guo, J. X., Chu, X. Z., and Song, M. M. 2006. Effect of phospholipid composition on characterization of liposomes containing 9-nitrocamptothecin. Drug Development and Industrial Pharmacy 32 (6): 719 - 726.
- Chu, C.-J., Dijkstra, J., Lai, M.-Z., Hong, K., and Szoka, F. C. 1990. Efficiency of cytoplasmic delivery by pH-sensitive liposomes to cells in culture. Pharmaceutical Research 7 (8): 824-834.
- Chu, W. H. and Lu, C. P. 2005. Role of microfilaments and microtubules in the invasion of EPC cells by *Aeromonas hydrophila*. Journal of Veterinary Medicine Series B 52 (4): 180-182.
- Connor, J. and Huang, L. 1985. Efficient cytoplasmic delivery of a fluorescent dye by pH-sensitive immunoliposomes. Journal of Cell Biology 101 (2): 582-589.
- Cooper, G. M. 2000. The Cell. Sinauer Associates, Inc.
- Corning Incorporated. 2009. Corning Life Science [online]. Available from: www.corning.com [2009, January 10]
- Crivellato, E., Candussio, L., Rosati, A. M., Bartoli-Klugmann, F., Mallardi, F., and Decorti, G. 2002. The fluorescent probe bodipy-FL-verapamil is a substrate for both P-glycoprotein and multidrug resistance-related protein (MRP)-1. The Journal of Histochemistry & Cytochemistry. 50 (5): 731-734.
- Cryan, S.-A., Devocelle, M., Moran, P. J., Hickey, A. J., and Kelly, J. G. 2006. Increased intracellular targeting to airway cells using octaarginine-coated liposomes: In vitro assessment of their suitability for inhalation. Molecular Pharmaceutics 3 (2): 104-112.
- Cuvier, C., Roblot-Treupel, L., Millot, J. M., Lizard, G., Chevillard, S., Manfait, M., et al. 1992. Doxorubicin-loaded nanospheres bypass tumor cell multidrug resistance. Biochemical Pharmacology 44 (3): 509-517.
- Dabholkar, R. D., Sawant, R. M., Mongayt, D. A., Devarajan, P. V., and Torchilin, V. P. 2006. Polyethylene glycol-phosphatidylethanolamine conjugate (PEG-PE)-based mixed micelles: Some properties, loading with paclitaxel, and

- modulation of P-glycoprotein-mediated efflux. International Journal of Pharmaceutics 315 (1-2): 148-157.
- Dantzig, A. H., Shepard, R. L., Cao, J., Law, K. L., Ehlhardt, W. J., Baughman, T. M., et al. 1996. Reversal of P-Glycoprotein-mediated Multidrug Resistance by a Potent Cyclopropyldibenzosuberane Modulator, LY335979. Cancer Research 56 (18): 4171-4179.
- Daugherty, A. L. and Mrsny, R. J. 1999. Regulation of the intestinal epithelial paracellular barrier. Pharmaceutical Science & Technology Today 2 (7): 281-287.
- Degim, Z. I., Ünal, N., Essiz, D., and Abbasoglu, U. 2004. The effect of various liposome formulations on insulin penetration across Caco-2 cell monolayer. Life Sciences 75 (23): 2819-2827.
- Deng, W.-j., Yang, X.-q., Liang, Y.-j., Chen, L.-m., Yan, Y.-y., Shuai, X.-t., et al. 2007. FG020326-loaded nanoparticle with PEG and PDLA improved pharmacodynamics of reversing multidrug resistance *in vitro* and *in vivo*. Acta Pharmacologica Sinica 28 (6): 913-920.
- Echevarria, M. and Verkman, A. 1992. Optical measurement of osmotic water transport in cultured cells. Role of glucose transporters. Journal of General Physiology 99 (4): 573-589.
- El-Sayed, M., Rhodes, C. A., Ginski, M., and Ghandehari, H. 2003. Transport mechanism(s) of poly (amidoamine) dendrimers across Caco-2 cell monolayers. International Journal of Pharmaceutics 265 (1-2): 151-157.
- Eneroth, A., Åström, E., Hoogstraate, J., Schrenk, D., Conrad, S., Kauffmann, H. M., et al. 2001. Evaluation of a vincristine resistant Caco-2 cell line for use in a calcein AM extrusion screening assay for P-glycoprotein interaction. European Journal of Pharmaceutical Sciences 12 (3): 205-214.
- Essodaïgui, M., Broxterman, H. J., and Garnier-Suillerot, A. 1998. Kinetic Analysis of Calcein and Calcein Acetoxymethylester Efflux Mediated by the Multidrug Resistance Protein and P-Glycoprotein. Biochemistry 37 (8): 2243-2250.
- Faassen, F., Vogel, G., Spanings, H., and Vromans, H. 2003. Caco-2 permeability, P-glycoprotein transport ratios and brain penetration of heterocyclic drugs. International Journal of Pharmaceutics 263 (1-2): 113-122.

- Fang, N., Wang, J., Mao, H.-Q., Leong, K. W., and Chan, V. 2003. BHEM-Chol/DOPE liposome induced perturbation of phospholipid bilayer. Colloids and Surfaces B: Biointerfaces 29 (4): 233-245.
- Fardel, O., Lecureur, V., and Guillouzo, A. 1996. The P-glycoprotein multidrug transporter. General Pharmacology: The Vascular System 27 (8): 1283-1291.
- Ferrec, E. L., Chesne, C., Artusson, P., Brayden, D., Fabre, G., Gires, P., et al. 2001. In vitro models of the intestinal barrier. Alternatives to Laboratory Animals 29: 649-668.
- Freshney, R. I. 2005. Culture of animal cells : a manual of basic technique. 5th ed. USA: Wiley-Liss.
- Fretz, M. M., Koning, G. A., Mastrobattista, E., Jiskoot, W., and Storm, G. 2004. OVCAR-3 cells internalize TAT-peptide modified liposomes by endocytosis. Biochimica et Biophysica Acta (BBA) - Biomembranes 1665 (1-2): 48-56.
- Gan, L.-S. L. and Thakker, D. R. 1997. Applications of the Caco-2 model in the design and development of orally active drugs: Elucidation of biochemical and physical barriers posed by the intestinal epithelium. Advanced Drug Delivery Reviews 23 (1-3): 77-98.
- Gheuens, E. E. O., van Bockstaele, D. R., van der Keur, M., Tanke, H. J., van Oosterom, A. T., and De Bruijn, E. A. 1991. Flow cytometric double labeling technique for screening of multidrug resistance. Cytometry 12 (7): 636-644.
- Gottesman, M. M. and Pastan, I. 1993. Biochemistry of multidrug resistance mediated by the multidrug transporter. Annual Review of Biochemistry 62: 385-427.
- Grace Bio Labs. 2009. Biological coating procedures for CultureWellTM, MultiSlipTM and SecureSlipTM glass coverslips [online]. Available from: www.gracebio.com [2008, May 1]
- Graham, J. M. and Higgins, J. A. 1997. Membrane analysis. Guildford: Biddles.
- Hämmerle, S. P., Rothen-Rutishauser, B., Krämer, S. D., Günthert, M., and Wunderli-Allenspach, H. 2000. P-Glycoprotein in cell cultures: a combined approach to study expression, localisation, and functionality in the confocal microscope. European Journal of Pharmaceutical Sciences 12 (1): 69-77.

- Hatzi, P., Mourtas, S., G. Klepetsanis, P., and Antimisiaris, S. G. 2007. Integrity of liposomes in presence of cyclodextrins: Effect of liposome type and lipid composition. International Journal of Pharmaceutics 333 (1-2): 167-176.
- Hidalgo, I. J. and Li, J. 1996. Carrier-mediated transport and efflux mechanisms in Caco-2 cells. Advanced Drug Delivery Reviews 22 (1-2): 53-66.
- Higgins, C. F., Callaghan, R., Linton, K. J., Rosenberg, M. F., and Ford, R. C. 1997. Structure of the multidrug resistance P-glycoprotein. Seminars in Cancer Biology 8 (3): 135-142.
- Higgins, C. F. and Gottesman, M. M. 1992. Is the multidrug transporter a flippase? Trends in Biochemical Sciences 17 (1): 18-21.
- Ho, N. F. H., Day, J. S., Barsuhn, C. L., Burton, P. S., and Raub, T. J. 1990. Biophysical model approaches to mechanistic transepithelial studies of peptides. Journal of Controlled Release 11 (1-3): 3-24.
- Holovati, J. L., Gyongyossy-Issa, M. I. C., and Acker, J. P. 2008. Investigating interactions of trehalose-containing liposomes with human red blood cells. Cell Preservation Technology. 6 (2): 14.
- Honjo, Y., Hrycyna, C. A., Yan, Q.-W., Medina-Perez, W. Y., Robey, R. W., van de Laar, A., et al. 2001. Acquired mutations in the MXR/BCRP/ABCP gene alter substrate specificity in MXR/BCRP/ABCP-overexpressing cells. Cancer Research 61 (18): 6635-6639.
- Huang, J., Si, L., Jiang, L., Fan, Z., Qiu, J., and Li, G. 2008. Effect of pluronic F68 block copolymer on P-glycoprotein transport and CYP3A4 metabolism. International Journal of Pharmaceutics 356 (1-2): 351-353.
- Hunter, J., Hirst, B. H., and Simmons, N. L. 1993. Drug absorption limited by P-glycoprotein-mediated secretory drug transport in human intestinal epithelial Caco-2 cell layers. Pharmaceutical Research 10 (5): 743-749.
- Hwang, T.-L., Lee, W.-R., Hua, S.-C., and Fang, J.-Y. 2007. Cisplatin encapsulated in phosphatidylethanolamine liposomes enhances the in vitro cytotoxicity and in vivo intratumor drug accumulation against melanomas. Journal of Dermatological Science 46 (1): 11-20.

- Iffert, T., Soldan, M., Moeller, A., and Maser, E. 2000. Modulation of daunorubicin toxicity by liposomal encapsulation and use of specific inhibitors in vitro. Toxicology 144 (1-3): 189-195.
- Imura, T., Otake, K., Hashimoto, S., Gotoh, T., Yuasa, M., Yokoyama, S., et al. 2002. Preparation and physicochemical properties of various soybean lecithin liposomes using supercritical reverse phase evaporation method. Colloids and Surfaces B: Biointerfaces 27 (2-3): 133-140.
- Institute from Stem Cell Reserch (ISCR). 2008. Basic operation of FACScan and FACS Calibur cytometers [online]. Available from: <http://www.iscr.ed.ac.uk/> [2008, November 1]
- Jansons, V. K., Weis, P., Chen, T.-h., and Redwood, W. R. 1978. In vitro interaction of L1210 cells with phospholipid vesicles. Cancer Research 38 (3): 531-535.
- Jones, A. T., Gumbleton, M., and Duncan, R. 2003. Understanding endocytic pathways and intracellular trafficking: a prerequisite for effective design of advanced drug delivery systems. Advanced Drug Delivery Reviews 55 (11): 1353-1357.
- Kapitza, S. B., Michel, B. R., van Hoogevest, P., Leigh, M. L. S., and Imanidis, G. 2007. Absorption of poorly water soluble drugs subject to apical efflux using phospholipids as solubilizers in the Caco-2 cell model. European Journal of Pharmaceutics and Biopharmaceutics 66 (1): 146-158.
- Kato, Y., Miyazaki, T., Kano, T., Sugiura, T., Kubo, Y., and Tsuji, A. 2008. Involvement of influx and efflux transport systems in gastrointestinal absorption of celiprolol. Journal of Pharmaceutical Sciences 9999 (9999): 1-11.
- Kau, S. and Maack, T. 1986. Mechanism of tubular uptake on human growth hormone in perfused rat kidneys. Journal of Pharmacology and Experimental Therapeutics 236 (3): 596-601.
- Kawakami, K., Nishihara, Y., and Hirano, K. 1999. Rigidity of lipid membranes detected by capillary electrophoresis. Langmuir 15 (6): 1893-1895.
- Ke, W., Zhao, Y., Huang, R., Jiang, C., and Pei, Y. 2008. Enhanced oral bioavailability of doxorubicin in a dendrimer drug delivery system. Journal of Pharmaceutical Sciences 97 (6): 2208-2216.

- Khalil, I. A., Kogure, K., Futaki, S., and Harashima, H. 2006. High density of octaarginine stimulates macropinocytosis leading to efficient intracellular trafficking for gene expression. Journal of Biological Chemistry 281 (6): 3544-3551.
- Kheirloom, A. and Ferrara, K. W. 2007. Cholesterol transport from liposomal delivery vehicles. Biomaterials 28 (29): 4311-4320.
- Knoll, G., Burger, K. N. J., Bron, R., Meer, G. v., and Verkleij, A. J. 1988. Fusion of liposomes with the plasma membrane of epithelial cells: Fate of incorporated lipids as followed by freeze fracture and autoradiography of plastic sections. The Journal of Cell Biology 107: 2511-2521.
- Kobayashi, T., Ishida, T., Okada, Y., Ise, S., Harashima, H., and Kiwada, H. 2007. Effect of transferrin receptor-targeted liposomal doxorubicin in P-glycoprotein-mediated drug resistant tumor cells. International Journal of Pharmaceutics 329 (1-2): 94-102.
- Kraayenhof, R., Sterk, G. J., Wong Fong Sang, H. W., Krab, K., and Epan, R. M. 1996. Monovalent cations differentially affect membrane surface properties and membrane curvature, as revealed by fluorescent probes and dynamic light scattering. Biochimica et Biophysica Acta (BBA) - Biomembranes 1282 (2): 293-302.
- Krishna, R. and Mayer, L. D. 2000. Multidrug resistance (MDR) in cancer: Mechanisms, reversal using modulators of MDR and the role of MDR modulators in influencing the pharmacokinetics of anticancer drugs. European Journal of Pharmaceutical Sciences 11 (4): 265-283.
- Lee, K.-D., Hong, K., and Papahadjopoulos, D. 1992. Recognition of liposomes by cells: In vitro binding and endocytosis mediated by specific lipid headgroups and surface charge density. Biochimica et Biophysica Acta (BBA) - Biomembranes 1103 (2): 185-197.
- Legrand, P., Vertut-Doi, A., and Bolard, J. 1996. Comparative internalization and recycling of different amphotericin B formulations by a macrophage-like cell line. Journal of Antimicrobial Chemotherapy 37 (3): 519-533.
- Lentz, K. A., Hayashi, J., Lucisano, L. J., and Polli, J. E. 2000. Development of a more rapid, reduced serum culture system for Caco-2 monolayers and

- application to the biopharmaceutics classification system. International Journal of Pharmaceutics 200 (1): 41-51.
- Li, C., Greenwood, T. R., and Glunde, K. 2008. Glucosamine-bound near-infrared fluorescent probes with lysosomal specificity for breast tumor imaging. Neoplasia 10 (4): 389-398.
- Lo, Y.-L. 2000. Phospholipids as multidrug resistance modulators of the transport of epirubicin in human intestinal epithelial Caco-2 cell layers and everted gut sacs of rats. Biochemical Pharmacology 60 (9): 1381-1390.
- Lo, Y.-L. 2003. Relationships between the hydrophilic-lipophilic balance values of pharmaceutical excipients and their multidrug resistance modulating effect in Caco-2 cells and rat intestines. Journal of Controlled Release 90 (1): 37-48.
- Lo, Y.-L., Liu, F.-i., and Cherng, J.-y. 2001. Effect of PSC 833 liposomes and Intralipid on the transport of epirubicin in Caco-2 cells and rat intestines. Journal of Controlled Release 76 (1-2): 1-10.
- Loetchutinat, C., Saengkhae, C., Marbeuf-Gueye, C., and Garnier-Suillerot, A. 2003. New insights into the P-glycoprotein-mediated effluxes of rhodamines. European Journal of Biochemistry 270 (3): 476-485.
- Lukanawonakul, A. 2005. Evaluation of liposomal composition on delivery of hydrophilic substances and P-glycoprotein substrates. Master's Thesis Department of Pharmacy, Faculty of Pharmaceutical Sciences, Chulalongkorn University.
- Ma, T. Y., Hoa, N. T., Tran, D. D., Bui, V., Pedram, A., Mills, S., et al. 2000. Cytochalasin B modulation of Caco-2 tight junction barrier: role of myosin light chain kinase. American Journal of Physiology-Gastrointestinal and Liver Physiology 279 (5): G875-885.
- Magalhães, A. C., Baron, G. S., Lee, K. S., Steele-Mortimer, O., Dorward, D., Prado, M. A. M., et al. 2005. Uptake and neuritic transport of scrapie prion protein coincident with infection of neuronal cells. Journal of Neurosciences 25 (21): 5207-5216.
- Mainprize, T. and Grady, L. T. 1998. Standardization of an in vitro method of drug absorption. Pharmacopeial Forum 24: 6015-1023.

- Mamdouh, Z., Giocondi, M.-C., Laprade, R., and Le Grimellec, C. 1996. Temperature dependence of endocytosis in renal epithelial cells in culture. Biochimica et Biophysica Acta (BBA) - Biomembranes 1282 (2): 171-173.
- Mamot, C., Drummond, D. C., Hong, K., Kirpotin, D. B., and Park, J. W. 2003. Liposome-based approaches to overcome anticancer drug resistance. Drug Resistance Updates 6 (5): 271-279.
- Manconi, M., Isola, R., Falchi, A. M., Sinico, C., and Fadda, A. M. 2007. Intracellular distribution of fluorescent probes delivered by vesicles of different lipidic composition. Colloids and Surfaces B: Biointerfaces 57 (2): 143-151.
- Massing, U. and Fuxius, S. 2000. Liposomal formulations of anticancer drugs: selectivity and effectiveness. Drug Resistance Updates 3 (3): 171-177.
- Matsui, H., Johnson, L. G., Randell, S. H., and Boucher, R. C. 1997. Loss of binding and entry of liposome-DNA complexes decreases transfection efficiency in differentiated airway epithelial cells. The Journal of Biological Chemistry 272 (2): 1117-1126.
- Mayer, L. D. and Shabbits, J. A. 2001. The role for liposomal drug delivery in molecular and pharmacological strategies to overcome multidrug resistance. Cancer and Metastasis Reviews 20 (1): 87-93.
- Michieli, M., Damiani, D., Ermacora, A., Masolini, P., Michelutti, A., Michelutti, T., et al. 1999. Liposome-encapsulated daunorubicin for PGP-related multidrug resistance. British Journal of Haematology 106: 92-99.
- Miller, C. R., Bondurant, B., McLean, S. D., McGovern, K. A., and O'Brien, D. F. 1998. Liposome-cell interactions in vitro: Effect of liposome surface charge on the binding and endocytosis of conventional and sterically stabilized liposomes. Biochemistry 37 (37): 12875-12883.
- Mishra, V., Mahor, S., Rawat, A., Dubey, P., Gupta, P. N., Singh, P., et al. 2006. Development of novel fusogenic vesosomes for transcutaneous immunization. Vaccine 24 (27-28): 5559-5570.
- Mistry, P., Stewart, A. J., Dangerfield, W., Okiji, S., Liddle, C., Bootle, D., et al. 2001. In vitro and in vivo reversal of P-glycoprotein-mediated multidrug

- resistance by a novel potent modulator, XR9576. Cancer Research 61 (2): 749-758.
- Molecular Probes. 2006. Dextran conjugates [online]. Available from: www.invitrogen.com [2009, February 10]
- Moriya, M. and Linder, M. C. 2006. Vesicular transport and apotransferrin in intestinal iron absorption, as shown in the Caco-2 cell model. American Journal of Physiology-Gastrointestinal and Liver Physiology 290 (2): G301-309.
- New, R. R. C. 1997. Liposomes A Practical Approach. New York: Oxford University Press Inc.
- Nikolova, A. N. and Jones, M. N. 1998. Phospholipid free thin liquid films with grafted poly(ethylene glycol)-2000: formation, interaction forces and phase states. Biochimica et Biophysica Acta (BBA) - Biomembranes 1372 (2): 237-243.
- Ozben, T. 2006. Mechanisms and strategies to overcome multiple drug resistance in cancer. FEBS Letters 580 (12): 2903-2909.
- Palm, C., Jayamanne, M., Kjellander, M., and Hällbrink, M. 2007. Peptide degradation is a critical determinant for cell-penetrating peptide uptake. Biochimica et Biophysica Acta (BBA) - Biomembranes 1768 (7): 1769-1776.
- Papahadjopoulos, D., Poste, G., and Schaeffer, B. E. 1973. Fusion of mammalian cells by unilamellar lipid vesicles: Influence of lipid surface charge, fluidity and cholesterol. Biochimica et Biophysica Acta (BBA) - Biomembranes 323 (1): 23-42.
- Pincet, F., Cribier, S., and Perez, E. 1999. Bilayers of neutral lipids bear a small but significant charge. The European Physical Journal B 11: 127-130.
- Pincet, F., Lebeau, L., and Cribier, S. 2001. Short-range specific forces are able to induce hemifusion. European Biophysics Journal 30 (2): 91-97.
- Pivčević, B. and Žaja, R. 2006. Pesticides and their binary combinations as P-glycoprotein inhibitors in NIH 3T3/MDR1 cells. Environmental Toxicology and Pharmacology 22 (3): 268-276.

- Pool, G., French, M., Edwards, R., Huang, L., and Lumb, R. 1982. Use of radiolabeled hexadecyl cholesteryl ether as a liposome marker. Lipids 17 (6): 5.
- Poste, G. and Papahadjopoulos, D. 1976. Lipid vesicles as carriers for introducing materials into cultured cells: Influence of vesicle lipid composition on mechanism(s) of vesicle incorporation into cells. Proceedings of the National Academy of Sciences of the United States of America 73 (5): 1603-1607.
- Price, P. J. 1975. Preparation and use of rat-tail collagen. Methods in Cell Science 1 (1): 43-44.
- Rege, B. D., Kao, J. P. Y., and Polli, J. E. 2002. Effects of nonionic surfactants on membrane transporters in Caco-2 cell monolayers. European Journal of Pharmaceutical Sciences 16 (4-5): 237-246.
- Rege, B. D., Yu, L. X., Hussain, A. S. H., and Polli, J. E. 2001. Effect of common excipients on Caco-2 transport of low-permeability drugs. Journal of Pharmaceutical Sciences 90 (11): 1776-1786.
- Romsicki, Y. and Sharom, F. J. 1999. The membrane lipid environment modulates drug interactions with the P-glycoprotein multidrug transporter. Biochemistry 38 (21): 6887-6896.
- Sætern, A. M., Skar, M., Braaten, Å., and Brandl, M. 2005. Camptothecin-catalyzed phospholipid hydrolysis in liposomes. International Journal of Pharmaceutics 288 (1): 73-80.
- Sambuy, Y., De Angelis, I., Ranaldi, G., Scarino, M. L., Stamatii, A., and Zucco, F. 2005. The Caco-2 cell line as a model of the intestinal barrier: influence of cell and culture-related factors on Caco-2 cell functional characteristics. Cell Biology and Toxicology 21 (1): 1-26.
- Sarkadi, B. and Müller, M. 1997. Search for specific inhibitors of multidrug resistance in cancer. Seminars in Cancer Biology 8 (3): 171-182.
- Sauna, Z., Smith, M., Müller, M., Kerr, K., and Ambudkar, S. 2001. The mechanism of action of multidrug-resistance-linked P-glycoprotein. Journal of Bioenergetics and Biomembranes 33 (6): 481-491.

- Schinkel, A. H. and Jonker, J. W. 2003. Mammalian drug efflux transporters of the ATP binding cassette (ABC) family: an overview. Advanced Drug Delivery Reviews 55 (1): 3-29.
- Schnatwinkel, C., Christoforidis, S., Lindsay, M. R., Uttenweiler-Joseph, S., Wilm, M., Parton, R. G., et al. 2004. The rab5 effector rabankyrin-5 regulates and coordinates different endocytic mechanisms. PLoS Biology 2 (9): 1363-1380.
- Seelig, A. 1998. A general pattern for substrate recognition by P-glycoprotein. European Journal of Biochemistry 251 (1-2): 252-261.
- Seelig, A. and Landwojtowicz, E. 2000. Structure-activity relationship of P-glycoprotein substrates and modifiers. European Journal of Pharmaceutical Sciences 12 (1): 31-40.
- Senior, J. H., Trimble, K. R., and Maskiewicz, R. 1991. Interaction of positively-charged liposomes with blood: implications for their application in vivo. Biochimica et Biophysica Acta (BBA) - Biomembranes 1070 (1): 173-179.
- Shargel, L., Wu-Pong, S., and Yu, A. B. C. 2005. Applied Biopharmaceutics & Pharmacokinetics. New York: McGraw-Hill.
- Sigma-Aldrich Co. 2009. Sigma-Aldrich [online]. Available from: <http://www.Sigmaaldrich.com/> [2007, December 1]
- Smith, C. G. and O'Donnell, J. T. 2006. The process of new drug discovery and development. Informa Health Care.
- Somero, G. N. 1978. Temperature adaptation of enzymes: Biological optimization through structure-function compromises. Annual Review of Ecology and Systematics 9: 1-29.
- Spernath, A., Aserin, A., Ziserman, L., Danino, D., and Garti, N. 2007. Phosphatidylcholine embedded microemulsions: Physical properties and improved Caco-2 cell permeability. Journal of Controlled Release 119 (3): 279-290.
- Sugawara, T., Kushiro, M., Zhang, H., Nara, E., Ono, H., and Nagao, A. 2001. Lysophosphatidylcholine enhances carotenoid uptake from mixed micelles by Caco-2 human intestinal cells. The Journal of Nutrition 131 (11): 2921-2927.

- Takano, M., Yumoto, R., and Murakami, T. 2006. Expression and function of efflux drug transporters in the intestine. Pharmacology & Therapeutics 109 (1-2): 137-161.
- Tenopoulou, M., Kurz, T., Doulias, P.-T., Galaris, D., and Brunk, U. T. 2007. Does the calcein-AM method assay the total cellular 'labile iron pool' or only a fraction of it? Biochemical Journal 403: 261-266.
- Tessner, T. G. and Stenson, W. F. 2000. Overexpression of MDR1 in an intestinal cell line results in increased cholesterol uptake from micelles. Biochemical and Biophysical Research Communications 267 (2): 565-571.
- Torchilin, V. P. and Weissig, V. 2003. Liposomes A Practical Approach. New York: Oxford University Press.
- Troost, J., Albermann, N., Emil Haefeli, W., and Weiss, J. 2004. Cholesterol modulates P-glycoprotein activity in human peripheral blood mononuclear cells. Biochemical and Biophysical Research Communications 316 (3): 705-711.
- Troutman, M. D. and Thakker, D. R. 2003. Rhodamine 123 requires carrier-mediated influx for its activity as a P-glycoprotein substrate in Caco-2 cells. Pharmaceutical Research 20 (8): 1192-1199.
- Tuma, P. L. and Hubbard, A. L. 2003. Transcytosis: Crossing cellular barriers. Physiology Review 83 (3): 871-932.
- Uchiyama, K., Nagayasu, A., Yamagiwa, Y., Nishida, T., Harashima, H., and Kiwada, H. 1995. Effects of the size and fluidity of liposomes on their accumulation in tumors: A presumption of their interaction with tumors. International Journal of Pharmaceutics 121 (2): 195-203.
- Uchiyama, Y., Yui, H., and Sawada, T. 2004. Adsorption and desorption behaviors of cationic liposome-DNA complexes upon lipofection in inside and outside biomembrane models using a dynamic quasi-elastic laser scattering method. Analytical Sciences 20 (11): 1537-1542.
- US FDA. 2006. Guidance for Industry: Drug interaction studies: Study design, data analysis, and implications for dosing and labeling [online]. Available from: www.fda.gov/cder/guidance/index.htm [2008, February 1]

- Utoguchi, N., Chandorkar, G. A., Avery, M., and Audus, K. L. 2000. Functional expression of P-glycoprotein in primary cultures of human cytotrophoblasts and BeWo cells[small star, filled]. Reproductive Toxicology 14 (3): 217-224.
- van der Sandt, I. C. J., Blom-Roosemalen, M. C. M., de Boer, A. G., and Breimer, D. D. 2000. Specificity of doxorubicin versus rhodamine-123 in assessing P-glycoprotein functionality in the LLC-PK1, LLC-PK1:MDR1 and Caco-2 cell lines. European Journal of Pharmaceutical Sciences 11 (3): 207-214.
- Varma, M. V. S., Ashokraj, Y., Dey, C. S., and Panchagnula, R. 2003. P-glycoprotein inhibitors and their screening: a perspective from bioavailability enhancement. Pharmacological Research 48 (4): 347-359.
- Voronina, S. G., Sherwood, M. W., Gerasimenko, O. V., Petersen, O. H., and Tepikin, A. V. 2007. Visualizing formation and dynamics of vacuoles in living cells using contrasting dextran-bound indicator: endocytic and nonendocytic vacuoles. American Journal of Physiology-Gastrointestinal and Liver Physiology 293 (6): G1333-1338.
- Wang, E.-j., Casciano, C. N., Clement, R. P., and Johnson, W. W. 2000. Cholesterol interaction with the daunorubicin binding site of P-glycoprotein. Biochemical and Biophysical Research Communications 276 (3): 909-916.
- Ward, P. D., Tippin, T. K., and Thakker, D. R. 2000. Enhancing paracellular permeability by modulating epithelial tight junctions. Pharmaceutical Science & Technology Today 3 (10): 346-358.
- Warren, L., Jardillier, J.-C., Malarska, A., and Akeli, M.-G. 1992. Increased accumulation of drugs in multidrug-resistant cells induced by liposomes. Cancer Research 52 (11): 3241-3245.
- Wasan, K. M. 2007. Role of Lipid Excipients in Modifying Oral and Parenteral Drug Delivery. USA: John Wiley & Sons, Inc.
- Watson, P., Jones, A. T., and Stephens, D. J. 2005. Intracellular trafficking pathways and drug delivery: fluorescence imaging of living and fixed cells. Advanced Drug Delivery Reviews 57 (1): 43-61.
- Wong, H. L., Bendayan, R., Rauth, A. M., Xue, H. Y., Babakhanian, K., and Wu, X. Y. 2006. A mechanistic study of enhanced doxorubicin uptake and retention in multidrug resistant breast cancer cells using a polymer-lipid hybrid

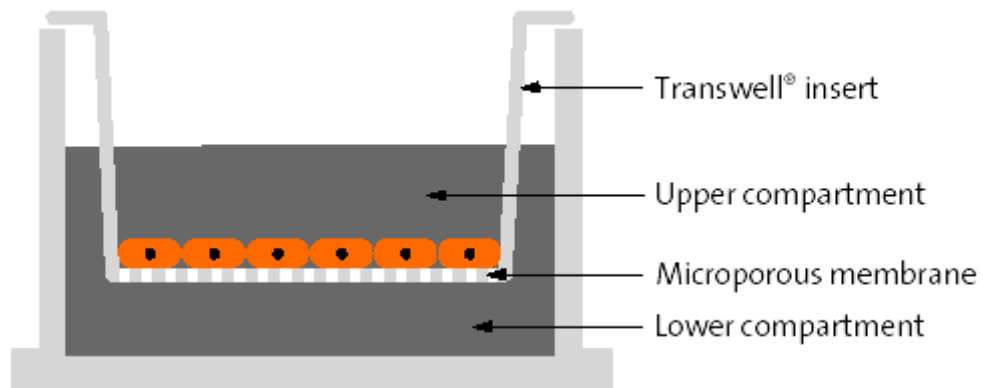
- nanoparticle system. Journal of Pharmacology and Experimental Therapeutics 317 (3): 1372-1381.
- Xia, C. Q., Liu, N., Yang, D., Miwa, G., and Gan, L.-S. 2005. Expression, localization, and functional characteristics of breast cancer resistance protein in Caco-2 cells. Drug Metabolism and Disposition 33 (5): 637-643.
- Yamashita, S., Furubayashi, T., Kataoka, M., Sakane, T., Sezaki, H., and Tokuda, H. 2000. Optimized conditions for prediction of intestinal drug permeability using Caco-2 cells. European Journal of Pharmaceutical Sciences 10 (3): 195-204.
- Zastre, J., Jackson, J., Bajwa, M., Liggins, R., Iqbal, F., and Burt, H. 2002. Enhanced cellular accumulation of a P-glycoprotein substrate, rhodamine-123, by caco-2 cells using low molecular weight methoxypolyethylene glycol-block-polycaprolactone diblock copolymers. European Journal of Pharmaceutics and Biopharmaceutics 54 (3): 299-309.
- Zhang, Y., Gupta, A., Wang, H., Zhou, L., Vethanayagam, R. R., Unadkat, J. D., et al. 2005. BCRP transports dipyridamole and is inhibited by calcium channel blockers. Pharmaceutical Research 22: 2023-2034.

APPENDICES

APPENDIX I

Transwell[®] inserts (Corning, 2006)

Transwell® inserts for transport studies (Corning, 2006)



Semipermeable membrane	= polycarbonate membrane (pore size = 3 μm)
Area of semipermeable membrane	= 4.71 cm^2 (6-well plate)
Apical volume	= 1.5 cm^3 (6-well plate)
Basolateral volume	= 2.6 cm^3 (6-well plate)

Average TEER \pm SD of the polycarbonate membranes (experimentally determined) =
 135.2 \pm 4.72 $\Omega\cdot\text{cm}^2$ (6-well plate)

APPENDIX II

**Components of the apical and basolateral buffers for transport study
(Mainprize and Grady, 1998)**

Apical buffer

Hank's balanced salt solution	935 ml
1 M D-Glucose monohydrate	25 ml
1 M MES Biological buffer	20 ml
125 mM Calcium chloride	10 ml
50 mM Magnesium chloride	10 ml
Adjusted with potassium hydroxide to a pH of 6.5	

Basolateral buffer

Hank's balanced salt solution	935 ml
1 M D-Glucose monohydrate	25 ml
1 M HEPES Biological buffer	20 ml
125 mM Calcium chloride	10 ml
50 mM Magnesium chloride	10 ml
Adjusted with potassium hydroxide to a pH of 7.4	

APPENDIX III

**Preparation of rat-tail collagen and coating procedures
for collagen-coated coverslips**

(Grace Bio-Labs, Inc. ;Price, 1975)

Protocol for preparation of rat-tail collagen

The following description is for preparation of collagen from one rat tail

- 1) Freeze tail in -20 °C refrigerator immediately after removal from donor rat. Keep frozen until ready for processing.
- 2) To process, remove rat tail from freezer and place in 150 x 15 mm Petri dish containing 70% ethanol for 20 minutes.
- 3) Cut the tip of the tail crosswise (about 2 cm from the tip) with sterile scissors, and pull skin back approximately 1/4 inch. The tendons will then be exposed.
- 4) Slowly pull out each tendon with sterile blunt tip forceps.
- 5) Place tendon in 150 x 15 mm sterile Petri dish containing sterile water.
- 6) Repeat 3, 4, and 5. Remove tendons one at a time from tendon bundle until all tendons have been pulled out.
- 7) Cut each tendon into small pieces with sterile scissors (If the tendons are tangled, they are difficult to mince.). Transfer pieces as minced to a sterile 250 ml beaker.
- 8) Soak the minced tendons obtained from one tail in 150 ml of acetic acid-water (1:1000) for 48 hours at 4 °C. Shake gently at 48 hours.
- 9) Transfer by pouring sterile tendon-acetic acid-water mixture into 50 ml centrifuge tubes. Centrifuge for 1/2 hour at approximately 2,000 xg at 4 °C.
- 10) Withdraw supernatant that is very viscous with a large bore pipette and recentrifuge supernatant at 4,000 xg at 4°C in 12 ml conical centrifuge tubes for 1/2 hour.
- 11) Store this supernatant at -20 °C.

Coating protocol for collagen-coated coverslips

- 1) Dilute rat-tail collagen solution 1:2 with 60% ethanol and spread over surface of sterile glass coverslip (30 μ l collagen solution per coverslip).
- 2) Immediately neutralize for 2 min with ammonium hydroxide vapors by placing the dish of coverslips in a covered dish containing filter paper wet with concentrated ammonium hydroxide. This will cause the collagen to gel.
- 3) Wash coverslips twice with sterile water.
- 4) Gently spread 50 μ l of collagen solution over the surface of the gelled collagen and air dry overnight under the UV light in laminar airflow hood.

APPENDIX IV

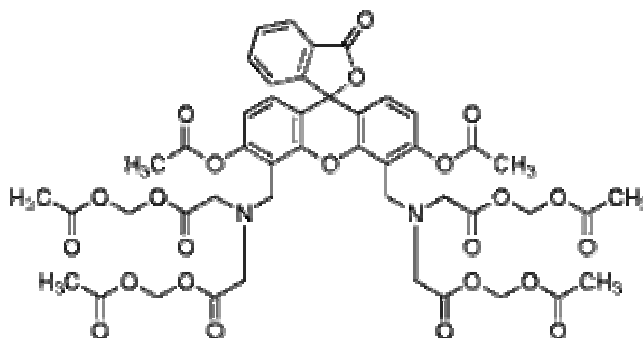
**Molecular structures of calcein AM, calcein, rhodamine 123,
and verapamil hydrochloride
(Sigma-Aldrich, 2009)**

Calcein AM (Sigma-Aldrich, 2009)

Synonym: Calcein *O,O'*-diacetate tetrakis(acetoxymethyl) ester

Empirical: C₄₆H₄₆N₂O₂₃

Structure:



(From Sigma-Aldrich, 2009)

Molecular weight: 994.86

Solubility: soluble in DMSO

Storage temperature: -20°C

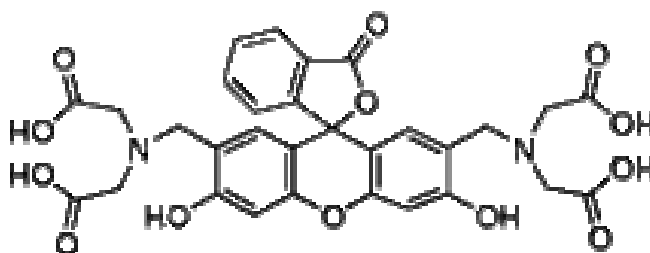
Calcein (Sigma-Aldrich, 2009)

Synonyms: Fluorescein-bis(methyliminodiacetic acid), Fluorexon,

Bis[*N,N*-bis(carboxymethyl)aminomethyl]fluorescein

Empirical: C₃₀H₂₆N₂O₁₃

Structure:



(From Sigma-Aldrich, 2009)

Molecular weight: 622.53

Solubility: clear orange to brown solution at 50 mg/ml in 1 M sodium hydroxide

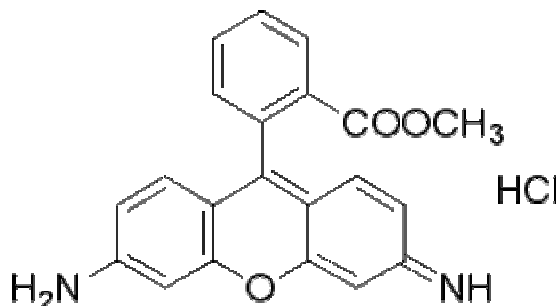
Storage temperature: store at room temperature

Rhodamine 123 (Sigma-Aldrich, 2009)

Synonym: 2-(6-Amino-3-imino-3H-xanthen-9-yl) benzoic acid methyl ester

Empirical: $C_{21}H_{17}ClN_2O_3$

Structure:



(From Sigma-Aldrich, 2009)

Molecular weight: 380.83

Solubility: soluble in 100% ethanol and water

Storage temperature: store at room temperature

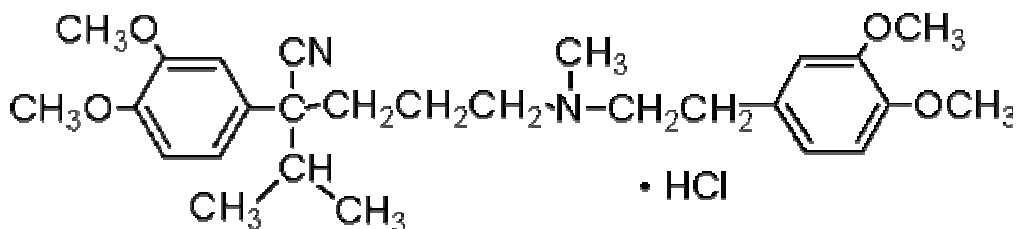
± Verapamil hydrochloride (Sigma-Aldrich, 2009)

Synonym: 5-[N-(3,4-Dimethoxyphenylethyl)methylamino]-2-(3,4-dimethoxyphenyl)-2-isopropylvaleronitrile hydrochloride

Empirical: $(CH_3O)_2C_6H_3CH_2CH_2N(CH_3)(CH_2)_3C[C_6H_3(OCH_3)_2][CH(CH_3)_2]CN \cdot$

HCl

Structure:



(From Sigma-Aldrich, 2009)

Molecular weight: 491.06

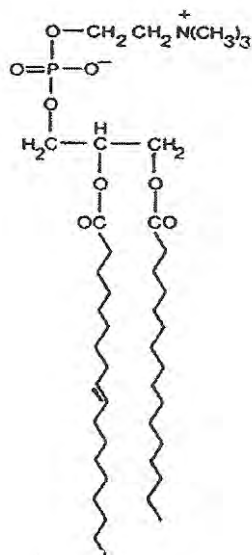
Solubility: methanol: 50 mg/ml, clear, colorless

Storage temperature: store at room temperature

APPENDIX IV

**Molecular structures of PC, DPPC, CH, DCP, and SA
(Graham and Higgin, 1997; Avanti Polar Lipids; Sigma-Aldrich, 2009)**

Molecular structure of phosphatidylcholine



(From Graham and Higgin, 1997)

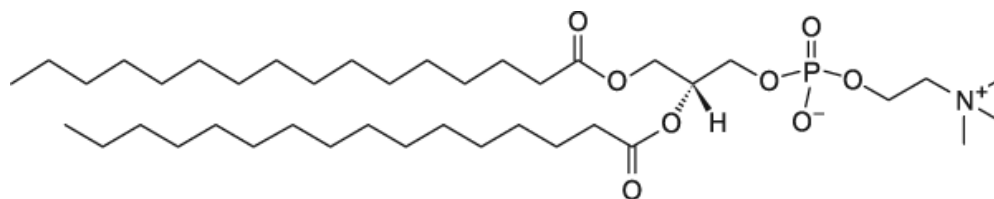
Dipalmitoylphosphatidylcholine (DPPC)

Synonym: 1,2-dihexadecanoyl-*sn*-glycero-3-phosphocholine

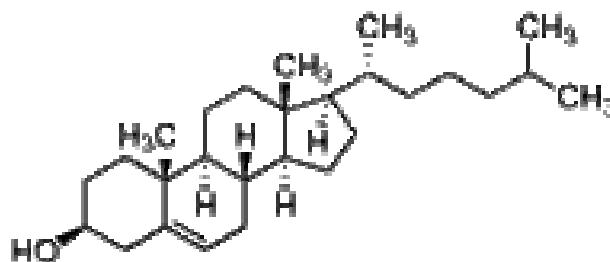
Empirical: C₄₀H₈₀NO₈P

Molecular weight: 734.04

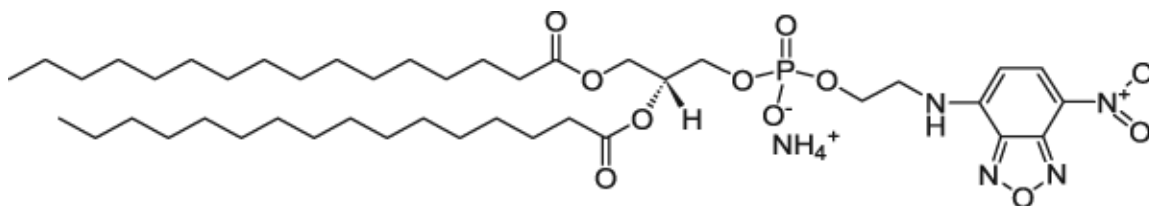
Structure:



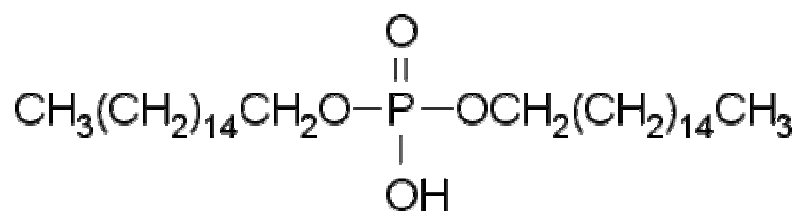
(From Avanti Polar Lipids)

Cholesterol**Synonym:** 3 β -Hydroxy-5-cholestene, 5-Cholesten-3 β -ol**Empirical:** C₂₇H₄₆O**Molecular weight:** 386.65**Structure:**

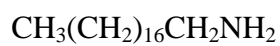
(From Sigma-Aldrich, 2009)

NBD-PE**Synonym:** 1,2-dipalmitoyl-*sn*-glycero-3-phosphoethanolamine-N-(7-nitro-2-1,3-benzoxadiazol-4-yl) (ammonium salt)**Empirical:** C₄₃H₇₈N₅O₁₁P**Molecular weight:** 872.08**Structure:**

(From Avanti Polar Lipids)

Dicetylphosphate (DCP)**Synonym:** dihexadecyl phosphate**Empirical:** C₃₂H₆₇O₄P**Molecular weight:** 546.85**Structure:**

(From Sigma-Aldrich, 2009)

Stearylamine (SA)**Synonyms:** 1-Aminooctadecane, octadecylamine**Empirical:** C₁₈H₃₉N**Molecular weight:** 269.51**Structure:**

(From Sigma-Aldrich, 2009)

APPENDIX IV

Standard curves of calcein and rhodamine 123

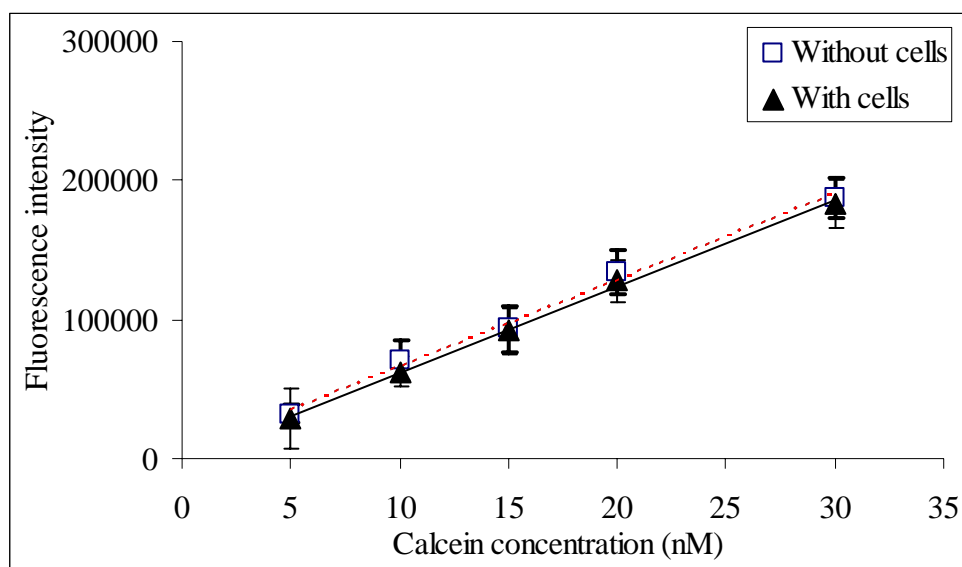


Figure 28: A representation of calibration curve of calcein in 1% Triton[®] X-100 in PBS

Without cells: $y = 6218.5x + 3975.9$, $R^2 = 0.9947$

With cells: $y = 6210.7x - 430.61$, $R^2 = 0.9981$

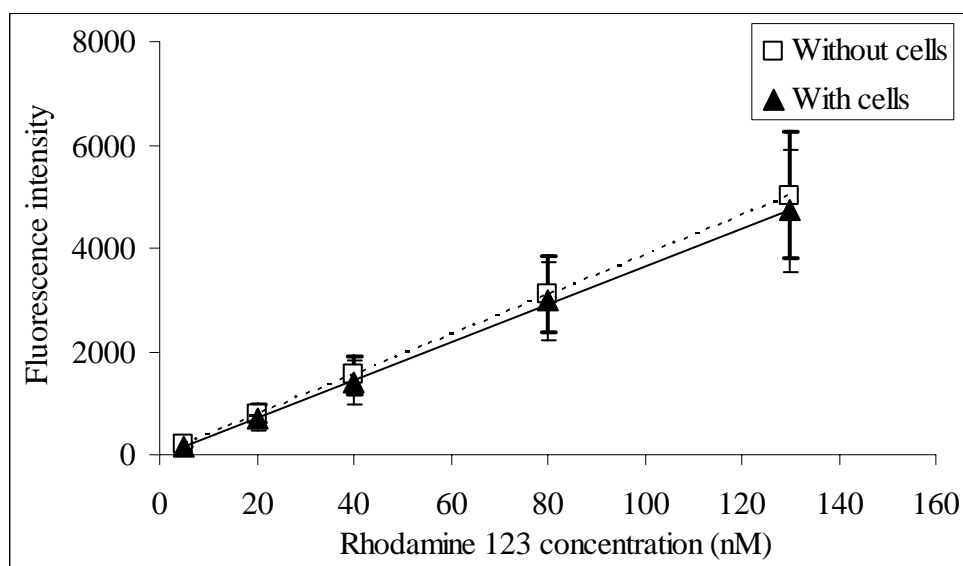


Figure 29: A representation of calibration curve of rhodamine 123 in 1% Triton[®] X-100 in PBS

Without cells: $y = 38.591x + 10.044$, $R^2 = 1$

With cells: $y = 36.846x - 41.339$, $R^2 = 0.9995$

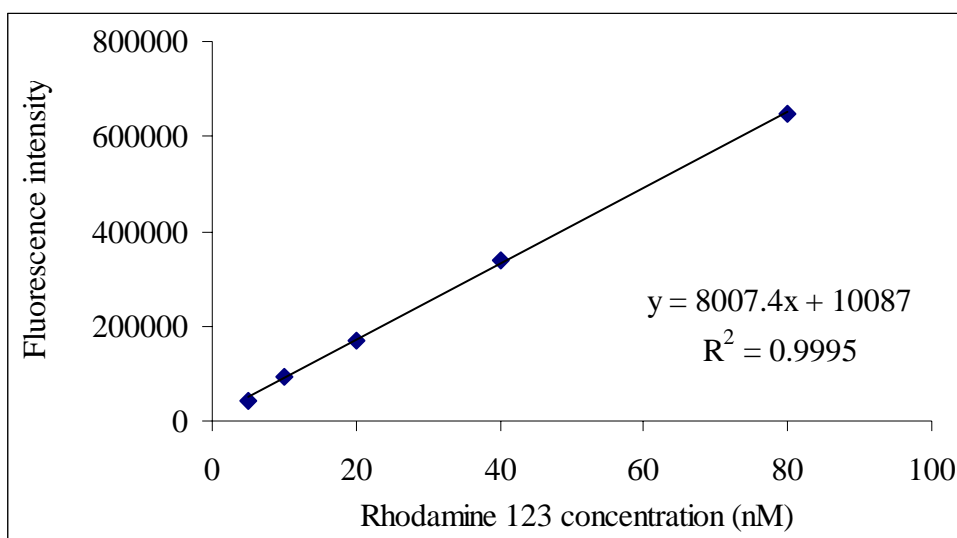


Figure 30: A representation of calibration curve of rhodamine 123 in the apical buffer

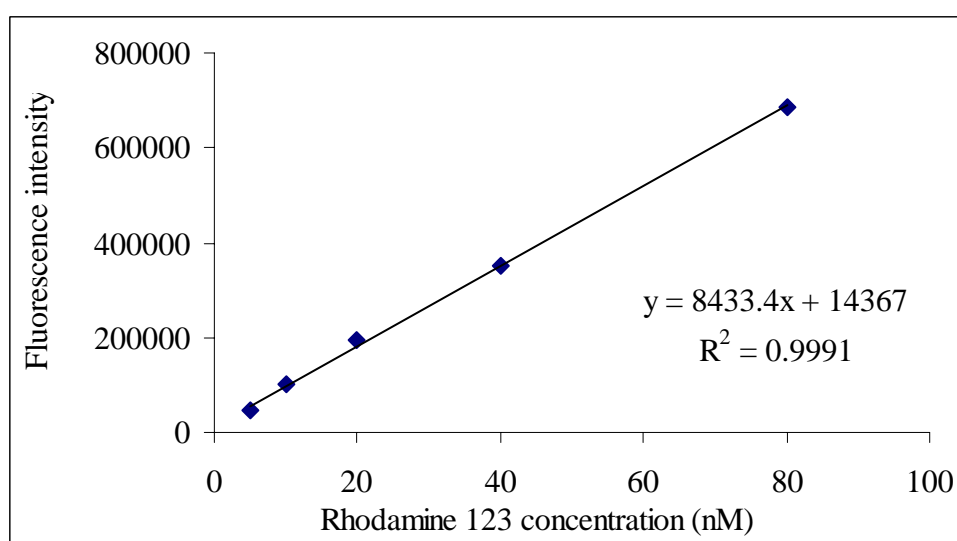


Figure 31: A representation of calibration curve of rhodamine 123 in the basolateral buffer

VITA

Miss Ing-orn Prasanchaimontri was born on November 13, 1980 in Bangkok, Thailand. She received the Bachelor of Pharmacy from Chulalongkorn University in 2003. Since graduation, she has worked at the Bioequivalence Study Center, Department of Medical Sciences, Ministry of Public Health. She entered the master's degree program in Pharmacy at Chulalongkorn University in 2006.